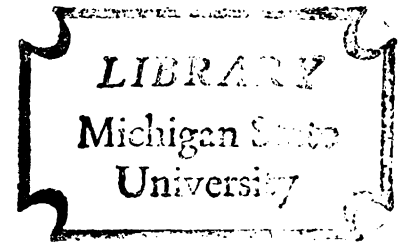


PLATOON DISPERSION DYNAMICS ON ARTERIAL STREETS
WITH ENTERING VEHICLES

Dissertation for the Degree of Ph. D.
MICHIGAN STATE UNIVERSITY
KIN KEUNG LAI
1977



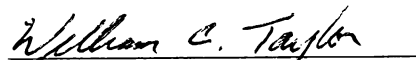
This is to certify that the
thesis entitled
PLATOON DISPERSION DYNAMICS ON
ARTERIAL STREETS WITH ENTERING VEHICLES

presented by

KIN KEUNG LAI

has been accepted towards fulfillment
of the requirements for

Ph.D. degree in Civil Engineering


Major professor

Date May 27, 1977

ABSTRACT

PLATOON DISPERSION DYNAMICS ON ARTERIAL STREETS WITH ENTERING VEHICLES

By

Kin K. Lai

The literature related to platoon dispersion was reviewed. A preliminary study of vehicular time headway within a platoon on arterial streets was conducted, and a stochastic model for the headway was developed, which was found to be a gamma distribution.

The results of the field study indicated no significant difference between the dispersion of platoons under light and medium flow mainstream traffic.

The dispersion of a platoon leaving from a signal and approaching a signal with or without entering vehicles was modeled as polynomial regressions with a degree of two. The model of dispersion of a passing platoon with entering vehicles was analyzed and related to the model of a dispersion platoon leaving an intersection with a signal.

Analytical models of the measures of effectiveness (that is, average merging delay, average delay before merging, and capacity) for entering vehicles under the influence of platoon dispersion were

developed. The best location of the entrance point, the distance for recovering the shape of the headway distribution after the entrance of sidestreet vehicles, and the optimal division of the input sources were determined by use of the models.

Simulation models were developed, and the validity of the analytical models were examined by using the simulation results.



PLATOON DISPERSION DYNAMICS
ON
ARTERIAL STREETS WITH ENTERING VEHICLES

By

Kin K. Lai

A DISSERTATION

Submitted to
Michigan State University
in partial fulfillment of the requirements
for the degree of

DOCTOR OF PHILOSOPHY

Department of Civil and Sanitary Engineering

1977

6107061

To My Mother and Father

ACKNOWLEDGMENTS

The author wishes to express his sincere appreciation to his major professor, Dr. William Taylor, for his valued guidance, assistance, and encouragement during the period of research and graduate study. As their friendship and his respect for Dr. Taylor have been satisfactorily developed, he sincerely cherishes as part of his accomplishment in this school.

He also wishes to thank Dr. John Kreer, Dr. Francis McKelvey, and Dr. Connie Shapiro, who, too, served on his guidance committee, for their helpful suggestions and interest in the research project.

Finally, the author especially wishes to express his deepest and heartfelt thanks to his wife, Alice, for her continual encouragement and understanding throughout the years of his graduate study.

TABLE OF CONTENTS

	Page
List of Tables	iv
List of Figures.	vii
List of Appendices	xi
 CHAPTER ONE	
INTRODUCTION	1
1.1 Background	1
1.2 Definition of the problem	2
1.3 The basic approach	2
 CHAPTER TWO	
REVIEW OF LITERATURE	6
 CHAPTER THREE	
THE DISTRIBUTION OF VEHICULAR HEADWAYS WITHIN PLATOONS	15
3.1 Introduction	15
3.2 The proposed distribution	15
3.3 Comparison with observed data	24
3.4 Goodness of fit test	26
3.5 Significance of results	28
 CHAPTER FOUR	
FIELD STUDIES PROCEDURES	30
4.1 Introduction	30
4.2 Determination of the input variables of the model	30
4.3 Selection of study sites	33

	Page
4.4 Sample size requirement	35
4.5 Field data collection	37
4.6 Results of field studies	37
CHAPTER FIVE	
MATHEMATICAL MODELING OF PLATOON DISPERSION	39
5.1 Introduction	39
5.2 Data analysis	39
5.3 Development of the mathematical models	43
5.4 Analysis of the mean headway for the passing platoon with entering vehicles	50
CHAPTER SIX	
SOME ANALYTIC CONSIDERATIONS OF QUEUEING	56
6.1 Introduction	56
6.2 Queueing consideration at the merging position	58
6.3 Queueing consideration before merging	67
6.4 Capacity and the best location of the minor stream	70
6.5 The required distance for recovering the shape of the headway distribution	75
6.6 Splitting flow to reduce delay of the entering vehicles	76
CHAPTER SEVEN	
SIMULATION ANALYSIS OF THE PROBLEM	82
7.1 Introduction	82
7.2 Development of the phase one model	83
7.3 Development of the phase two model	89

7.4 Development of the phase three model	92
7.5 Bvaluation of the results	97
CHAPTER EIGHT	
SUMMARY AND CONCLUSIONS	102
8.1 Summary of accomplishments	102
8.2 Applicability of models	106
APPENDICES	107
REFERENCES	139



LIST OF FIGURES

Figure	Page
1.1 Procedural flow chart	5
3.1 The negative exponential probability density function	17
3.2 The shifted exponential probability density function	18
3.3 The composite exponential cumulative distribution function	19
3.4 The normal probability density function	20
3.5 The lognormal probability density function	21
3.6 The gamma probability density function	23
3.7 The Weibull probability density function	24
3.8 Mean headway at different locations in the preliminary study	26
3.9 Standard deviation of headway at different locations in the preliminary study	26
5.1 Mean headway at different locations of platoon leaving from a signal	40
5.2 Mean headway at different locations of moving platoon with entering vehicles	40
5.3 Mean headway at different locations of platoon approach a signal	41
5.4 Mean headway at different locations of platoon leaving from a signal with the combination of light and medium flow	45
5.5 Mean headway at different locations of platoon approach a signal with the combination of light and medium flow.	46

Figure	Page
6.1 Translation of INTC	77
7.1 Physical characteristics of phase one model	84
7.2 Flow diagram for phase one model	86
7.3 Physical characteristics of phase two model	89
7.4 Flow diagram of phase two model	92
7.5 Flow diagram of phase three model	95

LIST OF TABLES

Table	Page
3.1 Degree of freedom for different distributions	28
3.2 Results of the goodness of fit test	29
4.1 Characteristics of the study sites	34
4.2 Standard deviation of headway at different locations in preliminary study	36
4.3 Sample size requirement at different locations	36
5.1 Results of the multiple comparisons of means for case 1	44
5.2 Results of the multiple comparisons of means for case 2	45
5.3 Equation results for $m = 2$	51
5.4 Equation results for $m = 3$	51
6.1 Percentage of the passing time at different locations	58
6.2 Calculate μ_t' for different T	65
6.3 Calculate $\sigma_t'^2$ for different T	65
6.4 Average merging delay $E(Z)$	66
6.5 Variance of merging delay $\text{Var}(Z)$	67
6.6 Calculate the expected queue size N	71
6.7 Calculate $E(W) = N/\lambda$	72
6.8 Calculate capacity for different T	74
6.9 Calculate $\delta \theta$ for different θ and λ	80
6.10 Calculate $\delta(1/3, 1/3, 1/3)$ for different	81
7.1 Simulation results of phase one model	85
7.2 Analytical results of phase one model	87



Table	Page
7.3 Greenshield's starting delay	90
7.4 Simulation results of phase two model	94
7.5 Simulation results of capacity	95
7.6 Simulation results of phase three model	97
7.7 Analytical results of phase two model	99
7.8 Analytical results of capacity	100
7.9 Analytical results of phase three model	101
7.10 U-statistic for the comparison of the analytical and the simulation results	101a

LIST OF APPENDICES

Appendix	Page
<u>Appendix I</u>	
Table I-1. The frequency of the headway sample within platoon leaving from a signal.	107
Table I-2. The frequency of the headway sample within platoons with entering vehicles.	108
Table I-3. The frequency of the headway sample within platoons approaching a signal.	109
Table I-4. Mean and standard deviation of headway within platoon for all cases.	110
<u>Appendix II</u>	
Table II-1. Incomplete gamma function $F = \int_0^{\infty} f(t)dt$.	111
Table II-2. Polynomial equations of $\int_0^{\infty} f(x) = a_0 + a_1t + a_2t^2 + a_3t^3 + a_4t^4$	112
Fig II-1. Plotting of $\int_0^{\infty} f(x)dx$	113
Table II-3. Formulation of $f_0(t) = \int_0^{\infty} f(x)dx / \int_0^{\infty} tf(t)dt$	114
Table II-4. Integrals of the forward recurrence time function F.	115
Table II-5. Calculate $M(t) = \int_0^T tf(t)dt$	116
Table II-6. Calculate $M_0(t) = \int_0^T tf_0(t)dt$	117
Table II-7. Calculate $N(t) = \int_0^T t^2 f(t)dt$	118
Table II-8. Calculate $N_0(t) = \int_0^T t^2 f_0(t)dt$	119



Appendix III

(A) Proof of μ_t^η	120
(B) Proof of EQ 6-11.	123
(C) Proof of EQ 6-15.	

Appendix IV

(A) Simulation program for Phase One model	125
(B) Simulation program for Phase Two model	127
(C) Simulation program for Phase Three model	132

CHAPTER ONE

INTRODUCTION

Background:

When the smooth flow of traffic is interrupted by some kind of traffic control device, such as signals, the downstream flow of traffic will usually take the form of a "platoon." As each platoon moves down the street it disperses, and its time length increases as the time-headways between successive vehicles increase. As a result, the whole platoon length increases when the platoon moves down from the signal. If there are entering sources downstream of the signal, the entering vehicles have two possibilities for entering traffic: while the platoon is passing the entrance point or after it has passed. In the first case, the entrance point would be expected to be a considerable distance from the signal so that there would be a large gap within the platoon and entering vehicles. In the second case, the entrance would be expected to be closer to the signal, platoon length would be shorter, and it would pass through earlier. Information about the behavior of vehicular platoons and how it affects entering vehicles is important to reduce delay time for entering vehicles.

The purpose of this dissertation is to investigate the dynamics of platoon dispersion. Specifically, to find a model for the dispersion of platoons and to use that model to investigate the effect on entering vehicles.

Definition of the problem:

The four objectives of this dissertation are as follows:

- (1) Develop a stochastic model for describing the dispersion of platoons approaching or leaving a signalized intersection, with or without entering vehicles.
- (2) Determine the delay time of entering vehicles before and upon merging.
- (3) Investigate the relationship between platoon dispersion and the capacity to accommodate vehicles entering downstream from the issuing intersection.
- (4) Determine an optimal system strategy for a traffic stream with variable vehicle entry points.

The basic approach:

Before discussing the approach of this dissertation, some definitions must be reviewed. Headway is the time between successive vehicles; theoretically it may range from zero seconds to infinity. In this dissertation, vehicular time headway was selected as the parameter for the platoon dispersion investigation. This parameter was chosen because it describes the interaction between vehicles in the car-following process, and it also describes the interaction in the merging process. Platoons include those vehicles queued at the intersection and those which join the queue after the light turns green, but within two seconds after the last queued vehicles arrived at the stop line. Since the behavior of the entering vehicles is mainly affected by the headways of the mainstream vehicles, vehicular headways will be used as a basis for the investigation of platoon

dispersion.

The research effort is divided into six principal phases. Phase 1 consists of a review of the literature describing platoon behavior. This review illustrates the differences between approach used here and those used in previous studies and also suggests avenues of future research.

Phase 2 is the development of a stochastic model of vehicle time headways within a platoon released from a signalized intersection. Using the results of Nemeth and Vecellio's report (23), the principal variables affecting platoon movement through linear signal systems are identified as signal spacing, signal offset, and platoon size. In order to study the variation of headway as the vehicles move down the signalized intersection, the next signal's coordination with the prior one is also considered. The next step is to study the relationship between headway and the distance from the signal, given various platoon sizes.

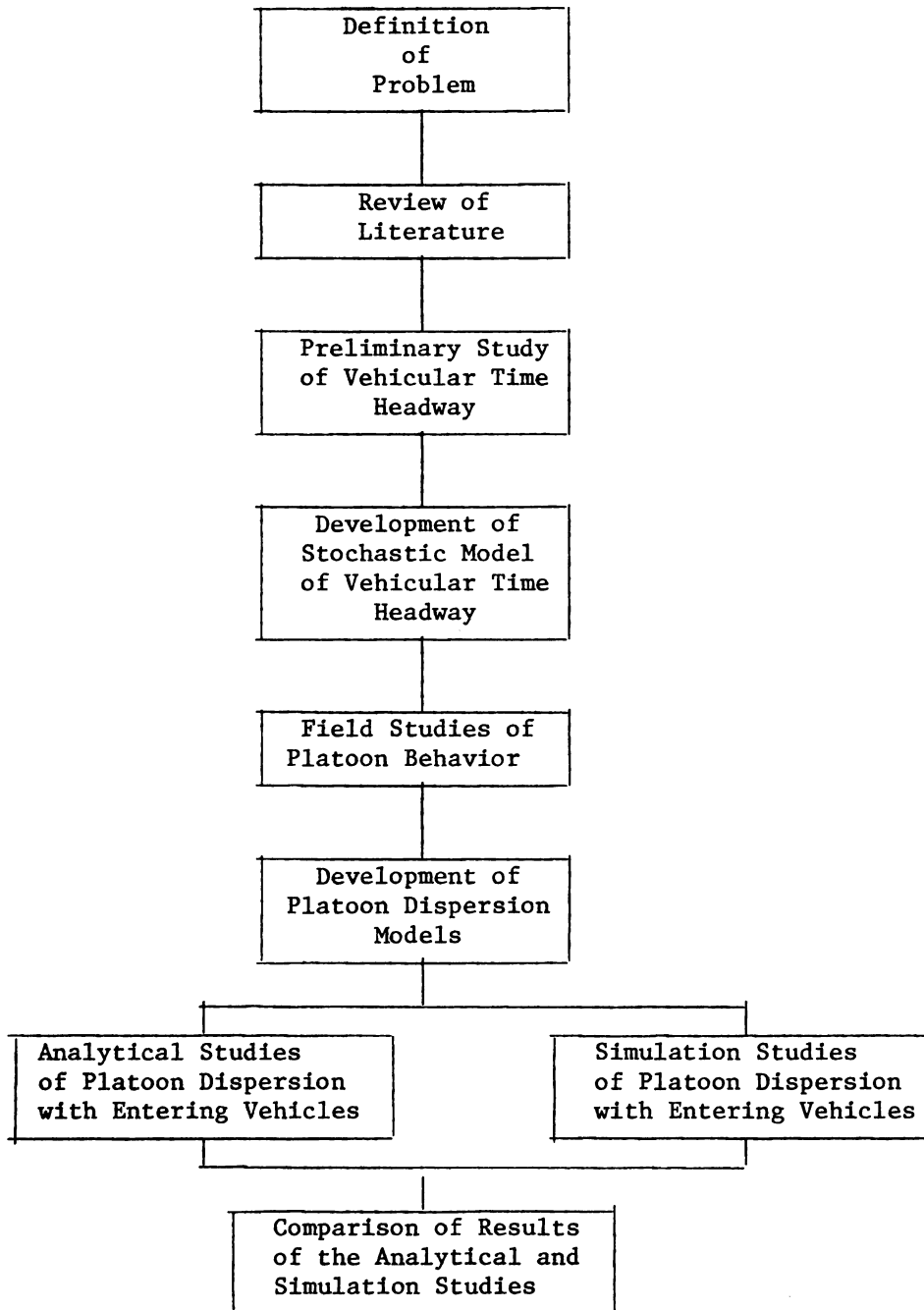
In Phase 3, data are collected under various conditions, that is, for different distances from the signal, different platoon sizes, and the presence or absence of entering vehicles.

In Phase 4, the data are analyzed and a regression model is developed to describe the relationship between the parameters of the headway model and the distance from the signal and platoon size.

Phase 5 studies platoon dispersion in connection with vehicles entering downstream from the signal. The effects of vehicles merging into the mainstream from any side street will be analyzed. The delay time of entering vehicles on the merging position and before merging

is determined, as are the optimal locations of the merging points. The relationships derived from Phase 4 are tested for the platoon after some vehicles merge into it. The distance required for the headway distribution to recover its original shape will be determined, and the possibility of splitting the entering flow into two or more entry points will also be investigated.

A computer simulation model is developed in Phase 6 to validate the analytical models. The analytical and simulation solutions of the same situation are compared. A flow chart illustrating the analytical procedures of the dissertation is shown in Figure 1-1.

Figure 1-1. Procedural Flow Chart



CHAPTER TWO

REVIEW OF THE LITERATURE

Numerous studies have been conducted on the behavior of traffic leaving a signalized intersection. Experimental work on the dispersion of traffic platoons has been reported by Lewis (19) (1958) and Graham and Chenu (10) (1962). Pacey (26) (1956) and Robertson (27) (1969) have proposed theoretical models describing this process, and Nemeth and Vecellio (23) (1973) have developed a simulation model for the dispersion of platoons. Grace and Potts (9) (1964) and Herman, Potts, and Rothery (15) (1964) have attempted to combine the theoretical and experimental aspects of platoon behavior. A review of these studies follows.

One of the early experimental studies was conducted by Lewis (19) in 1958. Platoon movement of traffic from an isolated signalized intersection was examined. The test site was a four-lane highway in Richmond, California. Observations of space-time data were made at five different locations downstream from a signalized intersection at distances up to 0.65 miles. Arrival time frequency distributions of the platoon at each of these five points were obtained. Analysis of this frequency distribution showed that three characteristics of platoon movement were linearly related to the distance downstream from the traffic signal. Those characteristics were (1) the maximum ordinates of the equivalent normal distribution of the arrival times of



the Nth vehicle, (2) the mean arrival time of the Nth vehicle, and (3) the time for the Pth percentile of vehicles in a platoon to pass a point. Lewis concluded that a progression diagram for distances up to the study limits could be plotted for all vehicles, which would allow greater success in timing the downstream signals than would occur using random selection.

Another experimental study was performed by Graham and Chenu (10) in 1962. Vehicles arrival time data also were collected at five locations downstream from a signalized intersection, at a distance of 1/35 mile, 1/4 mile, 1/2 mile, 3/4 mile, and one mile. The arrival time of each vehicle at each location was recorded. A graphic illustration of the dispersion of the platoon at various distances from the signal was provided by histograms plotting the frequency distribution of vehicle arrivals within each 5 percent increment of time - length of the platoon. The author concluded that at distances as great as one mile downstream from the signal, the vehicles still were "bunched," since 77 percent of the vehicles remained in the platoon at that location.

Pacey, (26) in an unpublished 1956 report, proposed a kinematic model to describe the dispersion of traffic platoons. He assumed that vehicle speeds in a platoon are normally distributed, so that the spread of the platoon can be accounted for and measured by the dispersion of vehicle speeds. Another assumption was that the speed of any individual vehicle remains constant as it moves down the road, that is, no interaction is assumed between vehicles. Based on these assumptions, Pacey formulated a distribution of travel time applicable



to traffic departing from a saturated signalized intersection. The derived travel time distribution was shown to be a function of the normality of vehicle speeds, the mean and variance of the speed distribution, and the distance over which travel times are distributed. The travel time distribution is as follows:

$$g(\tau) = \frac{1}{\tau s \sqrt{2\pi}} \exp. \left\{ -(1/\tau - \bar{v}/\alpha)^2 / 2s^2 \right\} \quad (2.1)$$

where τ = travel time (in seconds);

v = speed (in feet/sec.);

\bar{v} = mean of the speed distribution;

$s = \sigma/\alpha$;

σ = standard deviation of the speed distribution; and

α = distance over which the travel times are distributed
(in feet).

Pacey's model was compared with observations made at two sites on dual carriageways of the times after the green signal at which vehicles passed two points, one near the signals and one 600 yards beyond them. Especially for moderate traffic volumes, Pacey's model proved a good fit to the actual data.

A detailed theoretical study of Pacey's model was made by Grace and Potts (19) in 1964. They analyzed in detail the dispersion of a platoon as it moves down a street and emphasized the importance of allowing for this phenomenon to obtain efficient coordination of two traffic lights. A traffic density function was derived by the use of Pacey's model:

$$K(x, \tau) = \frac{1}{\sqrt{\pi}} \int_{-\infty}^{\infty} g \left\{ m(x) - 2.4z \sqrt{\frac{1}{\tau}} \right\} \exp(-z^2) dz \quad (2-2)$$

This is a well-known form of the solution of the one-dimensional diffusion equation,

$$\frac{\partial k}{\partial \tau} = \alpha^2 \left(\frac{\partial^2 k}{\partial \chi^2} \right) \quad (2.3)$$

where $g(x) = k(x,0)$ is a known function;

$k(x,t)$ = the traffic density, equal to the number of vehicles per unit road length at a given point x and at time t ;

χ = the distance down a highway;

m = average vehicle speed;

χ/m = offset time (in seconds);

$x = \chi/m - t$ preset time equal to the time added to the beginning of the green phase of the second signal to allow for the spreading of a platoon leaving a prior signal;

$\tau = \frac{1}{2} t^2$; and

α = diffusion constant.

If vehicle speeds are normally distributed with mean μ and variance σ^2 , then the diffusion constant is defined as μ/σ .

Grace and Potts applied their theoretical model to the design of progressive signal systems. For certain assumed initial conditions regarding the traffic density function, the diffusion equation was used to provide analytical solutions to the coordination of two successive signalized intersections, allowing for the dispersion of the platoon.

In 1964, Herman, Potts, and Rothery (15) conducted an experiment designed to test the kinematic model of traffic platoon behavior, in

particular, to test the detailed theoretical results obtained by Grace and Potts. Speed and arrival time of vehicles leaving an isolated intersection were measured at two locations, 757 feet and 2142 feet downstream from the signal. The results confirmed that the kinematic model accurately described the dispersion of platoons in medium volume traffic without interference. This was especially true for the lead vehicle in the platoon, while the behavior of the last vehicle varied from one platoon to another.

In 1969, Robertson (27) of Road Research Laboratory, England, developed a method to determine optimum fixed time traffic signal settings for a network of signalized intersections. In his "TRANSYT" model, a method was developed for predicting the dispersal of an average platoon of traffic. Observations were made at four locations in west London, where traffic leaving a signal travelled at least 1,000 feet before reaching another signal or major junction. Each location had four observation sites, one just beyond the traffic signal and the others at approximately 300, 600, and 1,000 feet downstream. The time of passage of every vehicle was recorded at each point. By further analysis of these observations, a recurrence relationship was established to predict flow at each site downstream from a traffic signal given the input flow, previously predicted flow, and a smoothing factor. The recurrence equation is as follows:

$$q'(i + t) = F.q(1) + (1-F). q'(i+t-1), \quad (2.4)$$

where $q(i)$ = the flow in the i th time interval of the initial platoon (in veh/hr.);

$q'(j)$ = the flow in the j th time interval of the predicted platoon (in veh/hr.);

t = 0.8 times the average journey time over the distance for which the platoon dispersal is being calculated;
and

F = a smoothing factor.

The smoothing factor, F , required for the best fit between the actual and calculated platoon shapes was found to be related to the journey time by the expression

$$F = \frac{1}{1 + 0.5F} \quad (2.5)$$

The author points out that it would be reasonable to expect that the smoothing factor required should also be a function of "site factors" such as road width, gradient, parking, and so forth, but these aspects have not yet been investigated.

The dispersion of a platoon of vehicles released from a signalized intersection has also been studied by Nemeth and Vecellio (1973), who developed a simulation model. Their purpose was to incorporate those variables affecting platoon movement into a model and to simulate the behavior of a group of vehicles as it passes through a series of signalized intersections.

Nine parameters were selected for inclusion in the variation analysis of platoon behavior:

- (1) traffic density;
- (2) traffic volume;
- (3) mean velocity;

- (4) standard deviation of velocity;
- (5) coefficient of variation of velocity;
- (6) mean spacing;
- (7) standard deviation of spacing;
- (8) coefficient of variation of spacing; and
- (9) mean time headway.

The time and distance variation of the nine parameters for the observed platoons were plotted. From this variation analysis, distance patterns were interpreted by the authors in relation to the spacing between signalized intersections, and time patterns were interpreted with respect to the values of the signal offsets. The authors concluded that these two variable, signal spacing and signal offset, affect platoon behavior.

Two other variables were also investigated to determine their influence on platoon behavior: platoon size and lane of travel. The F - test was used to test the mean velocity difference in different lanes, and velocity - time patterns for platoons of various sizes were plotted. The authors concluded that lane of travel has no significant effect on platoon behavior, but platoon size does.

Thus, the principal variables affecting platoon movement through linear signal systems were identified by Nemeth and Vecellio as signal spacing, signal offset, and platoon size. In their simulation model, the processing of traffic between intersections was achieved by relating traffic dispersion to site - related travel time parameters. The variables mentioned above were incorporated into a travel time distribution function. Using the data obtained at the study sites,

regression equations were derived for the travel time distribution parameters.

All the platoon studies reviewed thus far deal with platoons released from an isolated signalized intersection and traveling with no interference. In the experimental studies, such as that by Lewis and Chenu, no attempt was made to develop a model to describe the dispersion process.

The kinematic model developed by Pacey, investigated by Grace and Potts and validated through experiments carried out by Herman and others, is useful for more general applications. By collecting speed distribution data at actual locations, a value of the diffusion constant α can be computed and applied to the prediction of the spreading of platoons. Speed data obtained at different traffic volumes gave different α for low, medium, and high traffic flow. Since the kinematic model assumes that all vehicles travel at constant speeds normally distributed about a mean speed, many passing maneuvers and lane changes obviously have to take place in the platoon. As the volume increases, these maneuvers become more and more restricted, causing actual platoon behavior to deviate from the theory. Besides, the assumption of constant speed is not realistic near traffic signals. Herman stated that the best fit of actual data for the model is the front of the platoon at medium traffic volume.

The purpose of Nemeth's and Vecellio's simulation model was to generate mean delay and queue statistics at signalized intersections rather than attempt to predict the precise behavior of traffic between intersections.

The model developed by Robertson was a deterministic one, which only predicts average platoon behavior. Thus, flexibility was restricted.

From the above literature, it was found that several factors influence platoon dispersion, among them, distance from the signal, signal offset, and platoon size. As the platoon moves down from the signal, it will disperse, in other words, the gaps between vehicles will increase as the position of vehicles from the signal increases.

The approach taken in this dissertation differs in three aspects from the previous studies of platoon behavior. First, a stochastic model is developed to describe the dispersion of a platoon departing from and approaching a signalized intersection. Second, the case of allowing vehicles to enter the platoon downstream of the signal will be investigated. Third, the effect of platoon dispersion on the entering vehicles will be analyzed.

CHAPTER THREE

THE DISTRIBUTION OF VEHICULAR HEADWAYS WITHIN PLATOONS

This chapter seeks to develop an accurate and reliable model for describing the distribution of vehicular headways within platoons released from a signalized intersection. The distribution of headways can be found by observing the times of arrival of successive vehicles in a given lane at a point along the lane. The headway of the i th vehicle is defined as:

$$H_i = t_{i-1} - t_i, \quad (3.1)$$

where t_{i-1} is the arrival time of the vehicle ahead, and t_i is the arrival time of the i th vehicle. If many vehicles are observed, the distribution of H_i can be obtained, and one can investigate whether this variable can be described by some theoretical distribution function.

Vehicle headways are usually measured in seconds and theoretically may range from zero to infinity. A zero headway means a collision on the roadway, and an infinite headway represents an empty roadway. Thus, the theoretical distribution of headways must be continuous and positive. There are several distributions with these characteristics, and these will be discussed and compared below.

The proposed distribution:

It was first suggested by Adams (1) that the vehicles in light traffic passing a point at equal time intervals follow a Poisson distribution. If this is the case, the distribution of headways can be

shown to be described by the negative exponential distribution. The Poisson distribution gives the probability, or proportion of a number of equal time intervals, during which any number of vehicles, n , will arrive at a point:

$$P(x=n) = \frac{e^{-qt} (qt)^n}{n!}, \quad n=0,1,2,3,\dots \quad (3.2)$$

$$= 0 \quad \text{otherwise,}$$

where qt is the mean number of vehicles arriving during the time intervals of t seconds.

We are interested only in the probability of a headway greater than t seconds. This would mean that no arrivals occurred in t seconds:

$$P(H > t) = P(x=0). \quad (3.3)$$

Here, H is the headway. Thus,

$$P(H \geq t) = 1 - P(x=0)$$

$$= 1 - e^{-qt}. \quad (3.4)$$

This is the cumulative distribution function of the vehicular headway. Therefore, the probability density function of headway is:

$$f(t) = \frac{d}{dt} P(H \leq t)$$

$$= \frac{d}{dt} (1 - e^{-qt})$$

$$= qe^{-qt} \quad 0 \leq t < \infty$$

$$= 0 \quad \text{otherwise.} \quad (3.5)$$

If H is exponentially distributed, then $E(h) = 1/q$, and $\text{Var}(H) = 1/q^2$. This distribution has the interesting characteristic that the mean and the standard deviation are both the same. The density function is shown graphically in Figure 3-1.

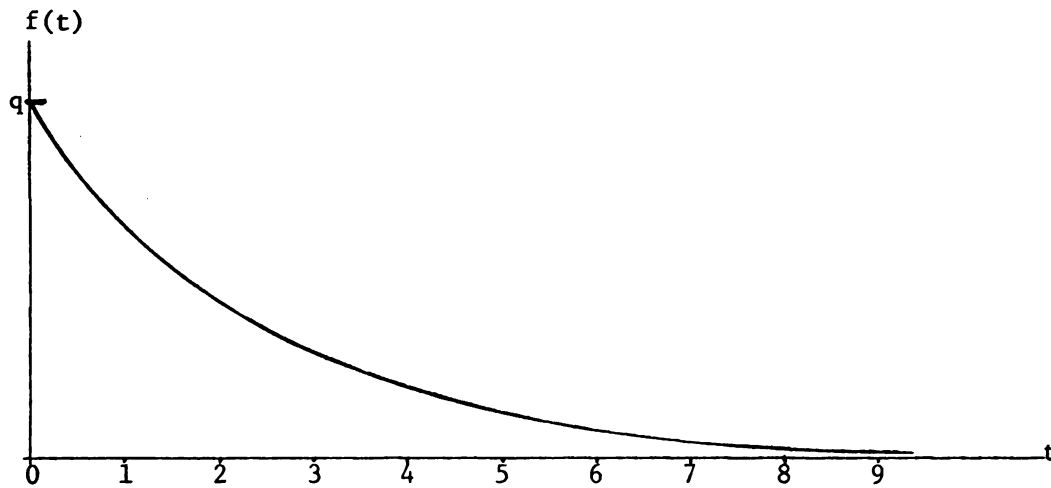
The negative exponential variates have a property, that is, no memory. If H is the headway and is negatively exponentially distributed,

it can be shown that

$$P(H > t + \mu | H > \mu) = P(H > t), \quad t, \mu > 0. \quad (3.6)$$

This equality shows the property of no memory. It implies that a knowledge of any headway gives no information at all about the length of the next headway. It is completely random.

Figure 3-1. The Negative Exponential Probability Density Function.



In Figure 3-1, it may be noticed that as the headways approach zero, the probability becomes larger. Applying this to our situation would assign higher probabilities to very low headways, which is not satisfactory. In the real situation, we know that the probability of a zero headway is, of necessity, zero.

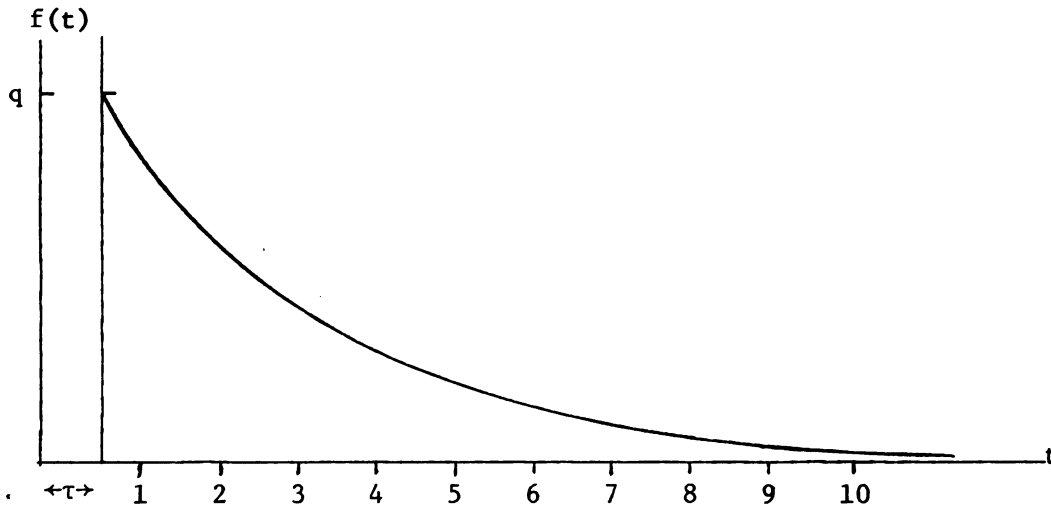
To take account of the fact that the negative exponential distribution exhibits too high a probability in the zone near zero headway, Newell (25) suggested that the headway distribution might conform to the negative exponential distribution if shifted to the right a distance of τ to allow for the existence of a certain fixed minimum

headway. Used by many researchers, the shifted negative exponential distribution is of the form

$$\begin{aligned} f(t) &= qe^{-q(t-\tau)} & t > \tau \\ &= 0, & \text{otherwise.} \end{aligned} \quad (3.7)$$

A diagram of the distribution is shown in Figure 3-2.

Figure 3-2. The Shifted Exponential Probability Density Function.



Another approach is to consider a composite distribution(11) of headways in which some vehicles are free-flowing and others are restrained in platoons behind another vehicles. If the proportion which is free-flowing is $(1-p)$, then the composite cumulative distribution function is the following:

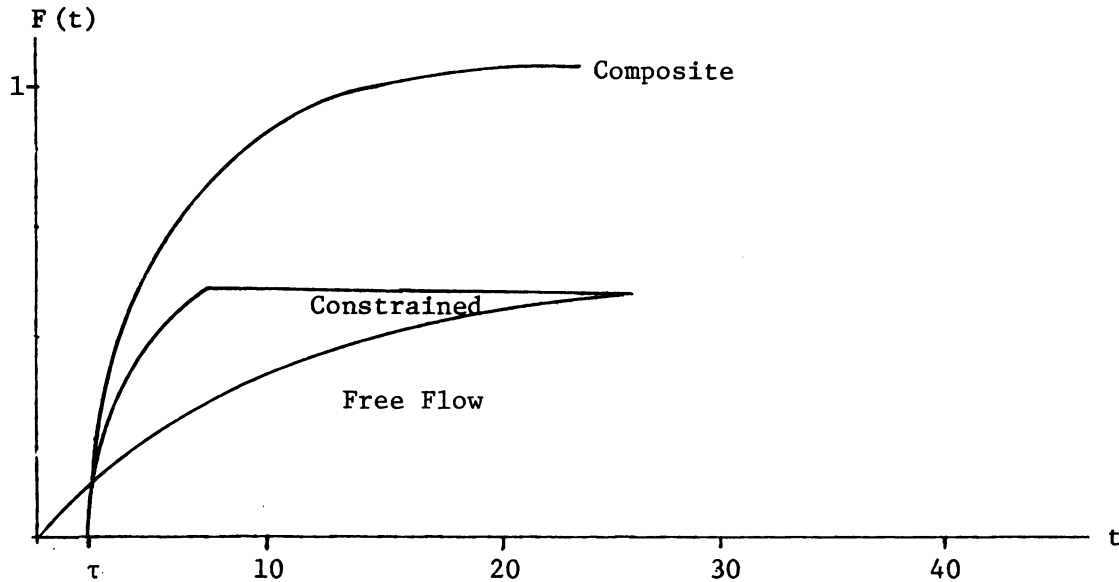
$$P(H > t) = (1-p)e^{-t/\bar{h}_1} + p e^{-(t-a)/(\bar{h}_2-a)} \quad (3.8)$$

where \bar{h}_1 = mean headway of free-flowing vehicles;

\bar{h}_2 = mean headway of constrained vehicles; and

a = minimum headway of constrained vehicles.

The diagram for the cumulative distribution (with $p = 0.5$) is shown in Figure 3-3. This composite distribution has also been used

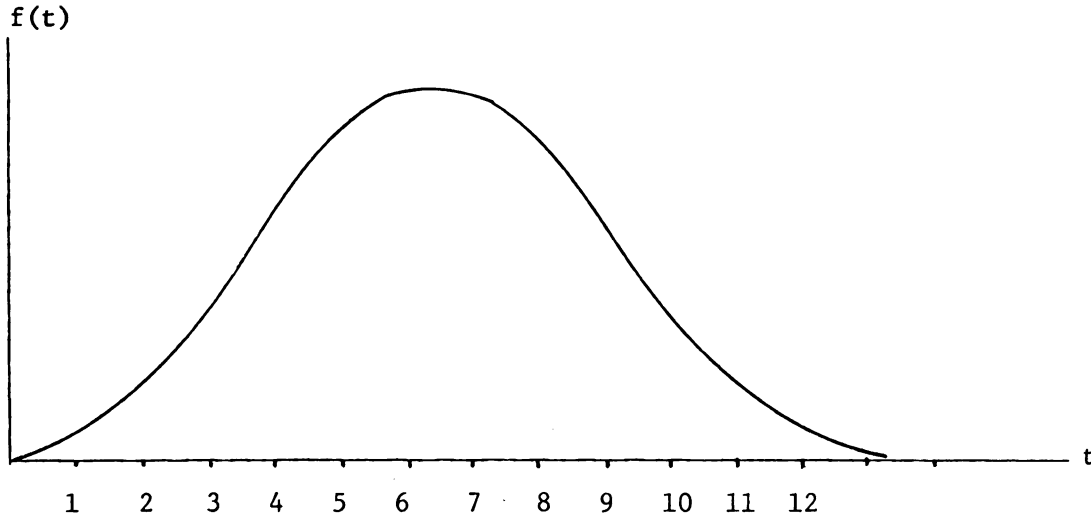
Figure 3-3. The Composite Exponential Cumulative Distribution Function.

in recent studies of traffic flow on two-lane urban streets (17).

A distribution which is most commonly used in phenomenal analysis is the normal distribution. It has several characteristics which recommends it to traffic engineers: (1) It is symmetrical, (2) it assigns a finite probability to every finite deviation, and (3) the mode and median are equal to mean. The probability density function is given by

$$f(t) = \frac{1}{\sigma\sqrt{2\pi}} \exp\{-(t-\mu)^2/2\sigma^2\}, \quad (3.9) \\ -\infty \leq t \leq \infty.$$

The distribution is completely specified by the location parameter μ and the scale parameter σ . A typical example of a normal probability density function is given in Figure 3-4.

Figure 3-4. The Normal Probability Density Function.

A distribution of particular interest which has been found to fit headway data quite well is the Log-normal distribution. Consider now the family of p.d.f's:

$$f(t) = \frac{1}{t\sigma\sqrt{2\pi}} \exp\left\{-\frac{(\ln Pt)^2}{2\sigma^2}\right\} \quad t > 0 \quad (3.10)$$

$$= 0, \quad \text{otherwise.}$$

The corresponding cumulative distribution function is

$$F(t) = \frac{1}{\sigma\sqrt{2\pi}} \int_0^t \exp\left\{-\frac{(\ln Pv)^2}{2\sigma^2}\right\} \frac{dv}{v}, \quad (3.11)$$

which, on writing $\{\ln(Pv)\}/\sqrt{\sigma} = \mu$,

becomes

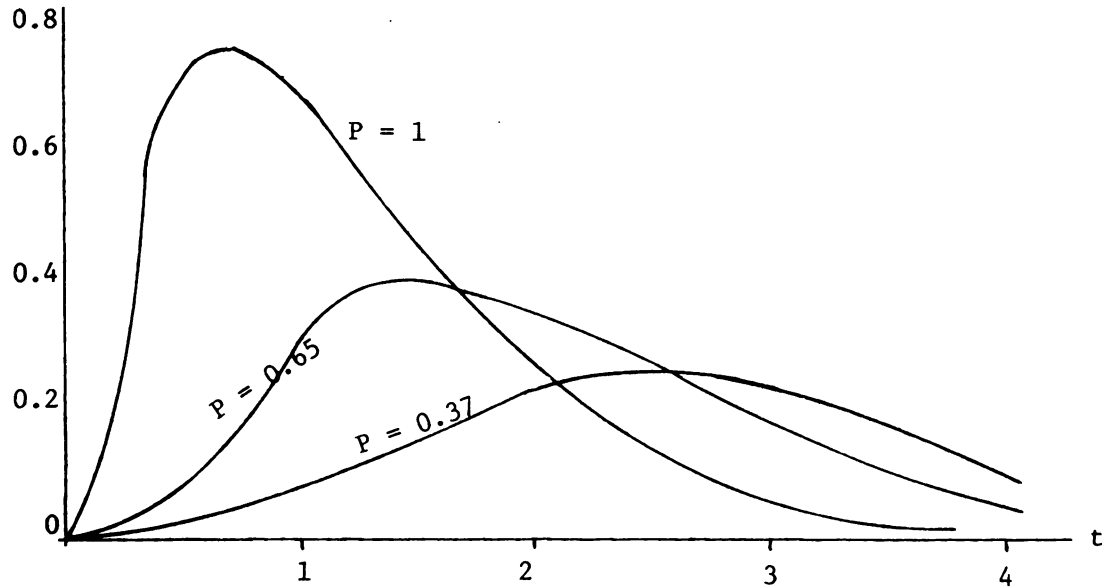
$$G\left(\frac{\ln t + \ln P}{\sigma}\right), \quad (3.12)$$

where

$$G(t) = \frac{1}{\sqrt{2\pi}} \int_{-\infty}^t \exp\left\{-\frac{\mu^2}{2}\right\} d\mu \quad (3.13)$$

is the standardized normal probability integral. The results show that the random variable $\ln X$ is normally distributed, hence the name log-normal distribution given to EQ (3.11). The mean of the distribution is $P^{-1} \exp(\frac{1}{2} \sigma^2)$, and the variance is $P^{-2} \exp(\sigma^2) (\exp(\sigma^2) - 1)$. For small values of σ^2 the distribution is nearly normal. For large values of σ^2 , the distribution has large positive skewness. A typical example of log-normal probability density function is shown in Figure 3-5.

Figure 3-5. The Log-normal Probability Density Function.



Tolle (26) proposed a more generalized version of a log-normal distribution by shifting the frequency curve by τ . The addition of a new parameter requires no new theory since in this case τ will be predetermined, and the probability density function is

$$f(t) = \frac{1}{(t-\tau)\sigma\sqrt{2\pi}} \exp \left\{ -\frac{[\ln P(t-\tau)]^2}{2\sigma^2} \right\} \quad t > \tau > 0 \quad (3.14)$$

$$= 0, \quad \text{otherwise.}$$

A distribution which has the correct general form of the negative exponential distribution but does not have the disadvantage of a sharp cutoff is the Erlang distribution:

$$f(t) = \frac{1}{(a-1)!b^a} t^{a-1} \exp(-t/b) \quad t \geq 0 \quad (3.15)$$

$$= 0, \quad \text{otherwise.}$$

where a is a positive integer. For $a = 1$, this is a negative exponential distribution. As a is increased, the density distribution becomes more peaked, indicating more regularity. As a approaches infinity, $f(t)$ becomes constant. That is, vehicles arrive at equal time intervals apart. Thus, a can be used as a measure of congestion.

A slightly more general distribution is obtained if a is permitted to be a non-integer to form the well-known Pearson type III distribution, or the gamma distribution. Its probability density function is

$$f(t) = \frac{1}{\Gamma(a)b^a} t^{a-1} \exp(-t/b) \quad t \geq 0 \quad (3.16)$$

$$= 0, \quad \text{otherwise,}$$

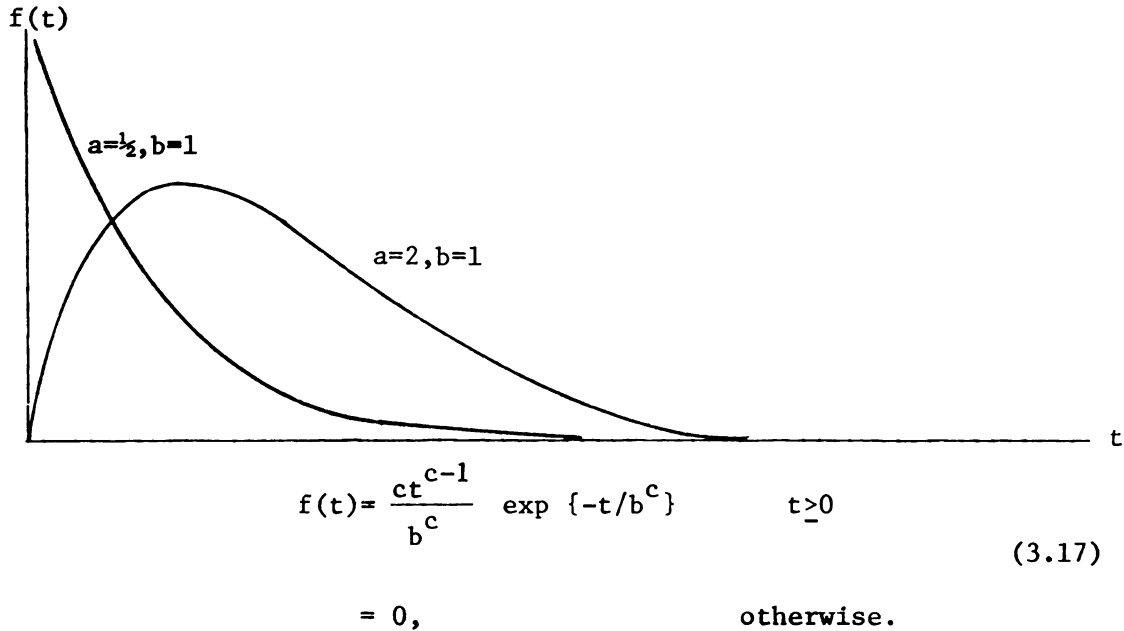
where $\Gamma(a)$ is called the gamma function and is defined by the formula

$$\Gamma(a) = \int_0^{\infty} z^{a-1} e^{-z} dz.$$

When $0 < a < 1$, the probability density function has an infinite ordinate at the origin: when $a > 1$, the p.d.f. is zero at the origin and has a single maximum at $b \cdot (a-1)$. A typical example of a gamma probability density function is shown in Figure 3-6. If a random variable, X , is described by a gamma distribution, then the mean is ab , and the variance is ab^2 .

The final distribution to be discussed is the Weibull distribution. This generates a family of curves as its parameters are given different values. When a random variable, X , has a Weibull distribution, its probability density function is:

Figure 3-6. The Gamma Probability Density Function.



The distribution depends on the two parameters b and c . The expected value and variance of the Weibull distribution are given by

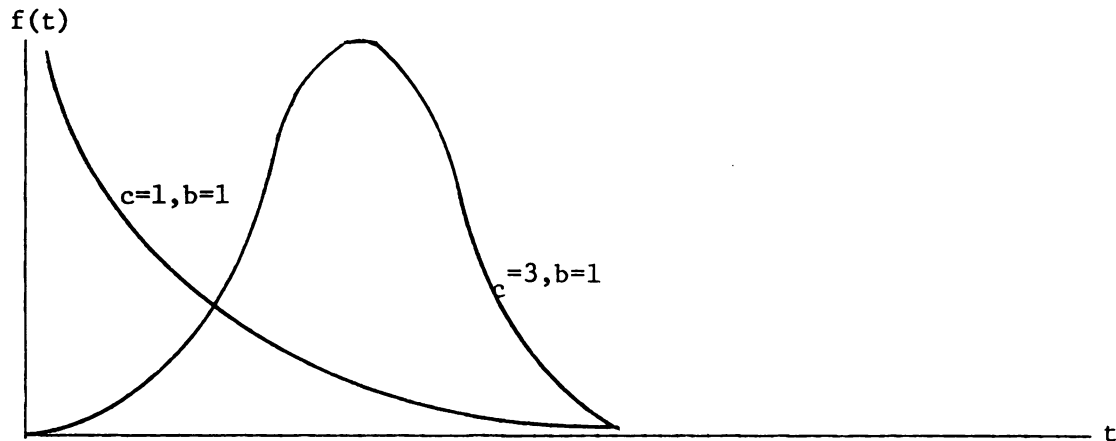
$$E(H) = b^{-1/c} \Gamma\left(\frac{1}{c} + 1\right),$$

$$\text{VAR}(H) = b^{-2/c} \{ \Gamma(2/c + 1) - (\Gamma(1/c + 1))^2 \} \quad (3.18)$$

A typical example of the probability density function of a Weibull distribution is shown in Figure 3-7.

The Weibull variate H with shape parameter $c=1$ is the exponential variate. It means that this distribution includes the case of random and nonrandom headway phenomena.

Figure 3-7. The Weibull Probability Density Function.



Comparison with observed data:

All the functions discussed previously have the characteristics of being the distribution of vehicular headways within platoons. This section describes the preliminary study of headway that was conducted by this author. In the study, field data were collected and compared with different theoretical distributions.

The results were to provide the variance and approximate changing pattern of headway along the road downstream from the signal, which information could be used to design the field study of a headway dispersion model. This information was necessary to determine the sample size with acceptable accuracy and the best location for the field study of the platoon dispersion model.

Seven of the eight distributions described above were compared with observed data:

- (1) negative exponential distribution;
- (2) shifted negative exponential distribution;
- (3) normal distribution;



- (4) shifted log-normal distribution;
- (5) gamma distribution;
- (6) Erlang distribution; and
- (7) Weibull distribution.

The composite negative exponential distribution was not chosen because in the case of platoon dispersion, the percentage of free-flow vehicles is almost zero.

Headway data were collected in the center lane of a three-lane arterial in East Lansing, Michigan. The total length of the block is 1,200 yards. These data were collected at four sites; 150, 300, 700, and 1,000 yards downstream from a signalized intersection. Observations were made in the morning from 8:00 a.m. to 11:00 a.m., and consisted of about 100 platoons with a total of 400 vehicles.

The site was selected because of the long distance between signals and because there were no interruptions from side streets. These factors are important in the formulation of a theoretical model of how a platoon is dispersed. The headway data were collected only from those "within platoon" in the center lane of the road. Here, "within platoon" includes all vehicles upstream of the traffic signal waiting for the signal to turn green and those vehicles which join the queue (within two seconds) prior to the last vehicle reaching the stop line. Turning vehicles and those merging from other lanes are excluded. One hundred data sets were collected at each of the four sites, and goodness of fit tests were performed.

The diffusion that took place throughout the section downstream from the intersection is shown in Figure 3-8, and the variance of the headways at different locations is shown in Figure 3-9.

Figure 3-8. Mean Headway at Different Locations in the Preliminary Study.

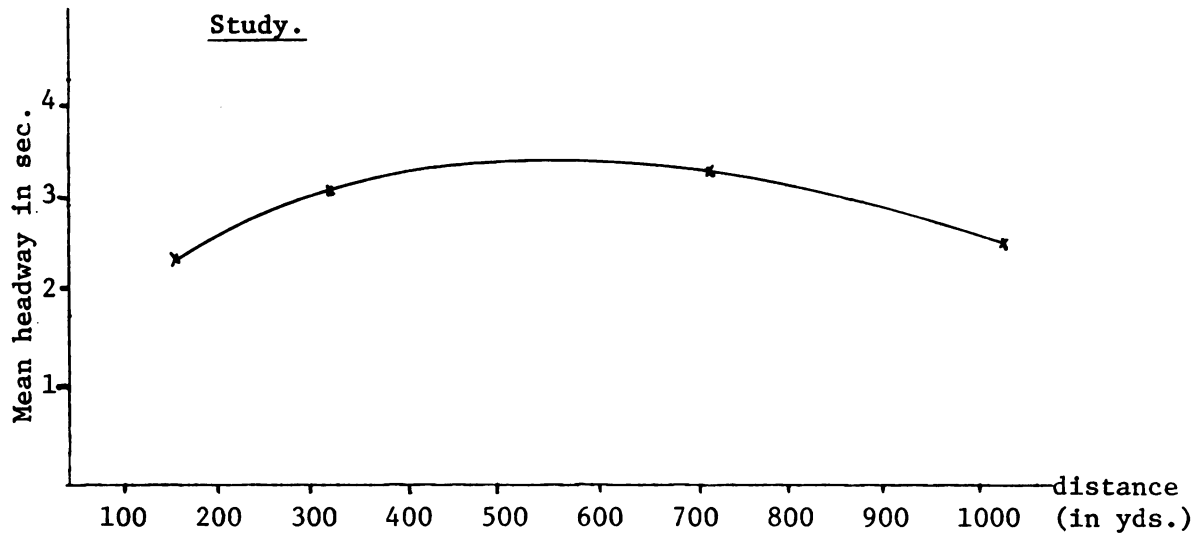
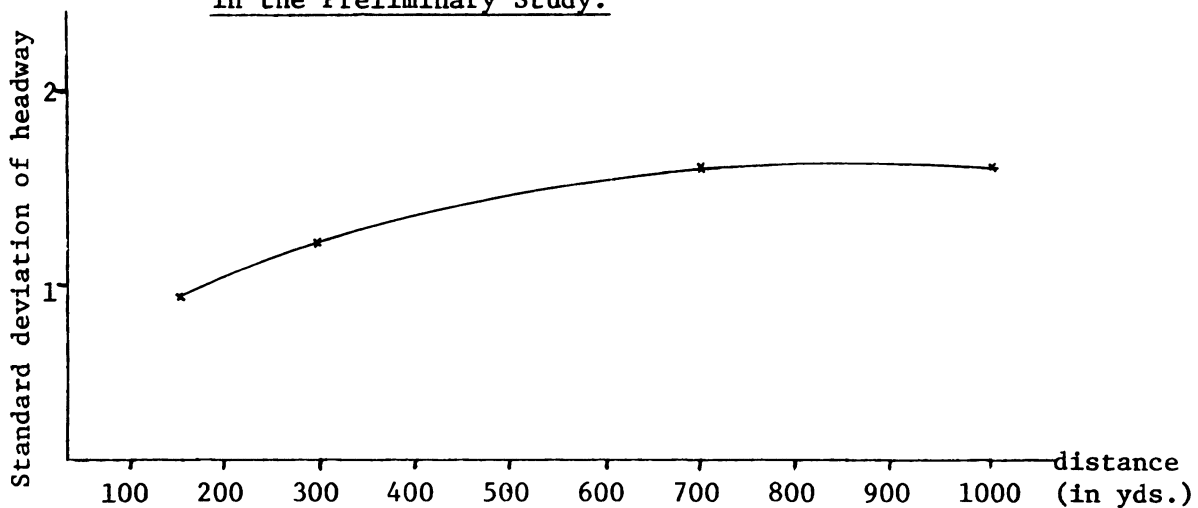


Figure 3-9. Standard Deviation of Headway at Different Locations in the Preliminary Study.



Goodness of fit test:

The degree of agreement between a theoretical probability distribution and the distribution of a set of sample observations constitutes a "goodness of fit" test. The assumption that our observations can be adequately described by a given theoretical probability distribution is



referred to as the null hypothesis. This test enables us to test this hypothesis for any probability distribution. "Goodness of fit" testing is accomplished by comparing the distribution of the observed data with the theoretical probability distribution specified in the null hypotheses.

The most common goodness of fit tests in engineering statistics are the Chi-square tests (5), and the Kolmogorov-Smirnov test (18). The former is very powerful for large samples on the order of $n \geq 100$. The latter is very powerful when each observation is treated as an individual cell, if grouping is unnecessary, and smaller samples can be effectively analyzed.

Since the sample size here was large, the Chi-square tests was applied, based on the test statistic

$$Q = \sum_{i=1}^n \frac{(O_i - E_i)^2}{E_i} \quad (3.19)$$

where n = number of cells;
 O_i = observed data points in cell i ; and
 E_i = expected data points in cell i .

When the null hypothesis is true, that is, E_i is the expected value of O_i , one would feel intuitively that experimental values of Q should not be too large. If the null hypothesis is true, the test statistic is a random variable asymptotically following a χ^2 distribution with $(n-p-1)$ degrees of freedom, where p is the number of unknown parameters. Using the table for χ^2 distribution, with $(n-p-1)$ degrees of freedom, find c so that

$$P(Q \geq c) = \alpha, \quad (3.20)$$

where α is the desired significance level of the test. The null hypothesis is rejected when the observed value of Q is at least as great as c .

In our Chi-square test, there are different degrees of freedom for different distributions, as shown in Table 3-1.

Table 3-1. Degree of Freedom for Different Distributions.

Distribution	Degree of Freedom
Exponential	$n - 2$
Shifted Exponential	$n - 2$
Normal	$n - 3$
Shifted Log-normal	$n - 3$
Erlang	$n - 3$
Gamma	$n - 3$
Weibull	$n - 3$

Significance of results:

The result of testing the hypothesis of fitting headways with the above proposed distributed by use of the Chi-square test is shown in Table 3-2.

Comparing the results of this testing, it can be seen that the gamma distribution is the best fit distribution for the observed platoon headways. It should be used as the basis for developing the platoon dispersion model. Due to Greenshield's constant starting delay, gamma distributed headway is true only starting close to the



signal, not at the signal

Table 3-2. Results of the Goodness of Fit Test.

Distribution	Location 1	Location 2	Location 3	Location 4
Exponential	165.8802	92.8429	117.6418	104.6973
Shifted Exponential	74.7796	52.3978	68.7166	47.0664
Normal	24.5386	5.6036	7.0281	10.9322
Shifted Log-normal	16.8066	15.1989	9.4884	10.3852
Erlang	12.0684	7.8025	7.2645	9.2501
Gamma	6.0743	3.6088	3.8878	3.5941
Weibull	13.7735	3.5490	4.5246	9.9915



CHAPTER FOUR

FIELD STUDIES PROCEDURES

Introduction:

The field studies of platoon dispersion are described and discussed in this chapter. The dispersion characteristics of platoons leaving a signalized intersection are separated into several sub-models for investigation. Specifically, three situations were investigated: (1) The behavior of a platoon leaving a signalized intersection; (2) the behavior of a moving platoon with entering vehicles from side streets downstream from the signal. (We assumed the location of the entrance at a distance where the average headway was in steady state.); and (3) the behavior of a platoon approaching a traffic signal.

To evaluate the dispersion behavior of a platoon down an arterial street, the changing pattern of the interaction between vehicles in the platoon was investigated, and headway between vehicles in the platoon was recorded.

Determination of the input variables of the models:

From the literature review, it was determined that several variables affect the behavior of platoon movement on arterial streets. Among them are the distance downstream from the traffic signal, signal offset, and platoon size. These three variables were investigated

and their influence on platoon behavior determined by the research staff of the Transportation Research Center, The Ohio State University (23) (1973).

Lewis (19) (1958) found that distance downstream from a traffic signal was linearly related with the arrival time of vehicles at a point. Since the time between successive arrivals is defined as headway, we can conclude from his study that distance downstream from the signal and headway have the same relation.

In Nemeth and Vecellio's experiments, they determined that improper signal offsets were one of the important factors causing traffic disturbances. This results in vehicle slowdowns or stoppages in platoons approaching a traffic signal. They also found that the initial acceleration characteristics of the smaller platoons (4 to 6 vehicles) are substantially different from those of the larger platoons (10 to 13 vehicles). Thus, it was reasonable to assume that headway would behave differently if the platoons varied in size.

In the preliminary study of headway reported in chapter 3, it was noted that the average headway of vehicles in a platoon increases in the initial state, reaches a steady state, and then decreases in the final 300 yards preceding the next signal. The influence of signal offset on average headways was also noted in our preliminary study. When the platoons were approaching the next signal, the average headway decreased due to vehicles slowing down when they observed a red signal. We would imagine that if the signal offset was well coordinated with the prior signal, then every vehicle might pass smoothly.

Bleyl (2) (1972) reported that 300 yards prior to a signal, the average speed profiles for all signal patterns are the same. He classifies the signal display into six categories:

- (1) a green signal indication from the moment the lead vehicle reaches a point approximately 300 yards in advance of the signal, at which point a red signal indication is given;
- (2) a red signal indication until the signal is reached;
- (3) a red signal indication from the moment the lead vehicle reaches a point approximately 300 yards in advance of the signal, at which point a green signal is given;
- (4) a green signal indication during the entire approach;
- (5) a flashing yellow signal;
- (6) no signal at all.

Bleyl found that the average speed profiles of the vehicles approaching the signal have no influence on the last four signal displays. From steady state car-following theory, it is reasonable to assume the average headway is independent of the signal timing until the lead vehicle in the platoon reacts to the signal displays of the first two categories.

Therefore, we concluded the following: (1) In the study of platoon dispersion leaving a signalized intersection (with or without entering vehicles), two independent variables to be considered are distance from the signal and platoon size; and (2) in the study of platoon approaching the next signal, only the reaction of the platoon's lead vehicle to the signal display of the first two categories noted above is to be considered.

Selection of study sites:

Having concluded that three factors (distance from the signal, platoon size, and signal offset) have a significant influence on platoon dispersion, it was decided that sites selected for data collection should eliminate other variables that might influence the dispersion. This meant that factors such as curb parking, grade, uncontrolled access from side streets, and opposing left turning traffic should be avoided.

Additional site requirements were that the volume vary so that the data would include different levels of platoon size. Also, the downstream signal spacing should be large enough for the study platoons to reach steady state flow.

Since the objective also was to study the dispersion of the platoon leaving the signalized intersection with the possibility of a downstream entrance, two sites were chosen. One was a section of an arterial street with a cross-street downstream from the signalized intersection, and the other was an arterial with no nearby cross-street. Both sites are on two-way signalized urban arterials located in Lansing, Michigan, the first on North Grand River Avenue between Logan Street and Airport Road, the second on Michigan Avenue between US-127 and Harrison Road. Platoon behavior was studied from the platoon formation point at the intersection of North Grand River and Airport Road and the intersection of Michigan and US-127. Some characteristics of the two sites are presented in Table 4-1.

In the last chapter, the results of the preliminary study of headways at various locations indicated the average headway of vehicles



Table 4-1. Characteristics of the Study Sites

Characteristics	Michigan Avenue Site	N.Grand River Avenue Site
Total length (yds.)	1,200	2,024
Lane	3	2
Max. speed (MPH)	35	45
Entrance point	0	2
Distance of the 1st entrance from the signal (yds.)	0	880

increases up to a distance of around 350 yards. Thus, four locations for data collection were established for Case One, 100, 200, 350, and 500 yards from the signal. It was believed that from these locations the behavior of the average headway could be traced through the transient state to the steady state.

Case Two involved the platoon approaching the next signal. Bleyl's paper assumed that 300 yards prior to the next signal, the average headway is in a steady state. Thus, three locations were selected for data collection, 100, 200, and 300 yards prior to the next signal.

Finally, Case Three concerned entering vehicles. It was assumed that the distance required to reach steady state after merging would be shorter than for platoons starting from the signal. Thus, the location for data collection were zero, 100, 200, and 300 yards from the entrance point.

Sample size requirement

In any experiment, estimating the statistical measures of a given phenomenon through a sampling technique requires determination of a sufficient and economical sample size. The sample for this study had to be large enough to produce results with acceptable accuracy, but cost and time were also considerations. Therefore, the minimum number of observations required for the estimation of platoons' average headway dispersion behavior was determined.

The headway of the vehicles within a platoon has been shown to be gamma distributed. If the number of data points from this distribution is sufficiently large, then the average will have a normal distribution according to the Central Limit Theorem.

If \bar{h} is the average of the observations from the sample, then

$$P(|\bar{h} - E(h)| \geq d) = \alpha, \quad (4-1)$$

where d is the chosen margin of error, and α is a small probability.

If we let d be 0.3 seconds and α be 0.05 seconds, we have the following equation to solve for n :

$$1.96 \frac{\sigma_0}{\sqrt{n}} = 0.3, \quad (4-2)$$

where σ_0 is the sample standard deviation. From Eq (4.2), we obtain

$$n = \frac{(1.96)^2 \sigma_0^2}{(0.3)^2}. \quad (4-3)$$

Using the preliminary study of headways discussed in Chapter 3, the sample standard deviation of headways at various locations downstream



from the signal are shown in Table 4-2.

Table 4-2. Standard Deviation of Headway at Different Locations.

Distance	150	300	700	1000
σ_0	0.98	1.22	1.63	1.64

The sample size required for the four locations of Case 1 are approximately as shown in Table 4-3.

Table 4-3. Sample Size Requirement at Different Locations.

Distance	100	200	350	500
n	40	70	120	120

The sample standard deviation in the steady state was the maximum and is approximately equal to 1.64. Using this sample standard deviation to calculate the required sample size for the second and third cases would give average headways for each locations within ± 0.3 seconds from the true mean with a probability of at least 0.95.

Data on the value of sample standard deviations for the headways of the vehicles approaching a signal or with entering vehicles were not available at this stage of the study. Therefore, the sample size for the second and the third cases was derived by using the sample standard deviation of the steady state.



Field data collection:

Field data were collected between 7:00 a.m. and 8:00 a.m. and 3:30 p.m. and 5:30 p.m. at the two sites on a number of days during fall and winter of 1976. These hours were selected because they are morning and evening peak traffic periods. On all occasions weather conditions were favorable, with good visibility and dry pavement.

Measuring headways of an entire platoon by stopwatch was impossible because of the speed with which it passed, especially large platoons. A photographic method was found to be more useful. A movie camera recorded the platoons as they passed each observation point along the street, and the headways between vehicles recorded. The camera used was an ARRIFLEX 16S/B camera equipped with a power operation unit. Film capacity was 100 feet, which yields approximately 5,120 exposures per roll. Eastman Plus - X negative black and white 16 mm film was used. The camera had variable speed control, and a speed of 8 frames per second was used during the data collection. A total of ten 100-foot rolls were used. The camera was mounted on a tripod at the selected locations to maintain a constant reference point.

Results of field studies:

Nemeth's and Vecellio's (22) (1971) field study tested the effect of platoon size on vehicle headways. Five categories were established: 9-10 vehicles, 12 vehicles, 16-17 vehicles, 20 vehicles, and over 20 vehicles. It was found that the effect of these platoon sizes on mean headway was not significant.



Therefore, for this study platoon size was grouped into three categories: under 5 vehicles; 6-9 vehicles, and over 9 vehicles. In general, platoons of under 5 vehicles are referred to as light flow, those with 6-9 vehicles as medium flow, and those with over 9 vehicles as heavy flow.

For the second case, moving platoons with entering vehicles from side streets downstream from the signal, data were only available under conditions of heavy flow on main and side streets.

The result of the field studies are tabulated in Appendix I.

CHAPTER FIVE

MATHEMATICAL MODELING OF PLATOON DISPERSION

Introduction:

From the results of the field study, statistical relationships were obtained for headway patterns downstream from the signal. The first part of this chapter describes tests performed to determine the effect of traffic volume on headway dispersion; the second part formulates mathematical models for platoon dispersion.

Data Analysis:

This section analyzes the data collected for platoons of different volume levels for different cases. The technique of multiple comparison of means (24) was used to determine whether or not the level of platoon volume had a statistically significant effect on the headway at different locations from the signal.

The effect of level of platoon volume on platoon dispersion for the three cases previously described is shown in Figures 5-1, 5-2, and 5-3. Figure 5-1 was plotted by calculating the average headway for platoons under three different levels of platoon volume at a number of downstream locations from the signal. Figure 5-2 plots the average headway for the moving platoon at a number of locations from the entrance with vehicles entering downstream. Figure 5-3 gives the average headway for platoons under different levels of platoon volume



Figure 5-1. Mean Headway at Different Locations of Platoon Leaving from a Signal.

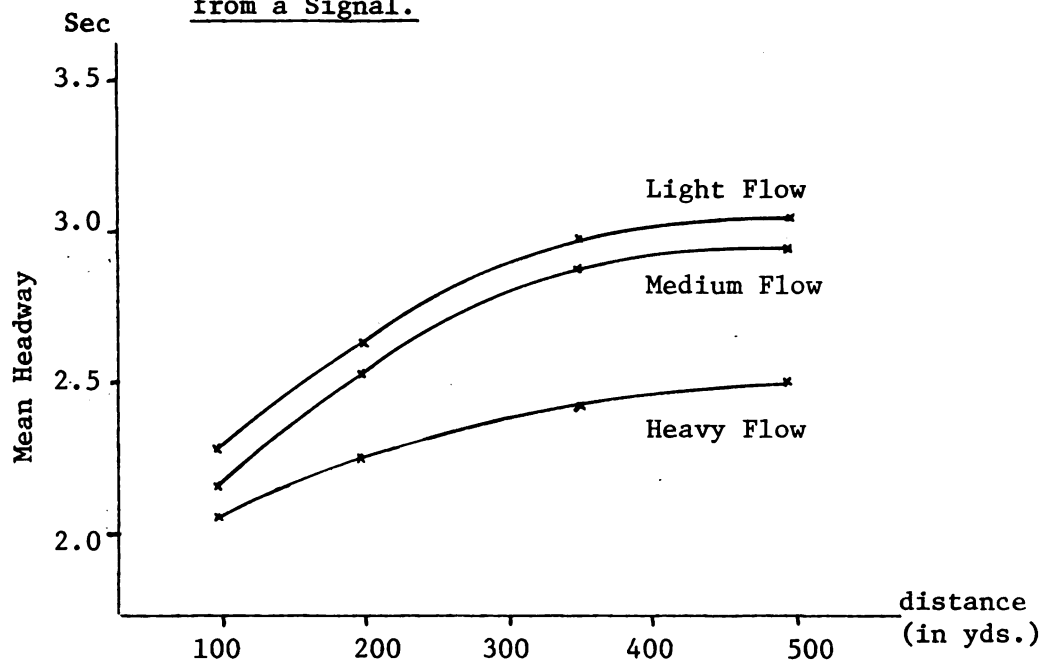
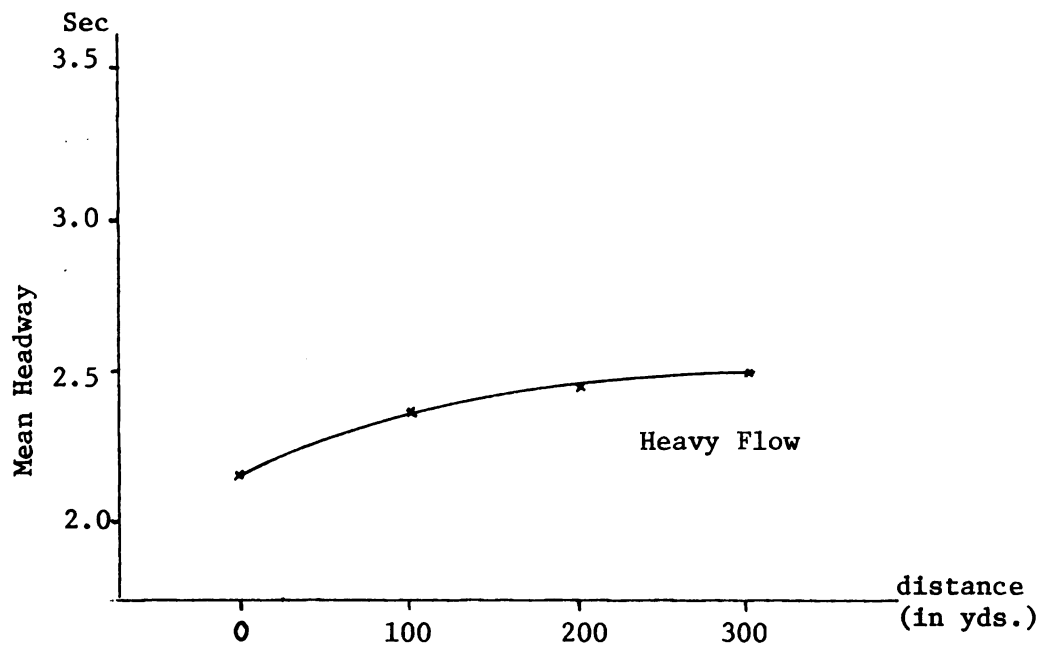
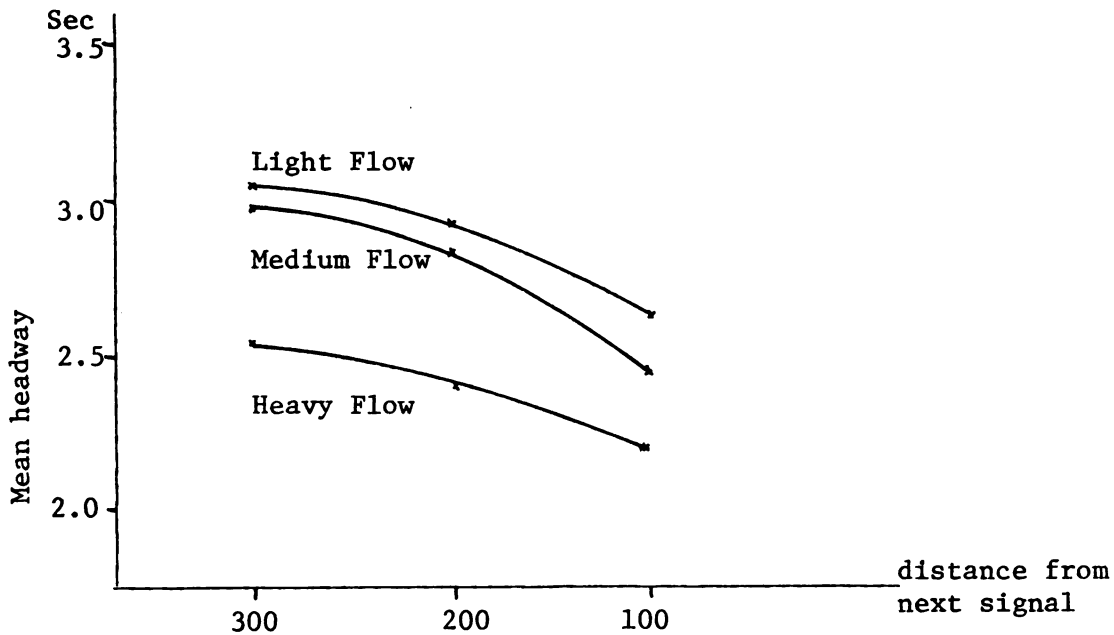


Figure 5-2. Mean Headway at Different Locations of Moving Platoon with Entering Vehicles.



1000000
(1000000)

Figure 5-3. Mean Headway at Different Locations of Platoon Approach a Signal.



at a number of locations approaching the next signal.

Multiple comparison of means requires the assumptions that the sample is from a normally distributed population having a mean M_i under different treatment (for example, three levels of platoon volume) with different variance. In mathematical notations, this can be stated as

$$X_{ij} \sim N(M_i, \sigma_i^2),$$

where $j=1, \dots, J$ is the number of treatments. The null hypothesis is

$$H_0 : M_i = M_j, \quad (5-1)$$



where $i, j=1, \dots, J$, and $i > j$.

In the previous section it was shown that the sample was not drawn from a normal distribution. But with fairly large sample sizes, where the Central Limit Theorem is applied, the mean is normally distributed.

In this study, data were collected under different treatments (platoon volume levels) at several locations from the signals. Thus, using a vector instead of a single variable, the new null hypothesis is defined as

$$H_0 : \begin{bmatrix} M_{i1} \\ M_{i2} \\ M_{i3} \\ \vdots \\ M_{ik} \end{bmatrix} = \begin{bmatrix} M_{j1} \\ M_{j2} \\ M_{j3} \\ \vdots \\ M_{jk} \end{bmatrix}, \quad (5-2)$$

where $i, j=1, \dots, J$, and $i > j$;

J = total number of treatments; and

K = total number of locations.

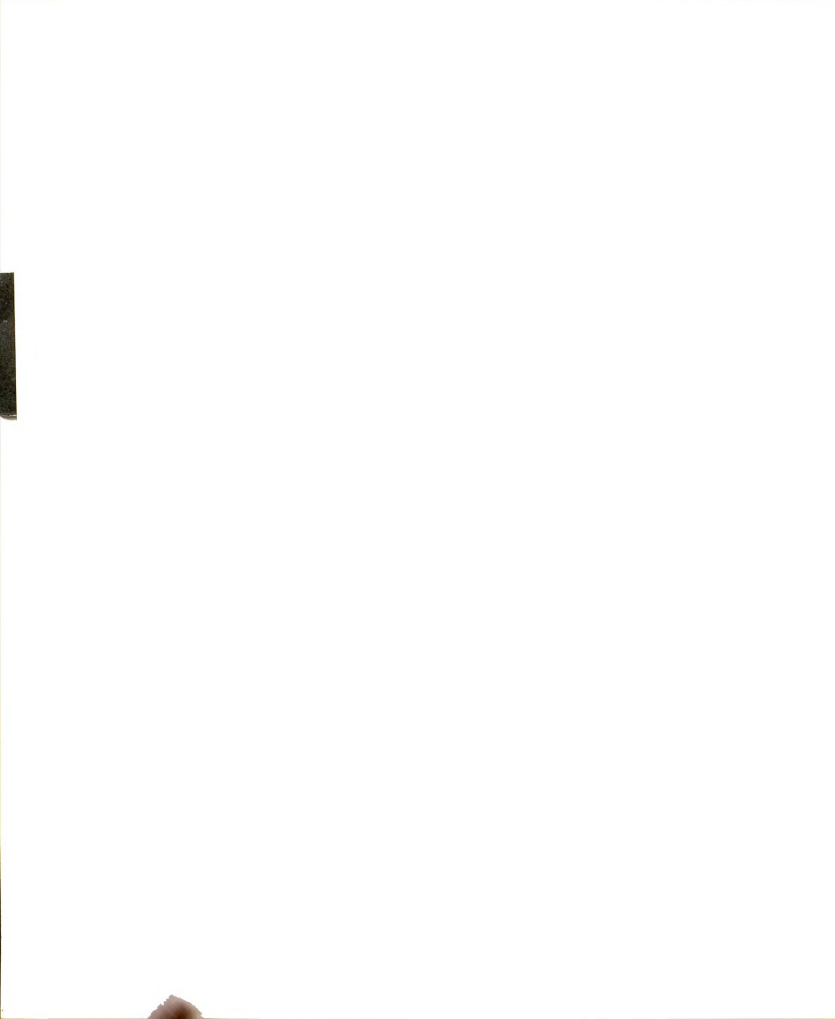
Eq (5-2) could be written as $\vec{M}_i = \vec{M}_j$,

and the test statistic may be written as

$$C_{\alpha k}^{ij} = Z_d \cdot S_{(\bar{x}_i - \bar{x}_j)}, \quad (5-3)$$

where Z_d = standardized normal statistic under level of significance α ;

$\vec{S}_{(\bar{x}_i - \bar{x}_j)}$ = a K -components vector, and its m th component is equal to $\sqrt{\frac{S_{im}^2}{\eta_1} + \frac{S_{jm}^2}{\eta_2}}$; and



S_{im} = the sample standard deviation of headway at location m under i th treatment.

Then the vector $\begin{vmatrix} \vec{M}_i & \vec{M}_j \end{vmatrix}$ is compared with $C_{\sigma k}^{ij}$ for all i and j , $i > j$. We reject H_0 if

$$\begin{vmatrix} \vec{M}_i & \vec{M}_j \end{vmatrix} \geq C_{\sigma k}^{ij} \quad (5-4)$$

and do not reject it otherwise. With the level of significance σ of each component of the vector, the level of significance for the whole vector is σk .

The results of the tests of the effect of platoon volume on headway at different locations are shown in Table 5-1, for the platoon leaving the signalized intersection, and Table 5-2, for the platoon approaching the next signal.

In both cases, the effect of light flow and medium flow on headway was of no significant difference. Therefore, these two categories were combined and labeled nonheavy flow. The results in mean headway after combining them are shown in Figures 5-4 and 5-5. The mean and standard deviation of headways for all cases are found in Table I-4 in Appendix I.

Development of the mathematical models:

The data analyzed in the previous section indicated that the relationships between distance and average headway spacing are non-linear. In other words, if we wanted to formulate this relationship in a mathematical form, it would not fit the form

$$F(x) = B_0 + B_1 x + E. \quad (5-5)$$



Table 5-1. Results of the Multiple Comparisons of Means for Case 1.

	m = 1	m = 2	m = 3	m = 4
$ M_3 - M_1 $ $C_{\alpha k}^{31}$	0.2043 0.4653	0.3386 0.3290	0.5687 0.2986	0.5464 0.3365
$ M_3 - M_2 $ $C_{\alpha k}^{32}$	0.1188 0.5076	0.2459 0.3802	0.4853 0.3425	0.4697 0.2944
$ M_2 - M_1 $ $C_{\alpha k}^{21}$	0.0855 0.4843	0.0927 0.3728	0.0834 0.3597	0.0767 0.3480

m: mth location from the signal;

1: light flow;

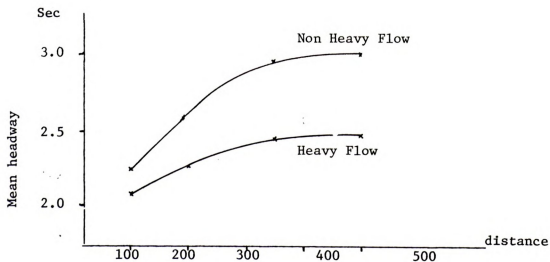
2: medium flow;

3: heavy flow;

$\alpha = 0.01$.

Table 5-2. Results of the Multiple Comparisons of Means for Case 3.

	m = 1	m = 2	m = 3
$ M_3 - M_1 $	0.4210	0.4300	0.5478
$C_{\alpha k}^{31}$	0.2546	0.2761	0.2688
$ M_3 - M_2 $	0.2393	0.3586	0.4790
$C_{\alpha k}^{32}$	0.2730	0.2823	0.2742
$ M_2 - M_1 $	0.1717	0.0714	0.0688
$C_{\alpha k}^{21}$	0.2628	0.2936	0.2752

Figure 5-4. Mean headway at different locations of platoon leaving from a signal with the combination of light and medium flow.

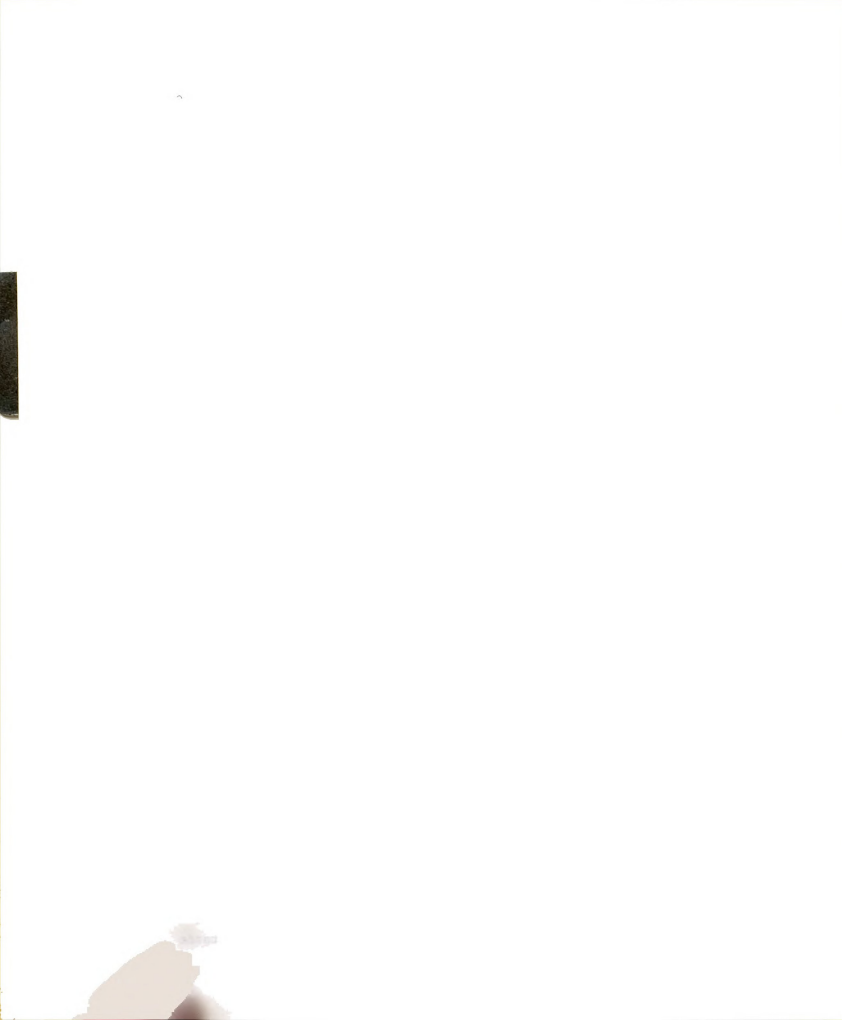
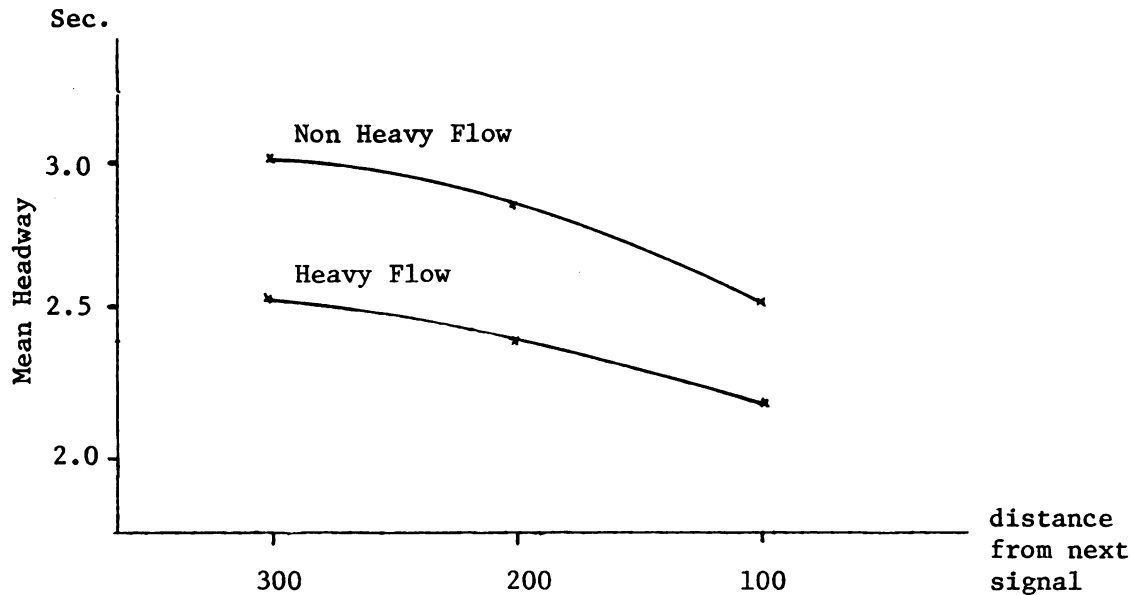


Figure 5-5. Mean Headway at Different Locations of Platoon Approach.

A nonlinear relationship can sometimes be approximated by an algebraic polynomial, which is intrinsically linear. Mathematically speaking, a polynomial in the base function $\{\phi_i(x)\}$ in any function of the form

$$P(x) = \alpha_0 + \alpha_1 \phi_1(x) + \alpha_2 \phi_2(x) + \dots + \alpha_m \phi_m(x), \quad (5-6)$$

where the α_i are constants. When the base functions are $1, x, x^2, x^3, \dots, x^n$, then a polynomial

$$P(x) = \alpha_0 + \alpha_1 x + \alpha_2 x^2 + \dots + \alpha_n x^n \quad (5-7)$$

is called an algebraic polynomial in one variable, and the polynomial is said to be of degrees n .

According to the Weierstrass Theorem (13), if $f(x)$ is a function continuous on $[a, b]$, and $\epsilon > 0$ is a given, when there exists

some integer n and an algebraic polynomial $p(x)$ of degree n , then

$$| f(x) - P(x) | < \epsilon \quad \text{for all } x \in [a, b].$$

Basically, the theorem says that it is reasonable to seek an algebraic polynomial approximation to any continuous function in a finite interval.

Thus, the problem now turns on the determination of the parameters of the polynomials.

The simplest method used to formulate the functional relationship of two variables is the polynomial interpolation method, in which the interpolating function passes through the given points exactly. But this method has two disadvantages: (1) It is accurate only for the points within the study interval, that is, not for extrapolation; and (2) it is accurate only for deterministic functions.

In our models, the average headway is a random variable which is normally distributed by the Central Limit Theorem. Furthermore, our data are "approximate", obtained experimentally. Therefore, in formulating the functional relationship, what is required is a method which allows the approximating function to differ from certain data points more than it does from others, since all data points are known only in what might be called a statistical sense. Least squares is such a method.

A quite general statement of the least squares theorem is as follows: The functional value $f(p_j)$ ($j=1, 2, \dots, n$) is given at a point p_j . A family of approximating functions,

$$Q_m(p_j, a_0, a_1, a_2, \dots, a_m), \quad (5-8)$$



is chosen, where $a_0, a_1, a_2, \dots, a_m$ are parameters. In the method of least squares, $a_0, a_1, a_2, \dots, a_m$ are determined such that

$$\sum_{j=1}^n \{f(p_j) - Q_m(p_j, a_0, a_1, \dots, a_m)\}^2 \quad (5-9)$$

is a minimum. For the determined values of $a_0, a_1, a_2, \dots, a_m$, say $\hat{a}_0, \hat{a}_1, \dots, \hat{a}_m$, the function $Q_m(p_j, \hat{a}_0, \hat{a}_1, \dots, \hat{a}_m)$ is the least squares approximation for the given data and the given approximating functions.

Since the approximating function is taken as an algebraic polynomial,

$$Q_m(x, a_0, a_1, a_2, \dots, a_m) = a_0 + a_1x + a_2x^2 + \dots + a_mx^m. \quad (5-10)$$

In order to minimize

$$\sum_{j=1}^n \{f(x_j) - a_0 - a_1x_j - a_2x_j^2 - \dots - a_mx_j^m\}^2, \quad (5-11)$$

the "normal" equation become:

$$a_0 \sum_{j=1}^n 1 + a_1 \sum_{j=1}^n x_j + a_2 \sum_{j=1}^n x_j^2 + \dots + a_m \sum_{j=1}^n x_j^m = \sum_{j=1}^n f(x_j);$$

$$a_0 \sum_{j=1}^n x_j + a_1 \sum_{j=1}^n x_j^2 + a_2 \sum_{j=1}^n x_j^3 + \dots + a_m \sum_{j=1}^n x_j^{m+1} = \sum_{j=1}^n x_j f(x_j);$$

and

$$a_0 \sum_{j=1}^n x_j^m + a_1 \sum_{j=1}^n x_j^{m+1} + a_2 \sum_{j=1}^n x_j^{m+2} + \dots + a_m \sum_{j=1}^n x_j^{2m} = \sum_{j=1}^n x_j^m f(x_j)$$

and must be solved.

A program for solving this set of equations is contained in a computer package available in the Computer Center, Michigan State University.

Five curves from Figures 5-2, 5-4, and 5-5 were formulated within the range of collected data, and M (degree of the equation) was assumed to be 2 and 3. From the figures, it was found that after the defined distance, steady state was reached. For convenience, specific notations were given to each of these five curves. They were:

NHL_i = i th location of the curve of mean headway for non-heavy flow of Case 1;

HL_i = i th location of the curve of mean headway for heavy flow of Case 1;

INT_i = i th location of the curve of mean headway of Case 2;

$NHAP_i$ = i th location of the curve of mean headway for non-heavy flow of Case 3;

HAP_i = i th location of the curve of mean headway for heavy flow of Case 3.

If i is replaced by c , this represents the whole curve.

After the equations were formulated, validity of the approximated

equations were examined and determined the degree of the polynomials. The coefficient of determination (7) which measures the proportion of total variation explained by the equation was used for this test. The coefficient of determination can be written as:

$$R^2 = \frac{\sum_{i=1}^n (\hat{f}(x_i) - \overline{f(x_i)})^2}{\sum_{i=1}^n (f(x_i) - \overline{f(x_i)})^2}, \quad (5-13)$$

where $\hat{f}(x_i)$ = the value of $f(x_i)$ estimated by the regression equation; and $\overline{f(x_i)}$ = the average of $f(x_i)$.

The results of the least squares approximation of the models and their coefficient of determination are shown in Table 5-3 for $M=2$ and Table 5-4 for $M=3$. From the results, it was found that $M=2$ gave the desired accurate approximation. From the two tables, it was found that the 3rd term of the degree three model did not give any additional accuracy to the model. Therefore, $M=2$ should be selected as the degree of the polynomials least squares approximation for the models.

Analysis of the mean headway for the passing platoon with entering vehicles:

Headway data for the passing platoon with entering vehicles were only available for heavy flow of the mainstream. In this section, the relationship between the mean headway for the passing platoon leaving a signalized intersection are analyzed. The results will be used as the basis for estimating the mean headway for the passing platoon with entering vehicles under non heavy flow.

Table 5-3. Equation Results for $m=2$: $f(x) = a_0 + a_1 y + a_2 y^2$ where
 $y = b_0 + b_1 X$.

	a_0	a_1	a_2	b	b_1	R^2
NHL _c	2.6981	0.1910	-0.0630	0.1000	-3	0.986
HL _c	2.3148	0.1015	-0.0264	0.1000	-3	0.995
INT _c	2.3639	0.0733	-0.0145	0.0133	-2	0.997
NHAP _c	2.8125	0.1199	-0.0275	0.0200	-4	0.996
NAP _c	2.4015	0.0720	-0.0337	0.0200	-4	0.994

Table 5-4. Equation results for $m=3$: $f(x) = a_0 + a_1 y + a_2 y^2 + a_3 y^3$
 where $y = b_0 + b_1 x$.

	a_0	a_1	a_2	a_3	b_0	b_1	R
NHL _c	2.6981	0.1910	-0.0630	-0.0200	0.1000	-3	0.987
HL _c	2.3148	0.1015	-0.0264	-0.0160	0.0100	-3	0.995
INT _c	2.3639	0.0733	-0.0145	-0.0054	0.0133	-2	0.997
NHAP _c	2.8125	0.1199	-0.0275	-0.0031	0.0200	-4	0.995
HAP _c	2.4015	0.0720	-0.0337	-0.0025	0.0200	-4	0.995

From Figure 5-4, it can be observed that the curve INT_c is similar to a portion of curve HL_c . In other words, if INT_c were shifted a constant distance, the two curves might be identical. The purpose of this section is to test this hypothesis.

The two curves can be written as

$$HL_c(x) = B_0 + B_1x + B_2x^2 \quad 100 \leq x \leq 500; \quad (5-14)$$

$$INT_c(x) = \alpha_0 + \alpha_1x + \alpha_2x^2 \quad 0 \leq x \leq 300. \quad (5-15)$$

Therefore, we want to test the null hypothesis

$$H_0 : INT_c(X) = HL_c(x + \theta), \quad (5-16)$$

or

$$H_0 : \begin{aligned} \alpha_0 &= \beta_0 + \theta \beta_1 + \theta^2 \beta_2 \\ \alpha_1 &= \beta_1 + 2\theta \beta_2 \\ \alpha_2 &= \beta_2 \end{aligned} \quad (5-17)$$

To simplify the analysis, this nonlinear hypothesis is changed to a linear one. A value of $\theta = 150$ yards is assumed, since the first data set of INT_c is approximately the midpoint of HL_1 and HL_2 .

To test the equality of this reduced model and the full model, an F-test (21) must be performed. The full model is defined as the original one, that is, EQ (5-14) and EQ (5-15). The reduced model might be written as:

$$HL_c(x) = \beta_0 + \beta_1x + \beta_2x^2, \quad 100 \leq x \leq 500; \quad (5-18)$$

$$\text{INT}_c(x) = (\beta_0 + 150\beta_1 + 150^2\beta_2) + (\beta_1 + 300\beta_2)x + \beta_2 x^2 \quad (5-19)$$

$$0 \leq x \leq 300.$$

We expect to find $\hat{\beta}_0, \hat{\beta}_1$ and $\hat{\beta}_2$ to minimize

$$Q = \sum_{i=1}^{n_1} (y_{1i} - \text{HL}_c(x_i))^2 + \sum_{i=1}^{n_2} (y_{2i} - \text{INT}_c(x_i))^2, \quad (5-20)$$

where y_{1i} = the mean headway of HL_c at i th location;
 y_{2i} = the mean headway of INT_c at i th location;
 n_1 = the total number of data points in HL_c ; and
 n_2 = the total number of data points in INT_c .

The test statistic then leads to

$$F = \frac{\{ \text{SSE(R)} - \text{SSE(F)} \} / m_1 - m_2}{\text{SSE(F)} / m_2}, \quad (5-21)$$

where SSE(R) = error sum of squares of the reduced model;

SSE(F) = error sum of squares of the full model;

$$m_1 = n_1 + n_2 - p_1;$$

$$m_2 = n_1 + n_2 - p_2;$$

p_1 = total number of parameters in the reduced model; and

p_2 = total number of parameters in the full model.

The test statistic then is compared with an F-distributed statistic

$F_{\alpha}((m_1 - m_2), m_2)$ under the level of significance α . The null hypothesis will be rejected if

$$F \geq F_{\alpha}((m_1 - m_2), m_2). \quad (5-22)$$

Solving for β_0, β_1 and β_2 to minimize Q , partial derivatives with respect to β_0, β_1 , and β_2 are taken to obtain the normal equations.

The resulting normal equations become:



$$\begin{aligned}
& \beta_0 \{n_1 + n_2\} + \beta_1 \left\{ \sum_{i=1}^{n_1} x_{1i} + 150n_2 + \sum_{i=1}^{n_2} x_{2i} \right\} + \beta_2 \left\{ \sum_{i=1}^{n_1} x_{1i}^2 + \sum_{i=1}^{n_2} x_{2i}^2 + 300 \sum_{i=1}^{n_2} x_{2i} + 150^2 n_2 \right\} = \\
& \left\{ \sum_{i=1}^{n_1} y_{1i} + \sum_{i=1}^{n_2} y_{2i} \right\} \\
& \beta_0 \left\{ \sum_{i=1}^{n_1} x_{1i} + 150n_2 + \sum_{i=1}^{n_2} x_{2i} \right\} + \beta_1 \left\{ \sum_{i=1}^{n_1} x_{1i}^2 + 150^2 n_2 + 300 \sum_{i=1}^{n_2} x_{2i} + \sum_{i=1}^{n_2} x_{2i}^2 \right\} + \\
& \beta_2 \left\{ \sum_{i=1}^{n_1} x_{1i}^3 + 150^3 n_2 + 67500 \sum_{i=1}^{n_2} x_{2i} + 450 \sum_{i=1}^{n_2} x_{2i}^2 + \sum_{i=1}^{n_2} x_{2i}^3 \right\} = \\
& \left\{ \sum_{i=1}^{n_1} y_{1i} x_{1i} + 150 \sum_{i=1}^{n_2} y_{2i} + \sum_{i=1}^{n_2} y_{2i} x_{2i} \right\} \quad (5-23)
\end{aligned}$$

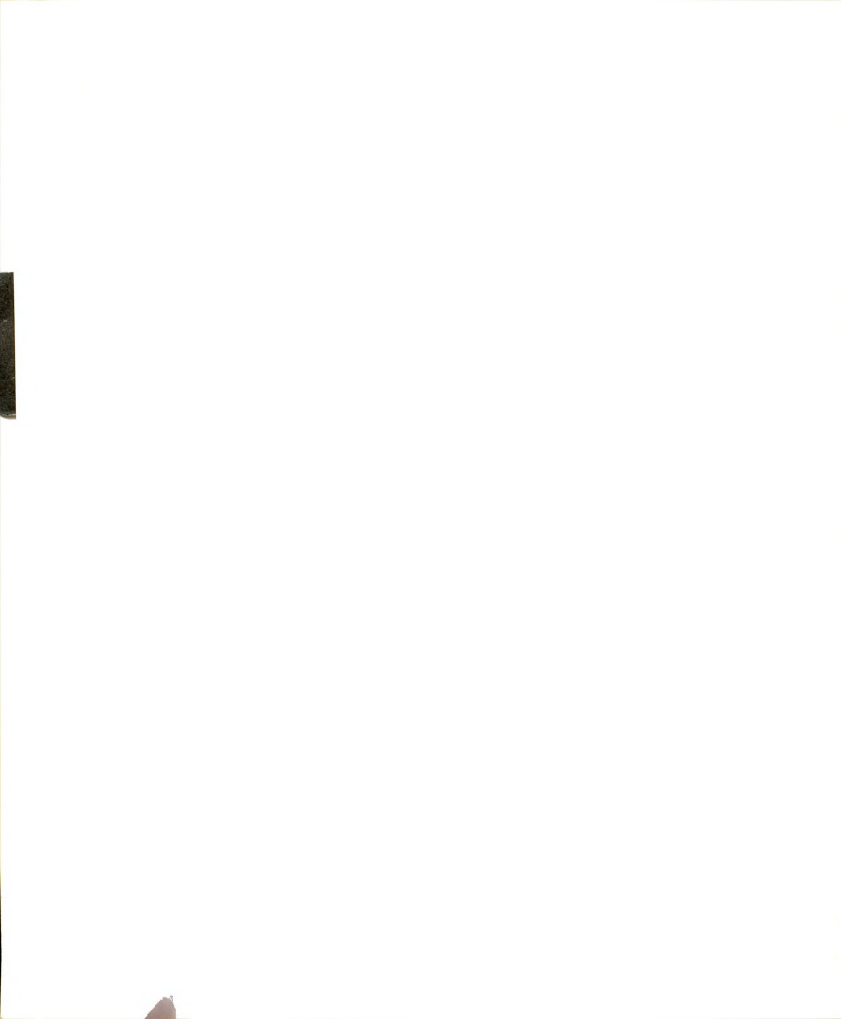
$$\begin{aligned}
& \beta_0 \left\{ \sum_{i=1}^{n_1} x_{1i}^2 + \sum_{i=1}^{n_2} (x_{2i} + 150)^2 \right\} + \beta_1 \left\{ \sum_{i=1}^{n_1} x_{1i}^3 + 150 \sum_{i=1}^{n_2} (x_{2i} + 150)^2 + \right. \\
& \left. \sum_{i=1}^{n_2} x_{2i} (x_{2i} + 150)^2 \right\} + \beta_2 \left\{ \sum_{i=1}^{n_1} x_{1i}^4 + (150)^2 \sum_{i=1}^{n_2} (x_{2i} + 150)^2 + 300 \sum_{i=1}^{n_2} x_{2i} \right. \\
& \left. (x_{2i} + 150)^2 + \sum_{i=1}^{n_2} x_{2i}^2 (x_{2i} + 150)^2 \right\} = \left\{ \sum_{i=1}^{n_1} y_{1i} x_{1i}^2 + \sum_{i=1}^{n_2} y_{2i} (x_{2i} + 150)^2 \right\}.
\end{aligned}$$

Solving Eq (5-23) for β_0, β_1 , and β_2 , we obtain

$$\begin{aligned}
\hat{\beta}_0 &= 1.84708 \\
\hat{\beta}_1 &= 0.00272 \\
\hat{\beta}_2 &= -0.00021.
\end{aligned} \quad (5-24)$$

Substituting $\hat{\beta}_0, \hat{\beta}_1$, and $\hat{\beta}_2$ into Eq(5-20), SSE(R) is obtained. The test statistic, F, is equal to 3.78. Under $\alpha = 0.05$, $F_{\alpha}(3.2) = 9.55$. Thus, the null hypothesis was not rejected.

The accepted hypothesis states that the INT_c curve is identical with the portion of HL_c starting from the location where the mean



headway is equal to the mean headway at the entrance point after the entering vehicles enter. This is reasonable because it implies that if both headway distributions have the same shape, they will have the same dispersion pattern. Therefore, for the case of non-heavy flow (where data were not available), the curve for platoon dispersion leaving the signal under non heavy flow is assumed to be valid for the case of entering vehicles.

CHAPTER SIX

SOME ANALYTIC CONSIDERATIONS OF QUEUEING

Introduction:

A number of theoretical papers (20) (28) have dealt with the queueing problem at unsignalized intersections where the minor street traffic is waiting for a sufficient gap to enter the main stream. Most papers have assumed that the arrival of both mainstream and minorstream traffic takes the Poisson distribution. However, in chapter 3 it was shown that the headway within a platoon is gamma distributed. We will also assume that the mainstream traffic is composed of a series of platoons with no vehicles between platoons. We will call the time between platoons "idle" time and the time when the platoon is passing a given point the "passing" time. Because of the dispersion of the platoon, idle time will decrease as the distance from the prior signal increases. Thus, in our queueing consideration, we have to separately consider these two conditions.

Another assumption is that the critical time gap is a step function. That is, the minor stream vehicles will accept the gap if it is greater than the critical time gap and reject it if the gap is less than the critical one. This assumption is suggested by the study by Blumenfeld (14), which showed that this assumption leads to no serious discrepancies in problems of engineering interests.

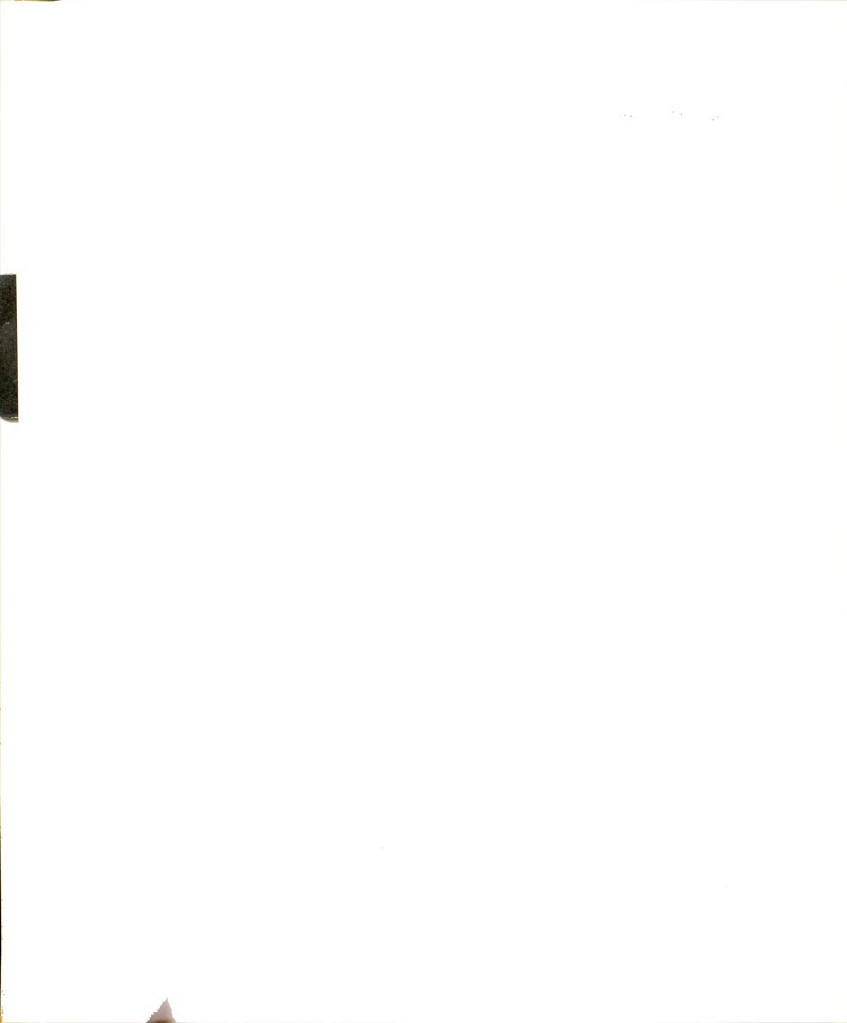


Multiple entry is permitted if the gap is sufficiently large, that is, if there is a critical time gap plus some move-up time for the second vehicles, and so on.

The notations used throughout this chapter are defined below.

$f(t)$ = main stream headway distribution;
 λ = arrival rate of minor stream (veh/sec);
 a, b = parameters of the mainstream headway distribution within a platoon (gamma distribution constants);
 s = cycle length;
 w_i = the headway of the i th vehicle within a platoon;
 v = moving up time (in seconds);
 n = average number of headway within a platoon;
 d = distance of the minor street from the nearest upstream signal (in yards); and
 t = critical gap time (in seconds).

Using these notations, we know that if the distance from the nearest upstream signal to the minor street and the average platoon size are given, chapter 4 can be used to calculate the parameters of the mainstream headway distribution within the platoon. Thus, in each cycle, platoon passing time will be equal to $\sum_{i=1}^n w_i$, and the idle time will be $s - \sum_{i=1}^n w_i$. We further assume that s is always greater than $\sum_{i=1}^n w_i$; otherwise, the platoon will merge. If we let $p = \sum_{i=1}^n w_i / s$, then $100xp$ percent of the time at locations i will be passing time, and $100x(1-p)$ percent will be "idle" time. We also assume that the cycle length equals 60 seconds, which is the actual cycle length of the signal at which field data were obtained. The



percentage of passing time and idle time for different locations from the signal is shown in Table 6-1.

Table 6-1. Percentage of the passing time at different locations.

	n	100 yds.	200 yds.	350 yds.	500 yds.
Nonheavy flow	6	0.2251	0.2567	0.2990	0.3002
Heavy flow	11	0.3482	0.3791	0.4088	0.4135

Queueing considerations at the merging position:

This section discusses the delay to a single vehicle waiting at a stop sign for a sufficiently large gap in the oncoming traffic. We first must define the terms "lag", which is different from gap. A lag is the interval of time between the arrival of a minor stream vehicle and the arrival of a major stream vehicle at the point where the streams cross. Assume that a vehicle arrives on the minor street at time $t=0$, and the driver waits for a gap greater than T seconds. There are two possibilities: The driver accepts the lag, or he rejects the lag and subsequently accepts a gap.

If we know the probability density function of the lag ($f_0(t)$) and the probability density function of the gap ($f(t)$), then we will accept a lag with probability

$$\int_T^{\infty} f_0(t) dt \quad (6-1)$$

and accept a gap with probability

$$\int_T^{\infty} f(t) dt. \quad (6-2)$$

Using the terminology of Renewal Theory, $f_0(t)$ is known as the forward recurrence time, which is shown by Cox (6) (1962) as

$$f_0(t) = \frac{\int_t^{\infty} f(x) dx}{\mu}, \quad (6-3)$$

where μ is the mean of the distribution $f(t)$. Therefore, $f_0(t)$ is a function of t , and the parameters of the headway distribution $f(t)$.

Let Eq (6-1) be denoted by F_0 and Eq (6-2) by F . We then further define a conditional probability, $H(t)$, as follows:

$H(t) = \text{Prob} \{ \text{A gap is accepted in the time interval } (t, t+dt) \text{ given that no gap was accepted in the interval } (0, t) \}$.

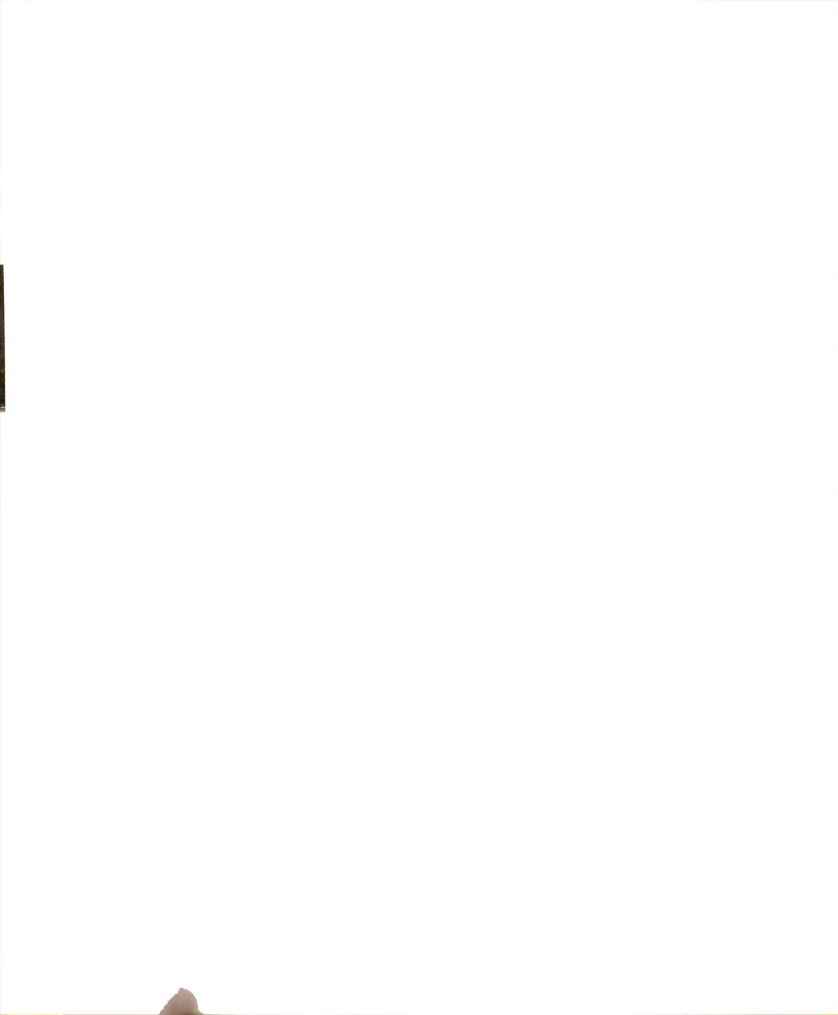
With these definitions we can write the probability density of the merging delay as

$$D(t) = \delta(t) F_0 + H(t) F, \quad (6-4)$$

where $\delta(t)$ is a Dirac delta function, which accounts for the cases of zero delay, that is the acceptance of the lag. The first term of Eq (6-4) indicates that if a lag is accepted with a probability of F_0 , the waiting time is zero. The second term of Eq (6-4) indicates that if a gap is accepted with a probability of F , then the waiting time is t .

By definition of a delta function,

$$\int_0^{\infty} \delta(t) dt = 1, \quad (6-5)$$



and

$$\int_0^{\infty} H(t) dt = 1, \quad (6-6)$$

where $H(t)$, $f(t)$, F_0 , and F are all positive functions. Thus, it is easily shown that $D(t)$ is a probability density function, since

$$\int_0^{\infty} D(t) dt = 1, \quad (6-7)$$

and

$$D(t) \geq 0 \quad \text{for all } t.$$

Let the Laplace Transform of $f(x)$ be $f^*(s)$, by

$$f^*(s) = \int_0^{\infty} e^{-\lambda t} f(t) dt.$$

Taking the Laplace Transform with respect to $D(t)$, the moment of the merging delay will be obtained. The proof is given in Appendix III. From Eq (6-4), we have

$$D^*(S) = FH^*(S), \quad (6-8)$$

In considering $H(t)$ of Eq (6-4), the mainstream vehicle that arrives in time $(t, t dt)$ must either have been the first vehicle to appear with density $f_0(t)$, and the lag was rejected, or a vehicle passed at $(t-x)$, and its gap was rejected. From this, we can write the equation satisfied by $H(t)$ as

$$H(t) = f_0(t) \{1 - \alpha(t)\} + \int_0^t H(x) f(t-x) (1 - \alpha(t-x)) dx; \quad (6-9)$$

where

$$\begin{aligned} \alpha(t) &= 0 & \text{if } 0 \leq t < T, \text{ and} \\ \alpha(t) &= 1 & \text{if } t \geq T. \end{aligned}$$

Let

$$G_0(t) = f_0(t) \{1 - \alpha(t)\}, \quad (6-10)$$



and

$$G(t) = f(t) \{ 1 - \alpha(t) \}.$$

Eq (6-9) then can be written as

$$H(t) = G_0(t) + \int_0^t H(t-x) G(t-x) dt. \quad (6-11)$$

Eq (6-11) becomes

$$H^*(S) = G_0^*(S) + H^*(S) G^*(S), \quad (6-12)$$

$$H^*(S) = \frac{G_0^*(S)}{1 - G^*(S)}, \quad (6-13)$$

The moment of the merging delay can be found from Eq (6-4) to be

$$\mu_t^n = (-1)^n \left(\frac{d^n}{ds^n} \right) D^*(s) \Big|_{s=0} \quad (6-14)$$

The proof of Eq (6-14) and the first and second moment are presented in Appendix III. The result is shown in Eq (6-15) and Eq (6-17) which is different from the result developed by Weiss and Maradudin (27) using the same model.

$$\mu_t^2 = \frac{1}{F} \int_0^\infty t \{ F G_0(t) + (1-F_0)G(t) \} dt. \quad (6-15)$$

If we let

$$M_0(t) = \int_0^\infty t G_0(t) dt, \text{ and}$$

$$M(t) = \int_0^\infty t G(t) dt,$$

Eq (6-15) becomes

$$\mu_t^1 = M_0(t) + \frac{1-F_0}{F} M(t), \quad (6-16)$$



and

$$\mu_t^2 = \frac{1}{F^2} \left\{ \int_0^\infty t^2 (F^2 G_0(t) + (1-F_0) F G(t) dt + 2 \int_0^\infty t G(t) dt \int_0^\infty t (F G_0(t) dt + (1-F_0) G(t)) dt \right\}. \quad (6-17)$$

Let

$$N_0(t) = \int_0^\infty t^2 G_0(t) dt, \text{ and}$$

$$N(t) = \int_0^\infty t^2 G(t) dt;$$

Eq (6-17) then becomes

$$\mu_t^2 = N_0(t) + \frac{1-F_0}{F} N(t) + \frac{2}{F} \mu_t^1 M(t). \quad (6-18)$$

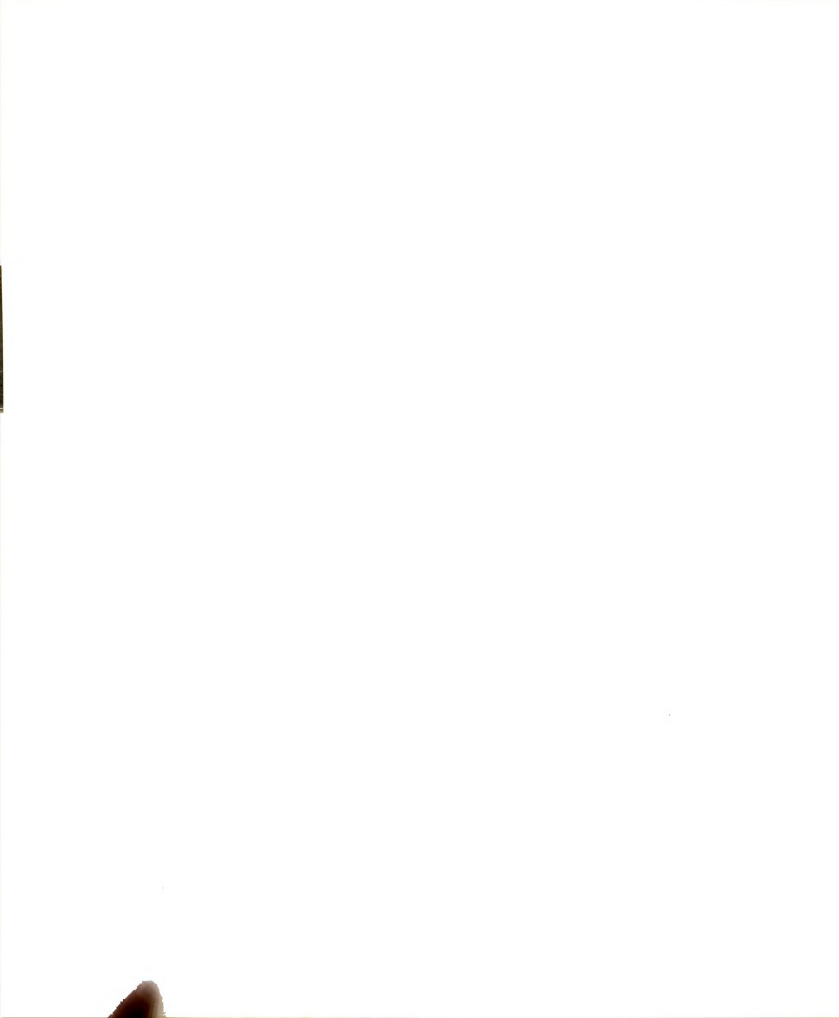
The variance of the merging delay is

$$\sigma_t^2 = \mu_t^2 - (\mu_t^1)^2. \quad (6-19)$$

In our headway model, $F(t)$ has been shown to be gamma distributed; thus

$$f(t) = \frac{1}{\Gamma(a)b^a} t^{a-1} e^{-t/b}, \quad t \geq 0 \quad (6-20)$$

where a and b are the parameters of distribution and are defined as real numbers.



In order to solve Eq (6-16) and Eq (6-18), $F_0(t)$, $F(t)$, $M_0(t)$, $M(t)$, $N_0(t)$, and $N(t)$ should be calculated first. By definition, F is the incomplete gamma function. Under different values of T , the value of F can be calculated by computer approximation for the different cases as defined in the last chapter. The result is presented in Table II-1 of Appendix II.

In calculating F_0 , which is defined as the integral of f_0 , f_0 is defined as

$$f_0(t) = \frac{\int_t^{\infty} f(x) dx}{\mu}, \quad (6-21)$$

which is an indefinite integral of the headway distribution divided by its mean.

There are several articles (18) which relate this indefinite integral to the cumulative Poisson distribution as

$$\int_t^{\infty} \frac{1}{\Gamma(a)_b} x^{a-1} e^{-\frac{x}{b}} dx = e^{-\frac{t}{b}} \sum_{i=0}^{a-1} \left(\frac{t}{b}\right)^i \frac{1}{i!}, \quad (6-22)$$

but this is only true when "a" is an integer.

Since "a" in gamma distribution is defined as a real number, a curve fitting an algorithm of f_0 for eight different cases is presented. The integral of $f(x)$ is approximated by computer, using nine different values of t ranging from 0 to 5. These nine points will plot all the curves of the resulting integral varying from one to 0.



By using the Lagrange polynomial interpolation technique (13), the proposed polynomial will pass through five alternative selected points. The value at the selected points and at the midpoints between them where one would expect the error to be the largest are then examined, substituting those values into the polynomial equations and comparing the results with the original data. The proposed polynomial is shown in Table II-2 of Appendix II. The curves plotted by the polynomial equations are presented in Figure II-1 of Appendix II.

The selected points and their midpoints are then substituted into the polynomial equations, and one finds that the upper bound of the deviation of the equation from the integral is 0.05. Thus, the polynomial equations can be accepted as a good fit to the indefinite integral $\int_t^\infty f(t)dt$.

f_0 is then equal to the proposed polynomial equation divided by the mean of the headway distribution; this result is shown in Table II-3, Appendix II.

F_0 is defined as the integral of f_0 ; by using computer approximation the result is shown in Table II-4 of Appendix II.

Again using the computer approximation, $M(t)$, $M_0(t)$, $N(t)$, and $N_0(t)$ under different T for different cases is calculated, as shown in Table II-5 through II-8 in Appendix II.

With this information, μ_t^1 and σ_t^2 are calculated under different T for different locations. These results are shown in Tables 6-2 and 6-3.



Table 6-2. Calculate μ_t^1 for Different T.

	T = 2	T = 3	T = 4	T = 5
NHL ₁	1.6307	9.6638	58.0139	404.4929
NHL ₂	1.1548	6.3097	36.0276	242.1522
NHL ₃	0.8327	3.6102	15.9985	79.9109
NHL ₄	0.8141	3.5847	15.8166	78.0859
HL ₁	1.9675	11.4557	65.9667	421.5800
HL ₂	1.5794	10.4827	57.8873	353.5397
HL ₃	1.2981	7.3444	44.9245	318.1406
HL ₄	1.2343	6.8330	39.2631	264.8093

Table 6-3. Calculate σ_t^2 for Different T.

	T = 2	T = 3	T = 4	T = 5
NHL ₁	3.3679	90.2583	3423.4429	164033.5986
NHL ₂	1.7437	43.2742	1331.2554	58892.3497
NHL ₃	0.9688	14.8524	273.7818	6473.0088
NHL ₄	0.9130	14.5814	267.9273	6210.7805
HL ₁	4.8569	139.6327	4417.0574	178135.4064
HL ₂	3.0980	115.0225	3560.0805	125251.8651
HL ₃	2.1631	60.1113	2062.0342	101547.4212
HL ₄	1.9678	50.4400	1577.5383	70388.9500

These results represent the merging delay for the minor stream vehicles while the mainstream platoon is passing, which occurs p percent of the time. The remaining $(1-p)$ percent of the time there will be no merging delay. Thus, the overall expected merging delay will be

$$E(Z) = P \mu_t^1 \quad (6-23)$$

and the variance will be

$$\text{Var}(Z) = p\sigma_t^2 + p(1-p)(\mu_t^1)^2 \quad (6-24)$$

The proof of Eq (6-24) is given in Appendix III, and the results are shown in Tables 6-4 and 6-5.

Table 6-4. Average Merging Delay $E(Z)$.

	T = 2	T = 3	T = 4	T = 5
NHL ₁	0.3670	2.1753	13.0589	91.0513
NHL ₂	0.2964	1.6197	9.2482	62.1604
NHL ₃	0.2489	1.0794	4.7835	23.8933
NHL ₄	0.2444	1.0761	4.7481	23.4413
HL ₁	0.6850	3.9888	22.9696	146.7941
HL ₂	0.5987	3.9739	21.9450	134.0269
HL ₃	0.5306	3.0024	19.3651	130.0558
HL ₄	0.5103	2.8254	16.2353	109.4986



Table 6-5. Variance of Merging Delay Var (Z).

	T = 2	T = 3	T = 4	T = 5
NHL ₁	1.2218	36.6041	1357.5797	65458.3323
NHL ₂	0.7020	18.7045	589.3893	26305.7369
NHL ₃	0.4349	7.1726	135.5082	3273.8831
NHL ₄	0.4131	7.0758	132.9663	3144.9319
HL ₁	2.5694	78.3968	2525.3985	102353.6166
HL ₂	1.7613	69.4613	2368.4217	76879.0861
HL ₃	1.2913	37.6053	1330.5592	65965.7520
HL ₄	1.1828	32.1745	1025.9936	46103.8799

Queueing Considerations before Merging:

Using the previous results, the average delay for a vehicle before merging and the average queue length of the minor stream can be developed.

In this section, Kendall's approach (16) for a queueing system with random inputs from the side and arbitrary service times is used to develop formulas for the average delay before merging and the average queue length.

Let $x(t_i)$ denote the number in the system at time t_i , where t_i is the time of completion of waiting of the i th vehicle. Let $X(t_i)$ be denoted by X_i . We can then write for all $m \geq 0$

$$X_{m+1} = X_m + A_{m+1} - \delta, \quad (6-25)$$



where δ is introduced as a random variable such that

$$\begin{aligned} \delta &= 0 & x_m &= 0 \\ &= 1 & x_m &> 0 \end{aligned} \quad (6-26)$$

In Eq (6-25) $A_{(m+1)}$, is the number of vehicles which arrived during the waiting time of the $(m+1)$ st vehicles arrival, say, Z_{m+1} , independent random variable, A_{m+1} can in general be denoted by A , and Z_{m+1} by Z . Then conditionally A is a Poisson variable of mean Z , given that Z is the duration time. Also assuming that the steady state solution exists, we can take the expected value of Eq (6-25) and obtain

$$E(X_{m+1}) = E(X_m) + E(A) - E(\delta). \quad (6-27)$$

Noting that $E(X_{m+1}) = E(X_m) = Nd$ in steady state, Eq (6-27) then becomes

$$Nd = Nd + E(A) - E(\delta), \quad (6-28)$$

$$\text{or} \quad E(\delta) = E(A). \quad (6-29)$$

The expected number of vehicles arriving during the merge waiting time of a vehicle is equal to the product of the arrival rate and the average merging waiting time, that is,

$$E(A) = \lambda E(Z). \quad (6-30)$$

Thus, we have

$$E(\delta) = \lambda E(Z). \quad (6-31)$$

Squaring both sides of Eq (6-25) and taking the expected value as before yields

$$\begin{aligned} E(X_{m+1}^2) &= E(X_m)^2 + E(A^2) + E(\delta^2) + 2E(X_m A) \\ &\quad - 2E(\delta X_m) - 2E(\delta A). \end{aligned} \quad (6-32)$$



Note that $\delta^2 = \delta$, $X_m \delta = X_m$, $E(X_{m+1}^2) = E(X_m^2)$,
and A is independent of X and δ . Thus, we have

$$E(A^2) + E(\delta) - 2E(X_m) + 2E(X_m) E(A) - 2E(\delta) E(A) = 0, \quad (6-33)$$

or

$$E(A^2) + \lambda E(Z) - 2\lambda^2 (E(Z))^2 - 2Nd + 2\lambda Nd E(Z) = 0, \quad (6-34)$$

or

$$Nd = \lambda E(Z) + \frac{E(A^2) - \lambda E(Z)}{2(1 - \lambda E(Z))}. \quad (6-35)$$

Now it is necessary to calculate $E(A^2)$, the second moment of the number of arrivals during the merge waiting time of any vehicle, and

$$\begin{aligned} E(A^2) &= \text{VAR}(A) + (E(A))^2 \\ &= \text{VAR}(A) + \lambda^2 (E(Z))^2, \end{aligned} \quad (6-36)$$

$$\text{where } \text{Var}(A) = E(\text{Var}(A|Z)) + \text{Var}(E(A|Z)). \quad (6-37)$$

The proof of Eq (6-37) is given in Appendix II. As mentioned earlier,

$A|Z$ is a Poisson variate and with mean λZ ; thus, $\text{Var}(A|Z) = \lambda Z$

and $E(A|Z) = \lambda Z$. Substituting into Eq (6-37), we obtain

$$\begin{aligned} \text{VAR}(A) &= E(\lambda Z) + \text{VAR}(\lambda Z) \\ &= \lambda E(Z) + \lambda^2 \text{VAR}(Z). \end{aligned} \quad (6-38)$$

By using Eq (6-38) in Eq (6-35), we finally obtain

$$Nd = \lambda E(Z) + \frac{\lambda^2 E(Z)^2 + \lambda^2 \text{VAR}(Z)}{2(1 - \lambda E(Z))}. \quad (6-39)$$



It has been shown that, (16) although N_d is the expected steady state system queue size at the time of a departure, it is equivalent to the expected steady system queue size at an arbitrary point in time. We denote this by N . Thus,

$$N = \lambda E(Z) + \frac{\lambda^2 \text{Var}(Z) + \lambda^2 (E(Z))^2}{2(1 - \lambda E(Z))}. \quad (6-40)$$

Eq (6-40) is often referred to as the Pollaczak-Khintchine formula. From it the expected waiting time in the system $E(W)$ (which includes the merging delay) can be obtained through the well-known Little's formula:

$$N = \lambda E(W), \quad (6-41)$$

or

$$E(W) = \frac{N}{\lambda}. \quad (6-42)$$

If $E(V)$ is the average waiting time for a vehicle before merging, then

$$E(V) = \frac{N}{\lambda} - E(Z). \quad (6-43)$$

The result of N and $E(W)$ under different T and different λ for different cases is shown in Tables 6-6 and 6-7.

Capacity and the Best Location of the Minor Stream

In calculating the capacity of the minor stream, it is assumed that a queue always exists on the minor street. For the installation of an entrance downstream from the signal, such as the entrance to a parking lot or shopping center, capacity at the entrance point would be expected to be the maximum. As before, the critical gap is T , and the move up time is v (which is the time required by the



Table 6-6. Calculate the Expected Queue Size N.

	$\lambda = 1/5$				$\lambda = 1/10$				$\lambda = 1/20$			
	T = 2	T = 3	T = 4		T = 2	T = 3	T = 4		T = 2	T = 3	T = 4	
NHL ₁	0.1026	1.8981	∞		0.0437	0.4812	∞		0.0201	0.1667	6.1558	
NHL ₂	0.0760	0.9548	∞		0.0337	0.2892	45.8117		0.0158	0.1099	2.0316	
NHL ₃	0.0685	0.4284	74.1148		0.0274	0.1547	1.9965		0.0131	0.0649	0.4992	
NHL ₄	0.0588	0.4250	61.6593		0.0269	0.1537	1.9552		0.0128	0.0646	0.4922	
HL ₁	0.2073	10.1207	∞		0.0848	1.1833	∞		0.0382	0.3467	∞	
HL ₂	0.1678	9.0993	∞		0.0711	1.1047	∞		0.0326	0.3316	∞	
HL ₃	0.1412	2.9341	∞		0.0614	0.6333	∞		0.0285	0.2186	26.4041	
HL ₄	0.1342	2.4118	∞		0.0586	0.5624	∞		0.0274	0.1997	9.3717	

Table 6-7. Calculate $E(w) = N/\lambda$

	$\lambda = 1/5$				$\lambda = 1/10$				$\lambda = 1/20$			
	T = 2	T = 3	T = 4	T = 2	T = 3	T = 4	T = 2	T = 3	T = 4	T = 2	T = 3	T = 4
NHL ₁	0.5130	0.4905	∞	0.4374	4.8120	∞	0.4014	3.3344	123.1160	0.4014	3.3344	123.1160
NHL ₂	0.3800	4.7740	∞	0.3370	2.8920	458.1170	0.3164	2.1996	40.6320	0.3164	2.1996	40.6320
NHL ₃	0.3420	2.1420	370.5740	0.2743	1.5467	19.9650	0.2612	1.2996	9.9840	0.2612	1.2996	9.9840
NHL ₄	0.2940	2.1250	313.2965	0.2686	1.5374	19.5520	0.2563	1.2920	9.8440	0.2563	1.2920	9.8440
HL ₁	1.0365	50.6035	∞	0.8480	11.8330	∞	0.7637	6.9360	∞	0.7637	6.9360	∞
HL ₂	0.8390	45.4965	∞	0.7114	11.0475	∞	0.6520	6.6320	∞	0.6520	6.6320	∞
HL ₃	0.7060	14.6705	∞	0.6136	6.3330	∞	0.5708	4.3720	528.0820	0.5708	4.3720	528.0820
HL ₄	0.6710	12.0590	∞	0.5860	5.6240	∞	0.5472	3.9940	187.4340	0.5472	3.9940	187.4340



second vehicle to move up to the first position after the first vehicle has left). Hence, with probability

$$\int_0^T f(t) dt \quad (6-44)$$

a gap is less than the critical gap. In general, for a gap of size $(T + (j-1)v, T + jv)$ with probability

$$\int_{T + (j-1)v}^{T + jv} f(t) dt, \quad (6-45)$$

j vehicles will enter the intersection. Thus, the capacity while the platoon is passing is

$$C_1 = q \sum_{j=1}^{\infty} j \int_{T + (j-1)v}^{T + jv} f(t) dt \quad (\text{veh/sec}). \quad (6-46)$$

If the move up time is v then the capacity during "idle" time is $\frac{1}{v}$ veh/sec. Thus, the overall capacity becomes

$$C = C_1 p + 1/v (1-p). \quad (6-47)$$

Since C_1 and p both vary with distance from the nearest signal, a table can be constructed showing the capacity at different distances from the signal for different average platoon sizes.

Assuming the move-up time to be two seconds, the result of C is tabulated in Table 6-8. For a specific value of critical gap T , the overall capacity is almost equivalent for different locations from the signal. Also, the capacity during the passing time is an increasing function and approaches steady state from 350 yards. The capacity during the idle time is a decreasing function and approaches

steady state from 350 yards.

Table 6-8. Calculated Capacity for Different T.

	T = 2	T = 3	T = 4	T = 5
NHL ₁	0.4444	0.4053	0.3850	0.3879
NHL ₂	0.4437	0.3996	0.3780	0.3726
NHL ₃	0.4352	0.3957	0.3520	0.3540
NHL ₄	0.4362	0.3957	0.3655	0.3535
HL ₁	0.4067	0.3498	0.3307	0.3266
HL ₂	0.4098	0.3390	0.3168	0.3113
HL ₃	0.4076	0.3351	0.3039	0.2967
HL ₄	0.4087	0.3362	0.3029	0.2947

During the calculation of C, it can be seen that almost 80 percent of the capacity was from idle time. One of our assumptions is that no mainstream vehicles are allowed between platoons. If that assumption is relaxed and mainstream vehicles are allowed passing during the idle time, we would expect the capacity during idle time to be an increasing function, the same as the capacity for passing time. In that case overall capacity would reach a maximum at 350 yards. That is the best location for the entrance when the mainstream vehicles are allowed passing between platoons.



The Required Distance for Recovering the Shape of the Headway

Distribution:

After the minor stream vehicles enter the main stream, the shape and the parameters of the headway distribution change. In this section, we will investigate the distance required by the new platoon (with the entering vehicles) to recover the original headway distribution after dispersion.

For the input vehicles, we consider only those vehicles waiting to enter the main traffic when a platoon is passing. If d and n are given, the passing time for the whole platoon is

$$\sum_{i=1}^n W_i = n \bar{w}, \quad (6-48)$$

where \bar{w} is the mean headway within the platoon. Thus, $\lambda \sum_{i=1}^n W_i$ vehicles will arrive to enter the mainstream during the passing time.

If the capacity $C_1 \sum_{i=1}^n W_i$ (see the last section; here we only consider the passing time) is greater than $\lambda \sum_{i=1}^n W_i$, then $\lambda \sum_{i=1}^n W_i$ vehicles will enter the mainstream during the platoon passing time. If $\lambda \sum_{i=1}^n W_i$ is less than $C_1 \sum_{i=1}^n W_i$, then $C_1 \sum_{i=1}^n W_i$ vehicles will enter the mainstream, and $(\lambda - C_1) \sum_{i=1}^n W_i$ vehicles will wait until the platoon has passed.

In the case where $\lambda \sum_{i=1}^n W_i$ vehicles enter the mainstream, platoon size becomes $((n+1) + \lambda \sum_{i=1}^n W_i)$. Using the model developed in the last section of chapter 5, the required distance can be determined.

In the case where demand exceeds the capacity during the passing time, only $C_1 \sum_{i=1}^n W_i$ can enter the traffic while the platoon is

passing. The new platoon size then is $((n + 1) + C_1 \sum_{i=1}^n W_i)$. Similarly, from chapter 5, we obtain the required distance.

An example will clarify how the models developed in chapter 5 can be used in this section. Suppose $\lambda=1/10$, the critical time gap is two seconds, and the entering point is 350 yards from the signal. Then

$$\lambda \sum_{i=1}^n W_i = \lambda n \bar{W} = 2.69 \approx 2 \text{ vehicles,}$$

and

$$C_1 \sum_{i=1}^n W_i = C_1 n \cdot \bar{W} = 7.4 \approx 7 \text{ vehicles,}$$

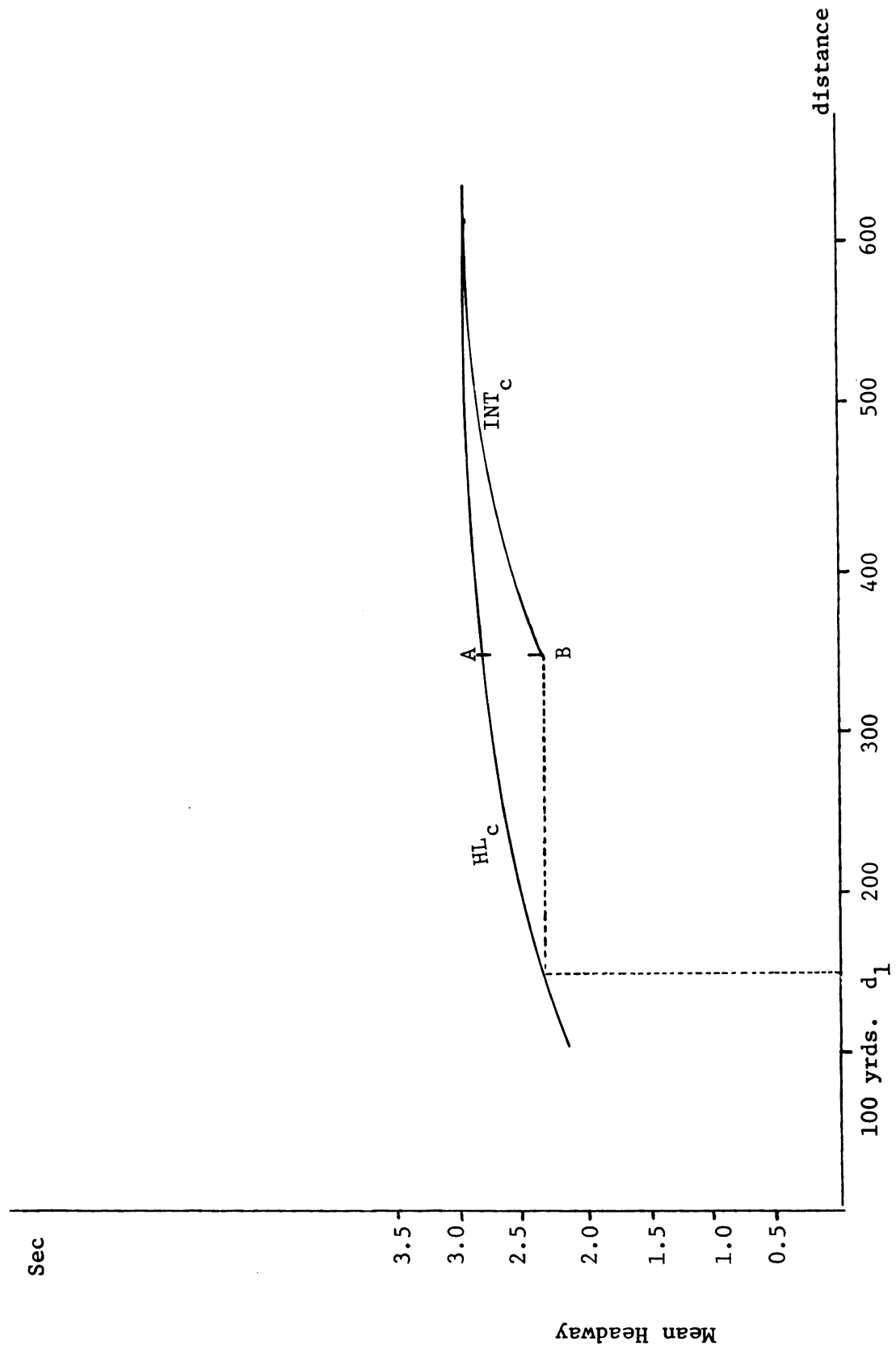
where the platoon is assumed to be in heavy flow. That means all two vehicles would be allowed to enter the mainstream while the platoon is passing. Platoon size after the minor street vehicles enter then becomes $((n + 1) + \lambda \sum_{i=1}^n W_i)$, which is equal to 14 vehicles. Therefore, with the same passing time $\sum_{i=1}^n W_i$, the platoon now consists of 14 vehicles. The average headway of the new platoon then became $\sum_{i=1}^n W_i / (\text{number of vehicles} - 1)$, or 2.08 seconds.

Referring to Figure 6-1, the mean headway would change from A to B after the minor street vehicles entered. We could also say the platoon is in the situation of being located at d_1 , since at d_1 the mean headway would be the same as B. According to the platoon dispersion behavior, the platoon would need $(350 - d_1)$ yards to recover its mean headway of A.

Splitting Flow to Reduce Delay of the Entering Vehicles:

In this section we will consider the problem of splitting the queue into two or more queues to reduce the delay of a queue of

Figure 6-1. Translation of INT_C



vehicles waiting to enter the mainstream traffic. The analysis uses the results of section three of this chapter, that is, the average waiting time in the system $E(W)$. If we split the queue into two streams, then we assume that the distance between the two entry points is sufficiently large so that the headway distribution returns to steady state after the first queue entry. While the technique developed in the section is applicable to any number of successive entry points, our discussion is limited to the possibility of splitting the queue into three entry streams.

Assuming θ to be the rate of splitting, where $0 \leq \theta \leq 1$, that is, if the rate of the minor street random arrival is λ , then we split the arrival into two Poisson streams, with arrival rate $\lambda \theta$ for the first entry and $(1 - \theta) \lambda$ for the second entry (if two streams are to be made). We then determine the optimal splitting, θ_{opt} .

For the case of two entry points, let us denote the distance of the first entry point from the signal as d_1 and the second as d_2 . If the average platoon size is n , then at d_1 the average waiting time in the system $E(w|d_1)$ is a function of d_1 , $\theta\lambda$, and n :

$$E(w|d_1) = f(d_1, n, \theta\lambda). \quad (6-49)$$

The average waiting time in the system at d_2 is

$$E(w|d_2) = g(d_2 - d_1, n + h(\theta\lambda), (1 - \theta)\lambda). \quad (6-50)$$

Eq (6-50) depends on $(d_2 - d_1)$, not d_2 alone, because there are vehicles entering upstream of d_2 . The calculation of the parameters of the platoon reaches point d_2 is different from the calculation of Eq (6-49).

The term $h(\theta\lambda)$ depends on the capacity at d_1 ; if arrivals at d_1 exceed capacity C , then C vehicles will enter the traffic; otherwise

θ λ will enter.

Eq. (6-49) and (6-50) are used to calculate the total mean waiting time in the system as a function of the parameters:

$$T(\theta) = \theta \cdot E(w|d_1) + (1-\theta)E(w|d_2). \quad (6-51)$$

Blumenfeld and Weiss suggested a parameter δ , (13) which can measure the improvement effected by queue splitting, that is,

$$\delta_{\theta} = \frac{T(1) - T(\theta)}{T(1)}. \quad (6-52)$$

The smaller the value of δ_{θ} , the greater the improvement effected by queue splitting.

Using the data from field studies, and assuming θ to be equal to $\frac{1}{2}$, $\frac{1}{3}$, $\frac{2}{3}$, $\frac{1}{4}$, and $\frac{3}{4}$. $\delta_{\frac{1}{2}}$, $\delta_{\frac{1}{3}}$, $\delta_{\frac{2}{3}}$, $\delta_{\frac{1}{4}}$, and $\delta_{\frac{3}{4}}$ are calculated by using Eq (6-52). The critical gap T is assumed to be 3 seconds. The result is shown in Table 6-9. There it is found that equal splitting, $\theta = \frac{1}{2}$, is the optimum splitting for two entry points.

Similar calculations are performed for splitting minor traffic into three streams. Assuming that equal splitting was better than the other splittings in three entry points.

Let d_1 , d_2 , and d_3 be the distances of three entry points. We have

$$T(\theta) = \theta_1 E(w|d_1) + \theta_2 E(w|d_2) + \theta_3 E(w|d_3), \quad (6-53)$$

where $\theta_1 + \theta_2 + \theta_3 = 1$, and θ_1 , θ_2 , and θ_3 are the splitting of the three entry points, respectively. The critical gap is assumed to be 3 seconds, and $\delta(1/3 \ 1/3 \ 1/3)$ is calculated. The results are shown in Table 6-10. It is found that $\delta(1/3 \ 1/3 \ 1/3)$ is better than $\delta_{\frac{1}{2}}$.

Table 6-9. Calculate $\delta \theta$ for Different θ λ .

	Splitting	NHL ₁	NHL ₂	NHL ₃	NHL ₄	HL ₁	HL ₂	HL ₃	HL ₄
$\lambda=1/5$	$(\frac{1}{2}, \frac{1}{2})$	0.5498	0.8019	1.6730	1.6850	0.1525	0.1632	0.4075	0.4663
	$(2/3, 1/3)$	0.5903	0.8070	1.2680	1.2750	0.2604	0.2697	0.4786	0.5555
	$(1/3, 2/3)$	0.6740	1.3006	2.6441	2.6310	0.1559	0.1702	0.4623	0.5555
	$(3/4, 1/4)$	0.6379	0.8929	1.1037	1.0840	0.3365	0.3452	0.5439	0.5808
	$(1/4, 3/4)$	0.7206	1.3728	2.9552	2.9778	0.1529	0.1684	0.4838	0.5808
$\lambda=1/10$	$(\frac{1}{2}, \frac{1}{2})$	0.7614	1.0708	1.7112	1.7191	0.4118	0.4309	0.6394	0.7101
	$(2/3, 1/3)$	0.7714	1.1540	1.7622	1.7672	0.5663	0.5806	0.7081	0.7679
	$(1/3, 2/3)$	0.8527	1.3120	2.2880	2.3006	0.4280	0.4526	0.6977	0.7679
	$(3/4, 1/4)$	0.8026	1.1650	1.7317	1.7356	0.6438	0.6551	0.8740	0.7811
	$(1/4, 3/4)$	0.8795	1.3922	2.4882	2.5024	0.4121	0.4382	0.7042	0.7811



The determination of splitting of the entry point not only depends upon the delay time, but also is a tradeoff between the costs and benefits from the splitting. Therefore, we cannot conclude that splitting into three is better than splitting into two, only that the delay time is decreased.

Table 6-10. Calculate δ (1/3,1/3,1/3) for Different λ .

	NHL ₁	NHL ₂	NHL ₃	NHL ₄	HL ₁	HL ₂	HL ₃	HL ₄
$\lambda=1/3$	0.2124	0.5427	1.4109	1.4249	*	*	*	0.1547
$\lambda=1/5$	0.4628	0.8811	1.6740	1.6688	0.1163	0.1262	0.3257	0.3894
$\lambda=1/10$	0.6958	1.0515	1.7998	1.8095	0.3642	0.3843	0.5785	0.6337

* Approaching zero due to infinity delay occurred in T(1).



CHAPTER SEVEN

SIMULATION ANALYSIS OF THE PROBLEM

Introduction:

The analytic results of the behavior of vehicles entering into stream with a dispersing platoon were developed in chapter 6. To validate the model, an experiment was performed. Verification of the entire range of the model would require extensive data at various volume levels, for the mainstream and entering traffic. It would be almost impossible to obtain sufficient data through field studies. Therefore, a computer simulation which could duplicate the real world situation was written.

A simulation model consists of two basic phases: input data generation and bookkeeping data generation. The Monte Carlo technique was used here to generate random events from some specified probability distribution. The models employed an event-oriented bookkeeping technique, updating the system status when events occur, recording relevant items, and calculating measures of the parameters of interest.

The analysis conducted for this study was divided into three stages. In the first stage a model was developed of a single unsignalized intersection at which vehicles were arriving from two directions, and right-of-way was given to the mainstream. The second



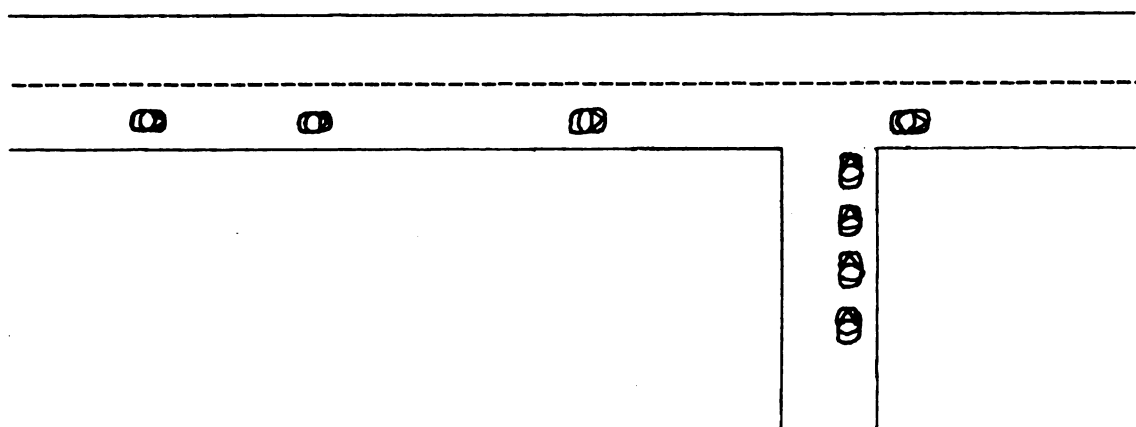
stage expanded the model to include a signalized intersection with a single sidestreet downstream. With this model, the simulation of platoons leaving the intersection every signal cycle and arriving at the sidestreet was conducted. The final stage was the extension of the second stage to include multiple entrances downstream from the signalized intersection.

The simulation models were designed such that the final results of the parameters of interest could be compared with the prior result to determine that steady state was reached. The programs were written in Fortran, and they were run on the CDC 6500 at Michigan State University.

Development of the Phase One Model:

The intersection used in the phase one simulation model was T-shaped, and the sidestreet was assumed to be a one-way street. Since it was established by Nemeth and Vecellio (1972) that the number of lanes exhibits no significant effect on platoon behavior, one lane of travel was assumed in the simulation model. To see the effect of entering vehicles on platoon dispersion, only right turns were permitted on the sidestreet. The physical characteristics of the phase one model are shown in Figure 7-1. Major street vehicles were given the right-of-way over entering vehicles whenever conflicts in entering occurred. Entering vehicles decelerated to a stop either at the intersection or in queue behind other stopped vehicles. It was assumed that an entering driver waiting to enter considers each time gap t in the mainstream traffic until he finds an acceptable



Figure 7-1. Physical Characteristics of Phase One Model Intersection.

gap T, which he believes to be of sufficient length to permit his safe entry. Blumenfeld and Weiss (4) have shown that this assumption of a fixed critical gap is fairly realistic for estimating delays and capacities.

Two input sources are involved in the present model: sidestreet arrivals and mainstreet arrivals. A common assumption made by many researchers (25) (14) is that arrivals from the sidestreet are random. In chapter 6 it was shown that the mainstreet headway conforms to a gamma distribution. Thus, for the simulation model, the interarrival time of the mainstreet vehicles was gamma distributed and that of side-street vehicles was random. The move-up time of the second vehicle in the sidestreet when the first vehicle entered traffic was assumed to be two seconds. Three parameters for the entering vehicles were recorded and measured in the simulation runs: average merging delay, average queue length and average total delay.

Briefly, the simulation was processed as follows. First, a side-street vehicle was generated, and its arrival time was recorded. Mainstreet vehicles were generated until it was found that the arrival



time of the sidestreet vehicle lay between the arrival time of two successive mainstreet vehicles. The critical gap was then compared to the available lag. If the lag was rejected, successive mainstreet headway was generated and compared to the critical gap until an acceptable gap was found. The time spent in the merging position was recorded, and another sidestreet vehicle was generated and checked to determine whether its arrival time preceded the leaving time of the prior vehicle. If not, no delay was recorded as occurring before moving into the merging position; if so, this delay was recorded. The process was repeated and new traffic was generated until the steady state solution was obtained. The logic flow diagram for the process is shown in Figure 7-2.

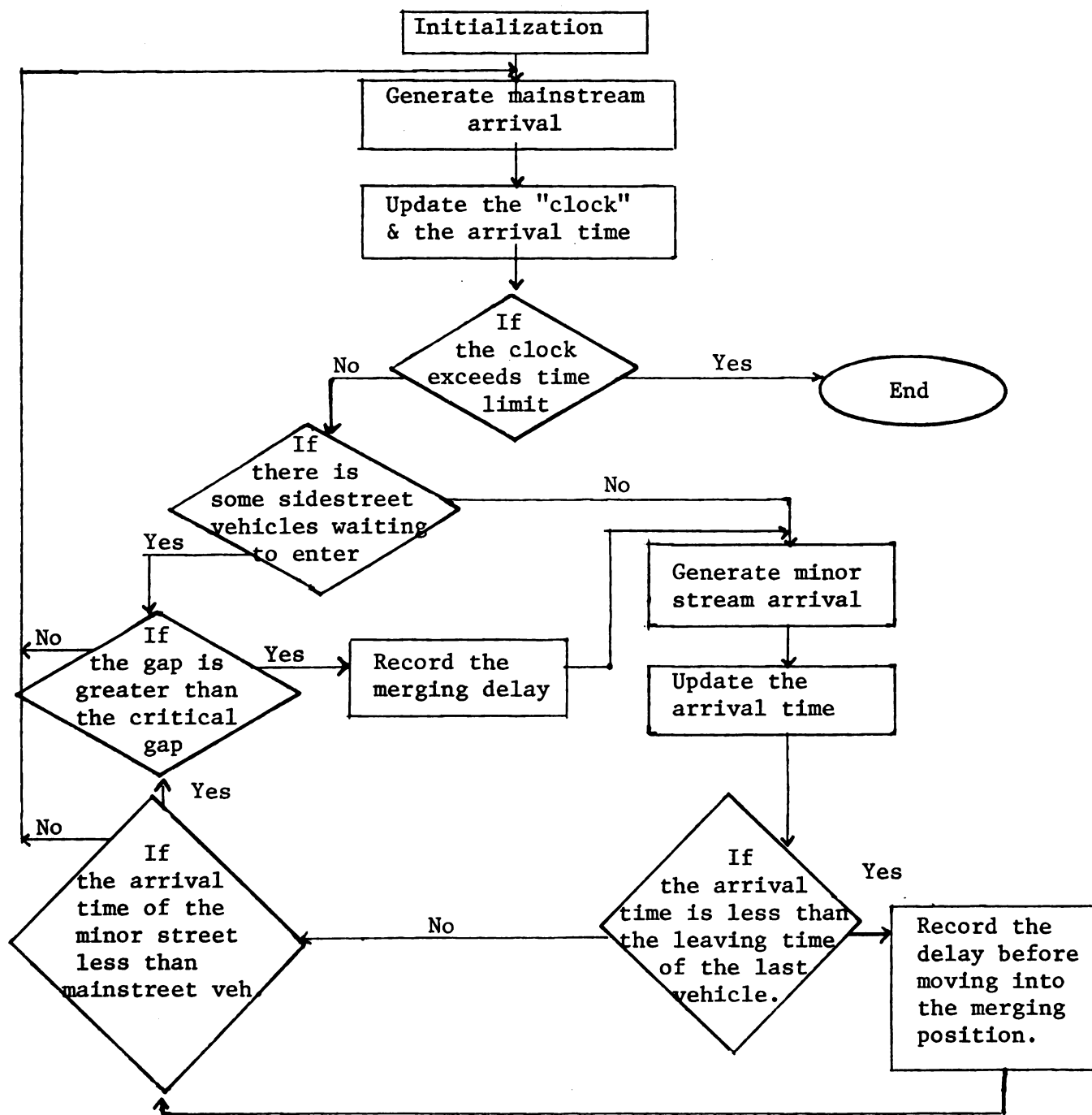
The program was run under different conditions for comparison with the analytic solution from chapter 6.

The results of the simulation program are shown in Table 7-1.

Table 7-1. Simulation Results of Phase One Model.

	Average Merging Delay		Average Delay Before Merging	
	Q = 350 vph	Q = 800 vph	Q = 350 vph	Q = 800 vph
T = 2	0.7011	1.9362	0.2211	0.4225
T = 3	4.2420	7.2350	8.1240	738.3500
T = 4	16.2400	42.2631	1024.5000	2104.0000

Note: Q = mainstream volume.

Figure 7-2. Flow Diagram for Phase One Model.



The results from Table 7-1 were run under a mainstreet volume 350 vph and 800 vph. On the average, this meant approximately 6 and 13 vehicles in the respective platoons. Minor street vehicles were assumed to arrive at the rate of 5 sec/veh., the entrance point was assumed to be 500 yards from the prior signal, and critical time gaps were assumed to be 2, 3, and 4 seconds. The simulation program is listed in Appendix IV.

The comparable analytic solutions were those formulas in chapter 6 with $p = 1$, that is, under 100 percent passing time. The mainstreet vehicles were passing the intersections at the same volume levels and critical gaps used in Table 7-1, and the results are shown in Table 7-2.

Table 7-2. Analytical Results of Phase One Model.

	Average Merging Delay		Average Delay Before Merging	
	Q = 350vph	Q = 800vph	Q = 350vph	Q = 800vph
T = 2	0.8141	1.2343	0.1882	0.4635
T = 3	3.5847	6.8330	9.6910	∞
T = 4	15.8166	39.2631	∞	∞

By the assumption of the analytical model, if the service rate is greater than the arrival rate, the average delay before merging will approach infinity. Therefore, three infinity delays appear in Table 7-2.

To compare the results of the two models (analytical and simulation), a standardized statistical test was introduced to indicate



the reliability of the model forecasts. The U-statistic (16) measures the statistical correlation between two sets of data; it measures the agreement between the forecast (analytical) and observed (simulation) item frequencies. The accuracy of the forecast is judged by the magnitude of the U - value. If the discrepancy between the observed and predicted mean values of the level of activity in a cell is small, there still could be poor agreement between measured and predicted results in individual cells, and the U - statistic can measure their significance.

The U-statistic is calculated as

$$U = \frac{\left\{ \frac{1}{n} \sum_{i=1}^n (S_i - C_i)^2 \right\}^{\frac{1}{2}}}{\left\{ \frac{1}{n} \sum_{i=1}^n (S_i)^2 \right\}^{\frac{1}{2}} + \left\{ \frac{1}{n} \sum_{i=1}^n (C_i)^2 \right\}^{\frac{1}{2}}}, \quad (7-1)$$

where S_i = the projected value of the i th cell;
 C_i = the observed value for the i th cell; and
 n = the number of cells in the distribution.

In general, a value of U less than 0.1 is considered good, a value between 0.1 and 0.3 average, and a value of greater than 0.3 poor.

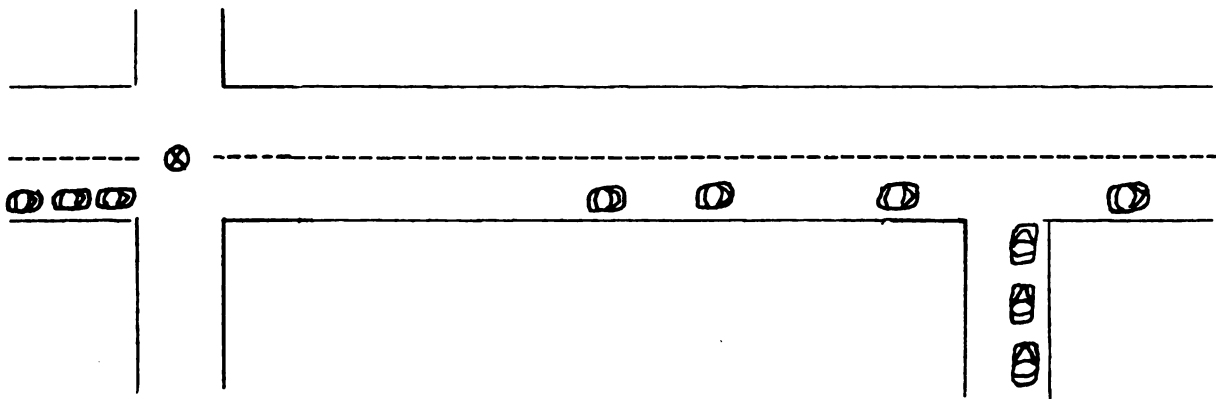
For the phase one model, the U-statistic was calculated for the average merging delay and the average delay before merging. It was found that the U-statistic for the average merging delay was 0.0518. The U-statistic for the average delay before merging was calculated using only finite values because of the possible infinity delay when the service rate is greater than the arrival. The U-statistic for the average delay before merging was 0.0878. Therefore, the reliability

of the analytical model for both delay parameters can be considered good. Thus, the phase one model can be used as the basis for development of the phase two and phase three models.

Development of the Phase Two Model:

The phase two model was developed to simulate a signalized intersection with a single downstream entrance. The physical characteristics of the model are shown in Figure 7-3.

Figure 7-3. Physical Characteristics of Phase Two Model.



The model was constructed to simulate the following conditions for the signalized intersection; (1) cycle length of 60 seconds, and (2) effective green time of 40 seconds.

A constant travel time (t) was assumed for the leading vehicle of the platoon traveling from the signalized intersection to the entrance, where $t = d / s$ (d is the distance of the entrance point from the signalized intersection, and s is the average speed of the vehicles, assumed here to be 30 mph).

The interarrival time for the vehicles at the signalized intersection and the entrance was assumed to be gamma distributed. At

the intersection, the starting delay was also considered. This was defined as the amount of time lost as successive vehicles in the queue moved across the intersection. The values determined by Greenshield, shown in Table 7-3, were used (12).

Table 7-3. Greenshield's Starting Delay.

Vehicle	Starting delay, in seconds
1	3.8
2	3.1
3	2.7
4	2.4
5	2.2
6	2.1
.

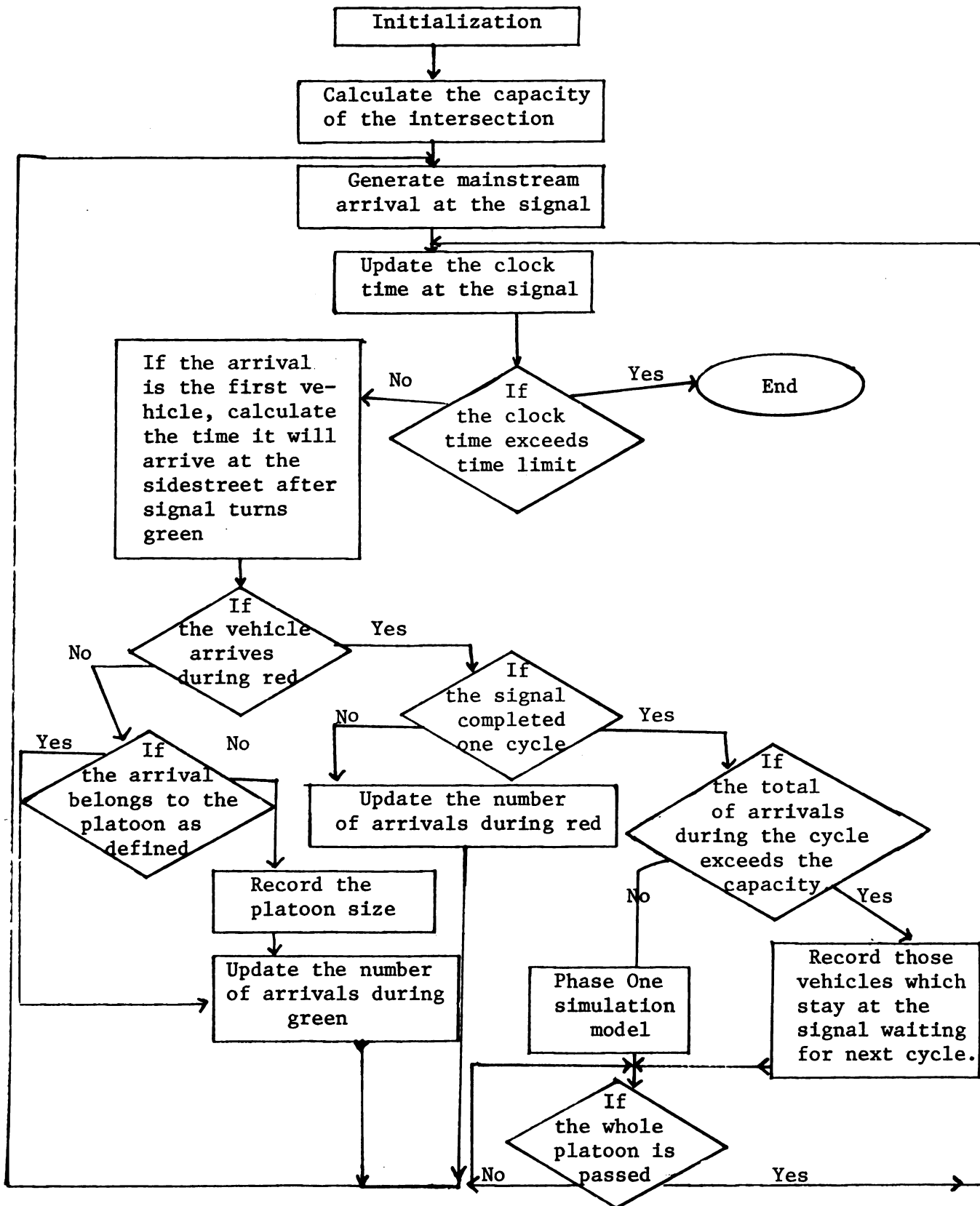
The merging operation of the entering vehicles of this model were considered to be the same as for the model developed for phase one, with the added condition that vehicles could enter the traffic freely between platoons. Thus, the average delay statistics from this model should be less than the average delay statistics from the phase one model.

The size of each platoon was recorded, with only those vehicles joining the queue within two seconds after the last stopped vehicle

left the intersection included in the definition. This information was used as input data for the dispersion model derived in chapter 5 and indicated the value of the headway parameters. The number of vehicles leaving the signal each cycle included those waiting in the queue during the red time plus those arriving during the green time. If the queue was so long that only a portion of it was permitted to leave the signal during the green time, then only those leaving vehicles were counted. Thus, the number of vehicle leaving the intersection in the simulation program for each signal cycle might be different from the "platoon size" defined previously. This platoon size was an input for the model.

When the signal turned green, vehicles were discharged from the intersection, and the first vehicle's arrival time at the entrance was calculated. Starting with this vehicle's arrival, headways with the parameters derived from the dispersion model in chapter 6 were generated. The entering process of the sidestreet vehicles followed the model developed for phase one. The passing vehicles in the mainstream were counted until all vehicles passed, at which time vehicles could enter freely between platoons. Average delay and queue statistics of the entering vehicles were recorded. The flow diagram of the phase two model is shown in Figure 7-4.

The program was run with different values for the critical gaps (2, 3, and 4 seconds), different levels of volume for the mainstreet (350 vph and 800 vph) and sidestreet (5 sec/veh. and 10 sec/veh.), and different locations of the entrance point (200 and 500 yards from the signal). The simulation program is listed in Appendix IV. The

Figure 7-4. Flow Diagram of Phase Two Model.

results of the simulation program are shown in Table 7-4.

Assuming the input source from the minor street to be a large value, the capacity at the entrance point would be equal to the total number of vehicles entering the mainstream traffic. The result is shown in Table 7-5.

Development of the Phase Three Model:

The extension of the single entrance model to one having more than one entrance was accomplished by defining a set of characteristics for each entrance added to the model. The physical characteristics of the model are shown in Figure 7-5. Two entrances downstream from the signalized intersection were assumed, with the merging traffic divided between two points. The assumptions for the second entrance were the same as in the analytic model in chapter 6, that is, the distance between the first and second entrance was assumed to be sufficient for the headway distribution to return to a steady state. Different levels of entrance flow and mainstream volume and different critical acceptance gaps were used as input to the simulation model under different entering flows. The flow diagram for the phase three model is shown in Figure 7-6.

The program was run with different values for entering splitting ($1/2$, $2/3$, and $3/4$). Different levels of mainstream volume (350 vph and 800 vph), and equal critical gap for the two entrances (3 seconds). The results of the simulation model are shown in Table 7-6. The comparison with the analytical results will be shown in the next section. The simulation program for the phase three model is listed in Appendix IV.

Table 7-4. Simulation Results of Phase Two Model.

				Average Merging Delay	Average Delay Before Merging
T = 2	d=200 yds.	$\lambda=1/5$	Q = 350	0.3124	0.1036
			Q = 800	0.6204	0.3045
		$\lambda=1/10$	Q = 350	0.3396	0.0824
			Q = 800	0.6572	0.1356
	d=500 yds.	$\lambda=1/5$	Q = 350	0.3824	0.0924
			Q = 800	0.6210	0.2013
		$\lambda=1/10$	Q = 350	0.3004	0.0625
			Q = 800	0.5931	0.1103
T = 3	d=200 yds.	$\lambda = 1/5$	Q = 350	1.8240	8.2436
			Q = 800	4.5362	45.5210
		$\lambda = 1/10$	Q = 350	1.6680	1.7523
			Q = 800	4.3210	8.0312
	d=500 yds.	$\lambda = 1/5$	Q = 350	1.4362	1.5024
			Q = 800	3.1124	11.2437
		$\lambda=1/10$	Q = 350	1.5341	0.6614
			Q = 800	3.0163	2.9326
T = 4	d=200 yds.	$\lambda = 1/5$	Q = 350	10.3651	845.6428
			Q = 800	24.1450	2410.2500
		$\lambda=1/10$	Q = 350	10.8765	532.7321
			Q = 800	23.6450	1172.6410
	d=500 yds.	$\lambda=1/5$	Q = 350	5.0210	357.3756
			Q = 800	19.3620	987.8800
		$\lambda = 1/10$	Q = 350	5.2524	22.8014
			Q = 800	20.2371	637.7875

Table 7-5. Simulation Results of Capacity.

			Capacity (veh/hr.)
T = 2	d = 200	Q = 350	1432
		Q = 800	1420
	d = 500	Q = 350	1483
		Q = 800	1415
T = 3	d = 200	Q = 350	1284
		Q = 800	1110
	d = 500	Q = 350	1324
		Q = 800	1138
T = 4	d = 200	Q = 350	1321
		Q = 800	1054
	d = 500	Q = 350	1217
		Q = 800	980

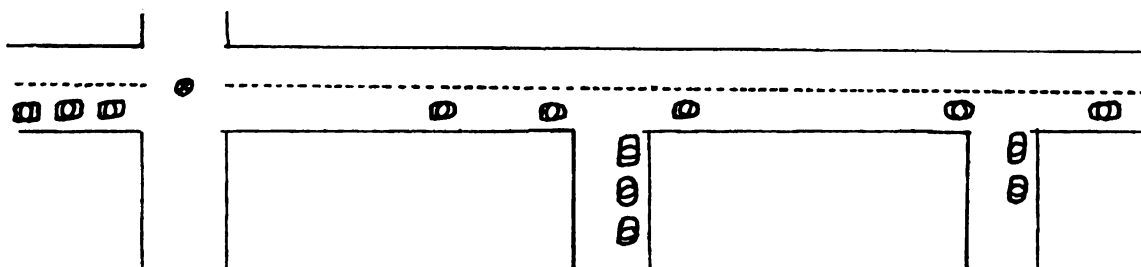
Figure 7-5. Physical Characteristics of Phase Three Model.

Figure 7-6. Flow Diagram of Phase Three Model.

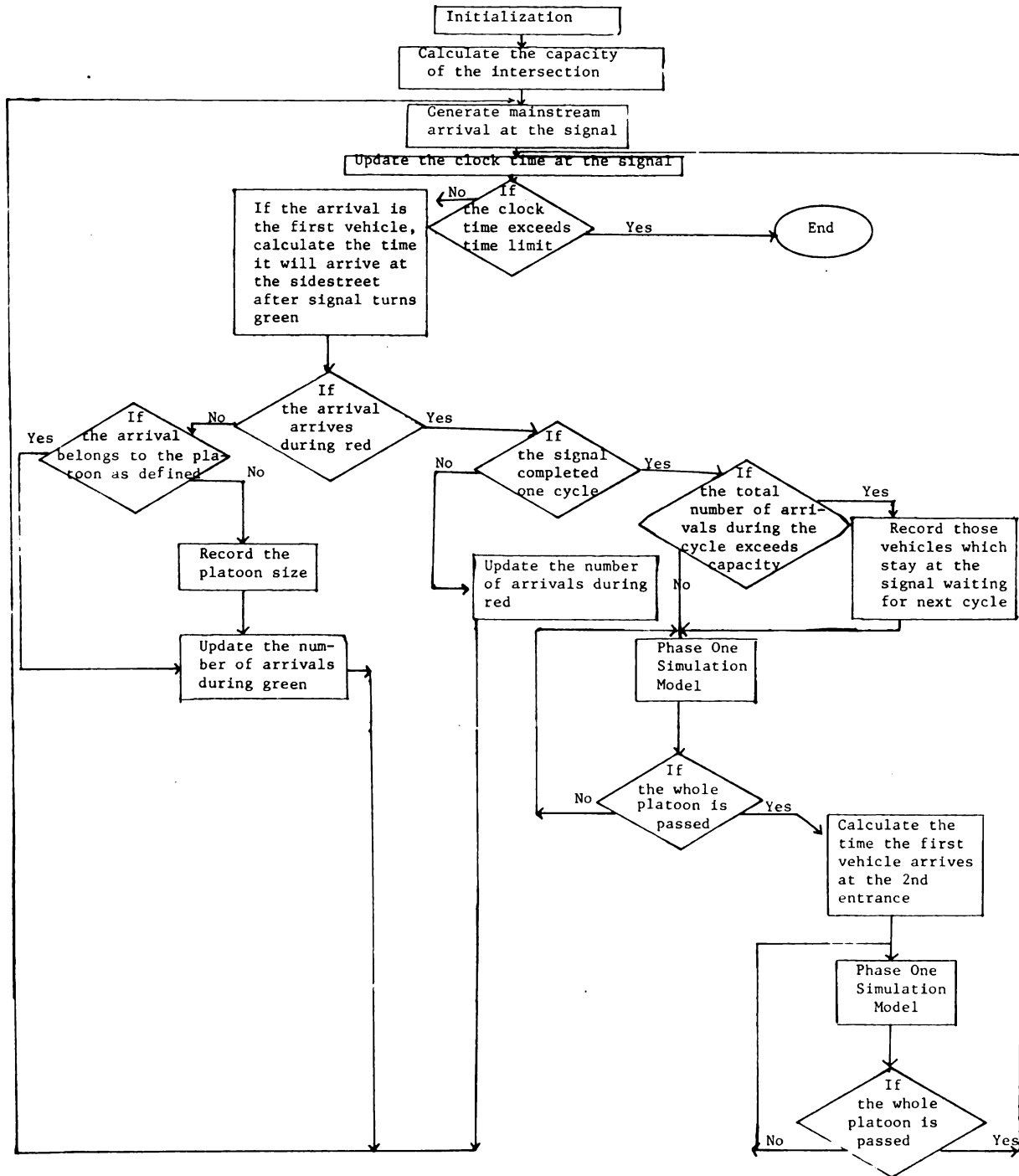


Table 7-6. Simulation Results of the Phase Three Model.

		Splitting	Average delay in the system
Q = 350	$\lambda = 1/5$	(1/2,1/2)	4.2139
		(2/3,1/3)	3.1056
		(3/4,1/4)	2.8314
	$\lambda = 1/10$	(1/2,1/2)	2.7652
		(2/3,1/3)	2.8042
		(3/4,1/4)	2.2981
Q = 800	$\lambda = 1/5$	(1/2,1/2)	6.1021
		(2/3,1/3)	8.1034
		(3/4,1/4)	7.7830
	$\lambda = 1/10$	(1/2,1/2)	4.2310
		(2/3,1/3)	4.8248
		(3/4,1/4)	5.3214

Evaluation of the Results:

For both the phase 2 and phase 3 models, the delay parameters and capacity were calculated using the analytical model developed in chapter 6; the results are shown in Tables 7-7, 7-8, and 7-9. After comparing the simulation results, the U-statistics was obtained and is shown in Table 7-10.

It was found that the predicted results from the analytical models agreed with the observed values from the simulation models. It was also found that the delay parameters from the analytical model were dominated by the results from the simulation models. This was because the assumption of platoon size differed between two phase models. In the analytical model, platoon size was composed of those vehicles waiting in the queue and joining the queue within two seconds after the last vehicle left the intersection. In the simulation model, platoon size was based on the total number of arrivals during a cycle. Therefore, more vehicles would pass through the downstream entrance point, and more delay and less capacity would occur. Since the U-statistic showed the differences between the analytical and simulation models were not significant, the feasibility of the platoon size assumption in the analytical model is implied.

Table 7-7. Analytical Results of Phase Two Model.

				Average Merging Delay	Average Delay Before Merging
T = 2	d=200 yds.	$\lambda=1/5$	Q = 350	0.2964	0.0836
			Q = 800	0.5987	0.2403
		$\lambda=1/10$	Q = 350	0.2964	0.0406
			Q = 800	0.5987	0.1127
	d=500 yds.	$\lambda=1/5$	Q = 350	0.2444	0.0496
			Q = 800	0.5103	0.1607
		$\lambda=1/10$	Q = 350	0.2444	0.0242
			Q = 800	0.5103	0.0757
T = 3	d=200 yds.	$\lambda=1/5$	Q = 350	1.6197	7.8707
			Q = 800	3.9739	41.5226
		$\lambda=1/10$	Q = 350	1.6197	1.2723
			Q = 800	3.9739	7.0736
	d=500 yds.	$\lambda=1/5$	Q = 350	1.0761	1.0489
			Q = 800	2.8254	9.2336
		$\lambda=1/10$	Q = 350	1.0761	0.4613
			Q = 800	2.8254	2.7986
T = 4	d=200 yds.	$\lambda=1/5$	Q = 350	9.2482	∞
			Q = 800	21.9450	∞
		$\lambda=1/10$	Q = 350	9.2482	448.8688
			Q = 800	21.9450	∞
	d=500 yds.	$\lambda=1/5$	Q = 350	4.7481	308.5483
			Q = 800	16.2352	∞
		$\lambda=1/10$	Q = 350	4.7481	14.8039
			Q = 800	16.2353	∞

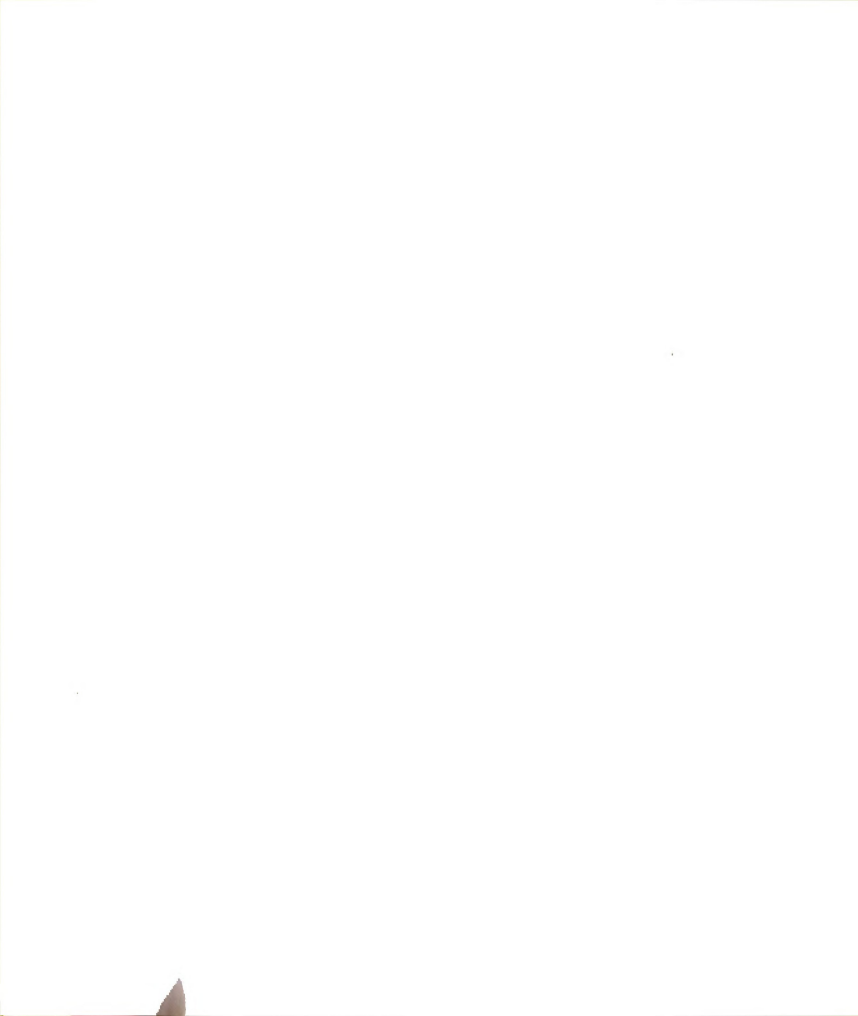


Table 7-8. Analytical Results of Capacity.

			Capacity (veh/hr.)
T = 2	d = 200	Q = 350	1597.32
		Q = 800	1475.28
	d = 500	Q = 350	1570.32
		Q = 800	1471.32
T = 3	d = 200	Q = 350	1438.56
		Q = 800	1220.40
	d = 500	Q = 350	1424.52
		Q = 800	1210.32
T = 4	d = 200	Q = 350	1360.80
		Q = 800	1140.48
	d = 500	Q = 350	1315.80
		Q = 800	1090.44

Table 7-9. Analytical Results of Phase Three Model.

		Splitting	Average Delay in the System
Q = 350	$\lambda = 1/5$	(1/2,1/2)	3.5807
		(2/3,1/3)	2.7095
		(3/4,1/4)	2.3035
	$\lambda = 1/10$	(1/2,1/2)	2.6430
		(2/3,1/3)	2.1020
		(3/4,1/4)	1.8907
Q = 800	$\lambda = 1/5$	(1/2,1/2)	5.6240
		(2/3,1/3)	6.6995
		(3/4,1/4)	7.0038
	$\lambda = 1/10$	(1/2,1/2)	3.9940
		(2/3,1/3)	4.3190
		(3/4,1/4)	4.3931

Table 7-10. U-statistic for the Comparison of the Analytical and the Simulation Results.

Model	Parameter	U-statistic
Phase 2	Average merging delay	0.06948
	Average delay before merging	0.81900
	Capacity	0.03720
Phase 3	Average delay in the system	0.07360



CHAPTER EIGHT

SUMMARY AND CONCLUSIONS

Summary of Accomplishments:

In this investigation of platoon dispersion dynamics on arterial streets with entering vehicles, vehicular time headway was selected as the parameter for the platoon dispersion model. This parameter was chosen because it describes the interaction between vehicles in the car-following process and the interaction in the merging process.

As stated in chapter 1, this dissertation followed a certain procedure. (1) A preliminary study of vehicular time headway within platoons was made. (2) A stochastic model of vehicular time headways within platoons was developed. (3) Field studies were made of platoon behavior. (4) Platoon dispersion models were developed. (5) Analytical studies were made of platoon dispersion with entering vehicles. (6) Simulation studies of platoon dispersion with entering vehicles were conducted. (7) The analytical and simulation results were compared. Vehicular time headway was modeled by the use of a fitted statistical distribution. Seven distributions which may characterize vehicular headways within platoons were used to test the goodness of fit. Those seven were the (1) negative exponential, (2) shifted negative exponential, (3) normal, (4) shifted lognormal,

(5) gamma, (6) Erlang, and (7) Weibull distributions. Using data from a preliminary study, a Chi-square goodness of fit test was performed, and it was found that the gamma distribution was the best fit.

Based on the statistical headway model and the results of the preliminary study, a field study was performed to investigate the dispersion of platoons leaving a signalized intersection and approaching a traffic signal with or without entering vehicles downstream. Two sites were selected for the field study, one on a section of an arterial street with a cross-street downstream from the signalized intersection and the other an arterial with no nearby cross-street. Locations for collecting data and sample size were determined by the results from the preliminary study.

Nemeth and Vecellio (1971) revealed that a platoon size of over 9 vehicles has no significant effect on mean headway. Therefore, platoon size was grouped into three categories in this field study: under 5 vehicles; 6-9 vehicles; over 9 vehicles, referred to as light, medium, and heavy flow, respectively.

Bleyl found that platoon dispersion is independent of a well-coordinated signal. Therefore, the present study did not consider the well-coordination of the prior signal as a factor in the dispersion of a platoon approaching a signal.

Because of the immediate successive appearance of the headway within a platoon, a movie camera (ARRIFLEX 16S/B) was used to record the platoons as they passed each data point, and the headway between vehicles was recorded.

For the case of moving platoons with entering vehicles downstream, data were only available under heavy flow conditions on main and side streets.

The mean headway at different locations under different platoon sizes was plotted (shown in Figures 5-1, 5-2, and 5-3).

Data analysis used a multiple comparison of means to examine the statistically significant effect of different levels of platoon volume on headway at different locations. It was found that light and medium flow did not have a significant effect on headway. Thus, these two categories were combined into a renamed non heavy flow category.

Data from the field study showed that the relationship between distance and mean headway was non linear. For the platoon leaving from a signal, the curve approached steady state after 350 yards. For the platoon approaching a signal, steady state was reached 300 yards from the next signal.

The polynomial least squares method was used to fit the curves, and the regression equations were fitted using 2 and 3 degrees. The validity of the equations were examined, and the degree was determined by the use of a coefficient of determination. The results were shown in Tables 5-4 and 5-5.

Headway data for the passing mainstream platoon with entering vehicles was only available under heavy flow. The relationship between the mean headway for a passing platoon with entering vehicles and the mean headway of a platoon leaving from a signal under heavy flow was analyzed. The results were used to estimate the mean



headway for a passing platoon with entering vehicles under non heavy flow.

An F-test was performed to test the hypothesis that the curves for a passing platoon with entering vehicles under heavy flow with a constant translation would be identical to the curve for the platoon leaving from a signal. The hypothesis was not rejected, and it was concluded that the curve for platoon dispersion leaving the signal under non heavy flow could be assumed valid for the case of entering vehicles.

To investigate the effect of platoon dispersion from a signal on entering vehicles, an analytical study was performed. Three measures of effectiveness (average merging delay, average delay before merging, and capacity at entrance point) for the entering vehicles were formulated under the influence of platoon dispersion. Using the results, the following determination was made: (1) the best location of the minor stream; (2) the required distance for recovering the shape of the headway distribution after sidestreet vehicles entered; and (3) the optimal splitting of sidestreet flow.

The best entrance location was found to be 350 yards from the signal if mainstream vehicles were allowed passing between platoons. An algorithm for calculating the required distance for recovering the shape of the headway distribution was determined. It was also found that equal splitting was better than non equal splitting for two entrance flows, and that splitting into three streams would offer some improvement over splitting into two.



To validate the analytical results of the behavior of the entering vehicles with dispersing platoons, computer simulation models were developed to replicate the real world situation. Using the U-statistic for comparison of the analytical and simulation results, it was found that their difference was not significant

Applicability of Models:

From the theoretical point of view, the models developed here will be helpful in understanding the complex behavior of traffic.

As a result of the investigation of the platoon dispersion characteristics of traffic leaving from a signalized intersection, approaching a signal, and passing sidestreets with entering vehicles, the models presented here can be used to coordinate successive traffic signals.

The models also can be used in future research in platoon dispersion, perhaps in the areas of entering vehicles permitted to make a left turn, multiple-lane maninstreets which permit lane changing, and the interaction of the opposite platoon dispersions on a two-way street.

APPENDICES

APPENDIX I



Table I-1. The frequency of the headway sample within platoon leaving from a signal.

Headways (in sec.)	Light Flow				Medium Flow				Heavy Flow			
	d1	d2	d3	d4	d1	d2	d3	d4	d1	d2	d3	d4
< 1	0	0	0	0	2	2	1	0	1	2	1	0
1.0-1.5	3	3	6	2	7	6	8	5	10	8	15	7
1.5-2.0	13	12	14	28	13	14	27	15	9	19	32	25
2.0-2.5	11	23	27	20	3	18	18	20	9	19	24	33
2.5-3.0	6	9	16	18	6	11	11	29	5	12	15	26
3.0-3.5	4	17	23	13	5	8	20	14	4	4	13	19
3.5-4.0	2	4	11	14	3	4	12	18	0	3	10	6
4.0-4.5	0	1	13	11	0	3	8	11	1	3	5	1
4.5-5.0	1	0	8	8	1	2	7	4	1	0	2	0
5.0-5.5	0	1	0	2	0	2	4	2	0	0	2	2
5.5-6.0	0	0	2	2	0	0	2	2	0	0	1	0
> 6.0	0	0	0	2	0	0	2	0	0	0	0	1

d1 : 100 yds. from the prior signal;

d2 : 200 yds. from the prior signal;

d3 : 300 yds. from the prior signal;

d4 : 500 yds. from the prior signal.

Table I-2. The frequency of the headway sample within platoons with entering vehicles.

Headways (in sec.)	d1	d2	d3	d4
<1	0	0	0	0
1.0-1.5	16	6	1	3
1.5-2.0	29	26	27	21
2.0-2.5	39	46	44	45
2.5-3.0	25	24	32	31
3.0-3.5	7	13	8	9
3.5-4.0	2	3	5	7
4.0-4.5	2	2	1	1
4.5-5.0	0	0	2	1
5.0-5.5	0	0	0	2
5.5-6.0	0	0	0	0
>6	0	0	0	0

d1 = next to the entrance point.

d2 = 100 from the entrance point.

d3 = 200 from the entrance point

d4 = 300 from the entrance point



Table I-3. The frequency of the headway sample within platoons approaching a signal.

Headways (in sec.)	Light Flow			Medium Flow			Heavy Flow		
	d1	d2	d3	d1	d2	d3	d1	d2	d3
< 1	0	0	0	1	0	0	2	1	0
1.0-1.5	7	5	2	15	8	4	19	10	8
1.5-2.0	18	13	13	33	13	10	35	19	23
2.0-2.5	34	18	21	26	20	25	26	33	27
2.5-3.0	30	32	28	16	28	30	18	23	28
3.0-3.5	18	25	33	12	26	27	12	18	20
3.5-4.0	9	16	15	11	16	12	4	14	8
4.0-4.5	2	4	4	3	2	3	3	1	4
4.5-5.0	1	4	3	2	4	5	0	0	1
5.0-5.5	1	2	1	0	1	2	1	1	1
5.5-6.0	0	1	0	0	2	1	0	0	0
> 6	0	0	1	0	0	0	0	0	0

d1 : 100 yds. from the next signal.

d2 : 200 yds. from the next signal.

d3 : 300 yds. from the next signal.

Table I-4. Mean and standard deviation of headway within platoon for all cases.

(A) Platoon leaving the signal

		150 yds.	200 yds.	350 yds.	500 yds.
Non heavy flow	M	2.2512	2.5670	2.9803	3.0024
	σ	0.855	0.8734	0.9878	0.9540
Heavy Flow	M	2.08975	2.2748	2.4533	2.4814
	σ	0.869	0.7921	0.8535	0.8633

(B) Platoon with entering vehicles.

		0 yds.	100 yds.	200 yds.	300 yds.
Heavy flow	M	2.1877	2.3523	2.4268	2.4886
	σ	0.8256	0.7923	0.8756	0.9324

(C) Platoon approaching the signal.

		100 yds.	200 yds.	300 yds.
Non heavy flow	M	2.5361	2.8857	3.0156
	σ	0.8245	0.8973	0.8524
Heavy flow	M	2.2110	2.4914	2.5022
	σ	0.8151	0.8122	0.8234



APPENDIX II



Table II-1. Incomplete Gamma Function $F = \int_T^{\infty} f(t) dt$.

	T = 2	T = 3	T = 4	T = 5
NHL ₁	0.5703	0.1793	0.0364	0.0055
NHL ₂	0.7216	0.2799	0.0646	0.0104
NHL ₃	0.8479	0.4522	0.1508	0.0354
NHL ₄	0.8617	0.4586	0.1564	0.0367
HL ₁	0.4859	0.1445	0.0299	0.0049
HL ₂	0.5965	0.1718	0.0368	0.0064
HL ₃	0.6733	0.2379	0.0504	0.0076
HL ₄	0.6936	0.2585	0.0583	0.0093

Table II-2. Polynomial Equations of $\int_t^\infty f(x)dx = a_0 + a_1t + a_2t^2 + a_3t^3 + a_4t^4$

	a_0	a_1	a_2	a_3	a_4
NHL ₁	1.0	0.2749	-0.3936	0.0825	-0.0041
NHL ₂	1.0	0.0629	-0.0211	-0.0667	0.0134
NHL ₃	1.0	-0.0762	0.1821	-0.1280	0.0185
NHL ₄	1.0	-0.1036	0.2259	-0.1454	0.0205
HL ₁	1.0	0.3402	-0.5611	0.1586	-0.0137
HL ₂	1.0	0.2474	-0.3192	0.0455	0.0009
HL ₃	1.0	0.1334	-0.1352	-0.0238	0.0086
HL ₄	1.0	0.1056	-0.0914	-0.0395	0.0103

Figure II-1. Plotting of $\int_t^\infty f(x)dx$.

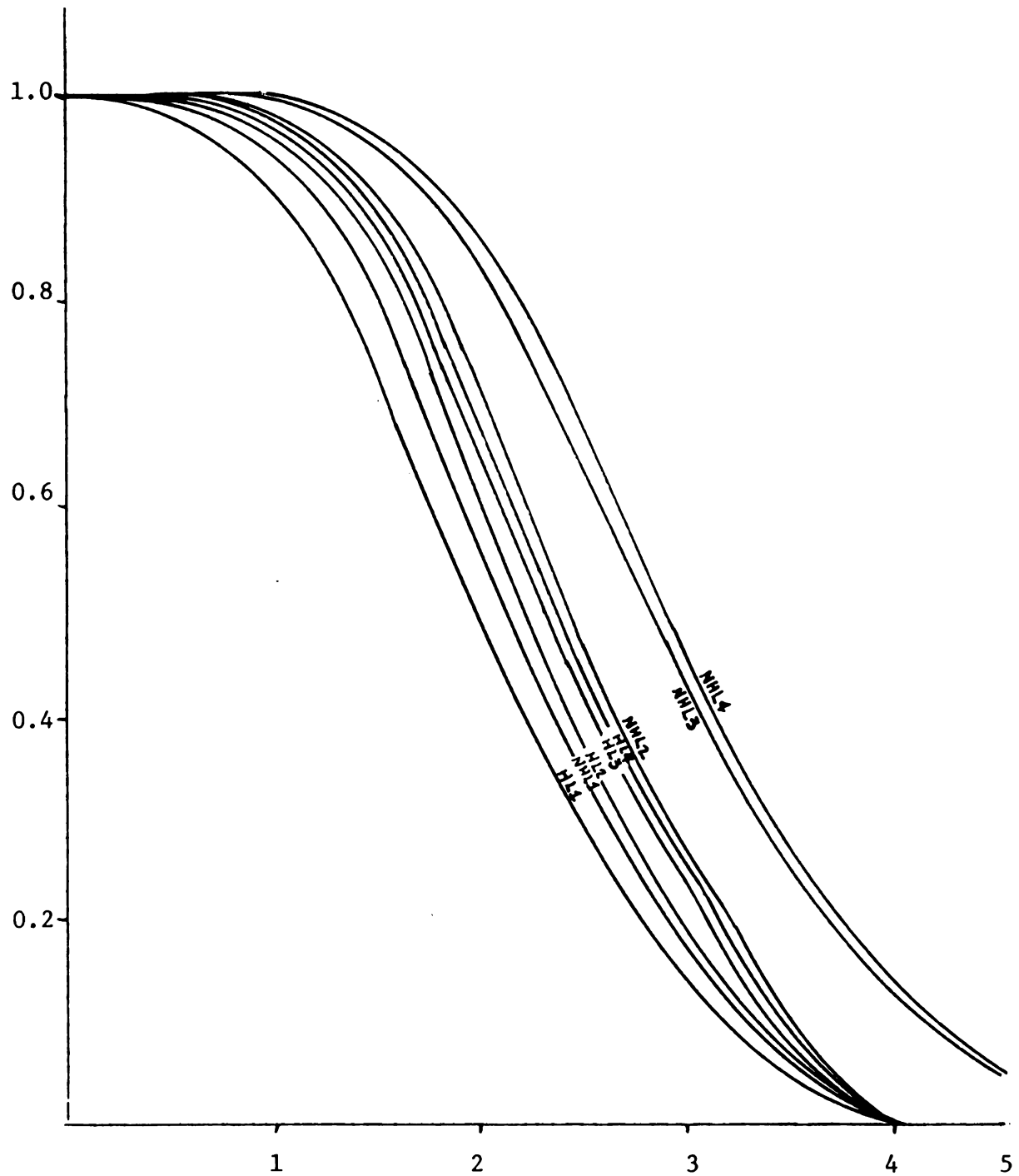


Table II-3. Formulation of $f_o(t) = \frac{\int_t^\infty f(x)dx}{\int_0^\infty t f(t)dt} = a_0 + a_1 t + a_2 t^2 + a_3 t^3 + a_4 t^4$

	a_0	a_1	a_2	a_3	a_4
NHL ₁	0.4442	0.1221	-0.1728	0.0366	-0.0018
NHL ₂	0.3895	0.0240	-0.0082	-0.0259	0.0052
NHL ₃	0.3344	-0.0254	0.0609	-0.0428	0.0061
NHL ₄	0.3330	-0.0345	0.0752	-0.0484	0.0068
HL ₁	0.4785	0.1628	-0.2685	0.0759	-0.0065
HL ₂	0.4396	0.1087	-0.1403	0.0200	0.0004
HL ₃	0.4076	0.0543	-0.0551	-0.0097	0.0035
HL ₄	0.4029	0.0425	-0.0368	-0.0159	0.0041



Table II-4. Integrals of the Forward Recurrence Time Function F_e

	T = 2	T = 3	T = 4	T = 5
NHL ₁	0.2041	0.0432	0.0092	0.0012
NHL ₂	0.2638	0.0670	0.0145	0.0020
NHL ₃	0.3377	0.1192	0.0423	0.0059
NHL ₄	0.3427	0.1192	0.0348	0.0052
HL ₁	0.1830	0.0413	0.0082	0.0011
HL ₂	0.1988	0.0342	0.0070	0.0007
HL ₃	0.2366	0.0521	0.0117	0.0015
HL ₄	0.2557	0.0631	0.0135	0.0018



Table II-5. Calculate $M(t) = \int_0^T t f(t) dt$

	T = 2	T = 3	T = 4	T = 5
NHL ₁	0.6457	1.6016	2.0861	2.2206
NHL ₂	0.4450	1.5394	2.2728	2.5093
NHL ₃	0.2512	1.2477	2.2850	2.7927
NHL ₄	0.2310	1.2480	2.3220	2.8258
HL ₁	0.7343	1.5649	1.9530	2.0622
HL ₂	0.6249	1.6627	2.1461	2.5264
HL ₃	0.5143	1.5825	2.2247	2.4116
HL ₄	0.4844	1.5594	2.2407	2.4546

Table II-6. Calculate $M_0(t) = \int_0^T t f_o(t)dt$

	T = 2	T = 3	T = 4	T = 5
NHL ₁	0.7297	1.1172	1.2309	1.2320
NHL ₂	0.7009	1.1785	1.3552	1.3560
NHL ₃	0.6365	1.1800	1.4860	1.4880
NHL ₄	0.6379	1.1878	1.4868	1.4890
HL ₁	0.7329	1.0733	1.1848	1.1870
HL ₂	0.7401	1.1357	1.2229	1.2240
HL ₃	0.7150	1.1621	1.3002	1.3010
HL ₄	0.7145	1.1813	1.3480	1.3490

Table II-7. Calculate $N(t) = \int_0^T t^2 f(t) dt$

	T = 2	T = 3	T = 4	T = 5
NHL ₁	1.0197	3.3879	5.0410	5.6300
NHL ₂	0.7356	3.4817	5.9962	7.0336
NHL ₃	0.4259	2.9666	6.5606	8.8032
NHL ₄	0.3949	2.9927	6.7119	8.9348
HL ₁	1.1198	3.1673	4.4910	4.9696
HL ₂	1.0078	3.5775	5.2211	5.7020
HL ₃	0.8402	3.5202	5.6994	6.5178
HL ₄	0.7940	3.4844	5.8184	6.7560

Table II-8. Calculate $N_o(t) = \int_0^T t^2 f_o(t) dt$

	T = 2	T = 3	T = 4	T = 5
NHL ₁	0.9116	1.8570	2.2393	2.2400
NHL ₂	0.9025	2.0766	2.6752	2.6760
NHL ₃	0.8361	2.1853	3.2337	3.2350
NHL ₄	0.8381	2.1735	2.9933	2.9960
HL ₁	0.8985	1.7271	2.1046	2.1060
HL ₂	0.9298	1.8930	2.1815	2.1820
HL ₃	0.9124	2.0078	2.4715	2.4730
HL ₄	0.9152	2.0613	2.6257	2.6300

APPENDIX III

(A) Proof of μ_t^n

$D(t)$ is the probability density function of the merging delay.

$$\text{and } D^*(s) = \int_0^\infty e^{-st} D(t) dt.$$

$$\text{Thus } (-1)^n \frac{d^n}{ds^n} D^*(s) \Big|_{s=0} = \int_0^\infty t^n D(t) dt = \mu_t^n$$

Since F_0 and F are constants, from EQ 6-3

$$D^*(s) = F_0 + H^*(t) F$$

by EQ 6-6

$$D^*(s) = F_0 + \frac{G_0^*(s)}{1-G^*(s)} F$$

$$\mu_t^1 = (-1) \frac{d}{ds} D^*(s) \Big|_{s=0} - F \frac{d}{ds} \frac{G_0^*(s)}{1-G^*(s)} \Big|_{s=0}$$

$$\frac{d}{ds} \frac{G_0^*(s)}{1-G^*(s)} \Big|_{s=0} = \frac{(1-G^*(s)) \frac{d}{ds} G_0^*(s) - G_0^*(s) \frac{d}{ds} (1-G^*(s))}{(1-G^*(s))^2}$$

$$= \frac{- \int_0^\infty t G_0(t) dt}{1 - \int_0^\infty G(t) dt} - \frac{\int_0^\infty G(t) dt \int_0^\infty t G(t) dt}{(1 - \int_0^\infty G(t) dt)^2} \quad (\text{EQ-1})$$

$$\text{Since } \int_0^\infty G(t) dt = \int_0^T f(t) dt = 1 - F$$

$$\text{and } \int_0^\infty G_0(t) dt = \int_0^T f_0(t) dt = 1 - F_0.$$

$$(\text{EQ-1}) = \frac{- \int_0^T f_0(t) dt}{F} - \frac{1 - F_0}{F} \int_0^T t f(t) dt$$

$$\mu_t^1 = -F \left(-M_0(t) - \frac{1 - F_0}{F^2} (M(t)) \right)$$

$$= M_0(t) + \frac{1 - F_0}{F} M(t)$$



$$\text{And } \mu_t^2 = \frac{d}{ds^2} D^*(s) \big|_{s=0} = F \frac{d^2}{ds^2} \frac{G_o^*(s)}{1-G^*(s)} \big|_{s=0}$$

$$\frac{d^2}{ds^2} \frac{G_o^*(s)}{1-G^*(s)} \big|_{s=0} = \frac{d}{ds} \left\{ \frac{d}{ds} D^*(s) \right\} = \frac{d}{ds} \frac{(1-G^*(s)) \frac{d}{ds} G_o^*(s) - G_o^*(s) \frac{d}{ds} (1-G^*(s))}{(1-G^*(s))^2}$$

$$= \left\{ (1-G^*(s))^2 \frac{d}{ds} \left[(1-G^*(s)) \frac{d}{ds} G_o^*(s) - G_o^*(s) \frac{d}{ds} (1-G^*(s)) \right] - ((1-G^*(s)) \frac{d}{ds} G_o^*(s) - G_o^*(s) \frac{d}{ds} (1-G^*(s))) \frac{d}{ds} (1-G^*(s))^2 \right\} / [1-G^*(s)]^4 \quad (\text{EQ -2})$$

$$\text{Since } \frac{d}{ds} (1-G^*(s))^2 = 2 (1-G^*(s)) \frac{d}{ds} G^*(s)$$

$$\text{and let } A = G^*(s), B = G_o^*(s)$$

$$(\text{EQ-2}) = (1-A)^2 \frac{d}{ds} \left[(1-A) \frac{d}{ds} B - B \frac{d}{ds} (1-A) \right] + 2 \left[(1-A) \frac{d}{ds} B - B \frac{d}{ds} (1-A) \right]$$

$$\cdot (1-A) \frac{d}{ds} A / [1-A]^4$$

$$= (1-A) \left[(1-A) \ddot{B} - \dot{B} \dot{A} + \dot{B} \dot{A} + B \ddot{A} \right] + \left[(1-A) \dot{B} + B \dot{A} \right] \cdot 2 \dot{A} /$$

$$(1-A)^3$$

$$= (1-A)^2 \ddot{B} + B(1-A) \ddot{A} + 2(1-A) \dot{A} \dot{B} + 2B(\dot{A})^2 / (1-A)^3$$

$$\text{Since } 1-A = F$$

$$\ddot{B} \big|_{s=0} = \int_0^T t^2 f_o(t) dt = N_o(t)$$

$$\ddot{A} \big|_{s=0} = \int_0^T t^2 f(t) dt = N(t)$$

$$\dot{A} \big|_{s=0} = \int_0^T t f(t) dt = M(t)$$

$$\dot{B} \big|_{s=0} = \int_0^T t f_o(t) dt = M_o(t)$$

$$A \big|_{s=0} = \int_0^T f(t) dt = 1 - F$$

$$B \big|_{s=0} = \int_0^T f_o(t) dt = 1 - F_o$$

$$\begin{aligned}
\mu_t^2 &= F \{ F^2 N_o(t) + (1-F_o) F N(t) - 2FM(t)M_o(t) - 2(1-F_o)M_o(t)^2 \} \\
&\quad / F^3 \\
&= N_o(t) + \frac{1-F_o}{F} N(t) + \frac{2}{F} M(t) \{ M_o(t) + \frac{1-F_o}{F} M(t) \} \\
&= N_o(t) + \frac{1-F_o}{F} M(t) + \frac{2}{F} M(t) \mu_t^1.
\end{aligned}$$

Q. E. D.

(B) Proof of EQ 6-11

Let the mean and the variance of the first kind, say group A, of the population (which has P percent) be M_1 and σ_1^2 , let the mean and the variance of the rest be M_2 and σ_2^2 . For the overall population, let the mean of M_3 and variance be σ_3^2 .

Obviously, we will have

$$M_3 = P \times M_1 + (1-P) M_2$$

$$\text{and } \sigma_3^2 = \frac{1}{N} \sum_{i=1}^n (X_i - M_3)^2 \quad (\text{EQ - 1})$$

where N is the population size, also we let N_1 be the size of group A, and N_2 be the size of the rest

Then EQ -1 will write,

$$\begin{aligned} &= \frac{1}{N} \left\{ \sum_{i \in A} (X_i - M_3)^2 + \sum_{i \in A} (X_i - M_3)^2 \right\} \\ &= \frac{1}{N} \left\{ \sum_{i \in A} (X_i - M_1 + M_1 - M_3)^2 + \sum_{i \in A} (X_i - M_1 + M_2 - M_3)^2 \right\} \\ &= \frac{1}{N} \left\{ \frac{N_1}{N_1} \sum_{i \in A} (X_i - M_1)^2 + N_1 (M_1 - M_3)^2 \right\} + \frac{1}{N} \left\{ \frac{N_2}{N_2} \sum_{i \in A} (X_i - M_2)^2 \right. \\ &\quad \left. + N_2 (M_2 - M_3)^2 \right\} \\ &= \frac{N_1}{N} \sigma_1^2 + \frac{N_1}{N} (M_1 - M_3)^2 + \frac{N_2}{N} \sigma_2^2 + \frac{N_2}{N} (M_2 - M_3)^2 \end{aligned}$$

Noting that, in our case

$$M_2 = 0, \sigma_2^2 = 0 \text{ and } M_3 = PM_1$$

$$\sigma_3^2 = P \sigma_1^2 + P (M_1 - PM_1)^2 + (1-P) (P M_1)^2$$



$$= P \sigma_1^2 + P (1 - P) M_1^2$$

Q. E. D.

(C) Proof of EQ 6-15.

Since for any random variable Z , X and any constant a , we have

$$E (Z - a)^2 = E (Z - E(Z))^2 + (E (Z) - a)^2$$

Using the relation

$$E (Z) = E (E(Z|X))$$

Then

$$\begin{aligned} \text{VAR} (Z|X) &= E ((Z - E(Z))^2 | X) \\ &= E ((Z - E(Z|X))^2 | X) + (E (Z|X) - E(Z))^2 \end{aligned}$$

By taking expectation of both sides, we obtain,

$$\text{VAR} (Z) = E (\text{VAR} (Z|X)) + \text{VAR} (Z|X).$$

Q. E. D.



APPENDIX IV

SIMULATION PROGRAM FOR PHASE ONE MODEL.

```

PROGRAM MERGE1(OUTPUT=65)
DIMENSION ARRMP(1000),XLEAV(1000)
I=J=0
T=3,
TWAIT=ABTT=TWATF=0
ARRMI=0
TLMIT=3600.
TMOVE=2.
M=0
YK=9.9046
YA=3.3
EXP=5.
1 IF(YK.GE.1)GO TO 91
YK=1
GO TO 93
91 JK=YK
YKC=JK
YQ=YK-YKC
R=RANF(1)
IF(R.LT.YQ)GO TO 92
YK=YKC
GO TO 93
92 YK=YKC+1
93 K1=YK
TR=1.0
DO 95 I1=1,K1
R=RANF(1)
95 TR=TR*R
Y=-ALOG(TR)/YA
ABTT=ABTT+Y
IF(ABTT.GE.TLMIT)GO TO 999
IF(J.GT.0)GO TO 15
2 X=-EXP*ALOG(RANF(1))
ARRMI=ARRMI+X
I=I+1
J=J+1
ARRMP(I)=ARRMI+TMOVE
IF(I.EQ.1)GO TO 14
IF(ARRMP(I).GE.XLEAV(I-1))GO TO 14
WAITB=XLEAV(I-1)-ARRMP(I)+TMOVE
TWATB=TWATB+WAITB
M=M+1
ARRMP(I)=XLEAV(I-1)+TMOVE
14 CHECK=ARRMP(I)
IF(CHECK.GT.ABTT)GO TO 1
15 GAP=ABTT-CHECK
IF(GAP.GE.T)GO TO 13
CHECK=ABTT
GO TO 1
13 J=J-1
XLEAV(I)=CHECK
WAIT=XLEAV(I)-ARRMP(I)
TWAIT=TWAIT+WAIT
GO TO 2

```



999 XI=I

XM=M

126

AVWM=TWAIT/XI

AVWS=TWATB/XM

PRINT 99,AVWM,AVWS,I

99 FORMAT(* AVE MERGING DELAY=*,F10.4,*)

AVE DELAY BEFORE MERGI

CNG=*,F10.4,*) TOTAL DIBOR VOL=*,I5)

END



C
C
C
C
C
C
C

SIMULATION PROGRAM FOR PHASE TWO MODEL.

```

PROGRAM MERGE2(OUTPUT=65)
DIMENSION XHEAD(50),XAT(100),XLT(100)
XHEAD(1)=3.8
XHEAD(2)=6.9
XHEAD(3)=9.6
XHEAD(4)=12.0
XHEAD(5)=14.2
DO 150 II=6,50
XHEAD(II)=XHEAD(II-1)+2.1
150 CONTINUE
SP=14.5
EXP=10.
TMOVE=2.
DIST=500.
T=3.
FLOW=1000.
XLIMIT=3600.
N=0
XLVLT=0
NJA=0
NIAS=0
IPASS=0
TIMSS=0.
TIMMS=0.
JL=0
NNOCY=0
ABT=0.
ABIT=0.
JJ=0
GT=40.
RT=20.
IAS=0
JA=0
XLT(1)=0
WAITS=0
WAIT=0
ABAT=-EXP*ALOG(PANF(1))
IPS=0
IM=0
JPS=0
XLVLT=0.
LDIWG=0
KDIWG=0
IWR=0
IWG=0
MSIG1=0
CT=GT+RT
NWG=0
NWR=0
FARRT=DIST/SP
152 JJ=JJ+1
IF(CT-XHEAD(JJ))1,151,151
151 N=N+1

```

```

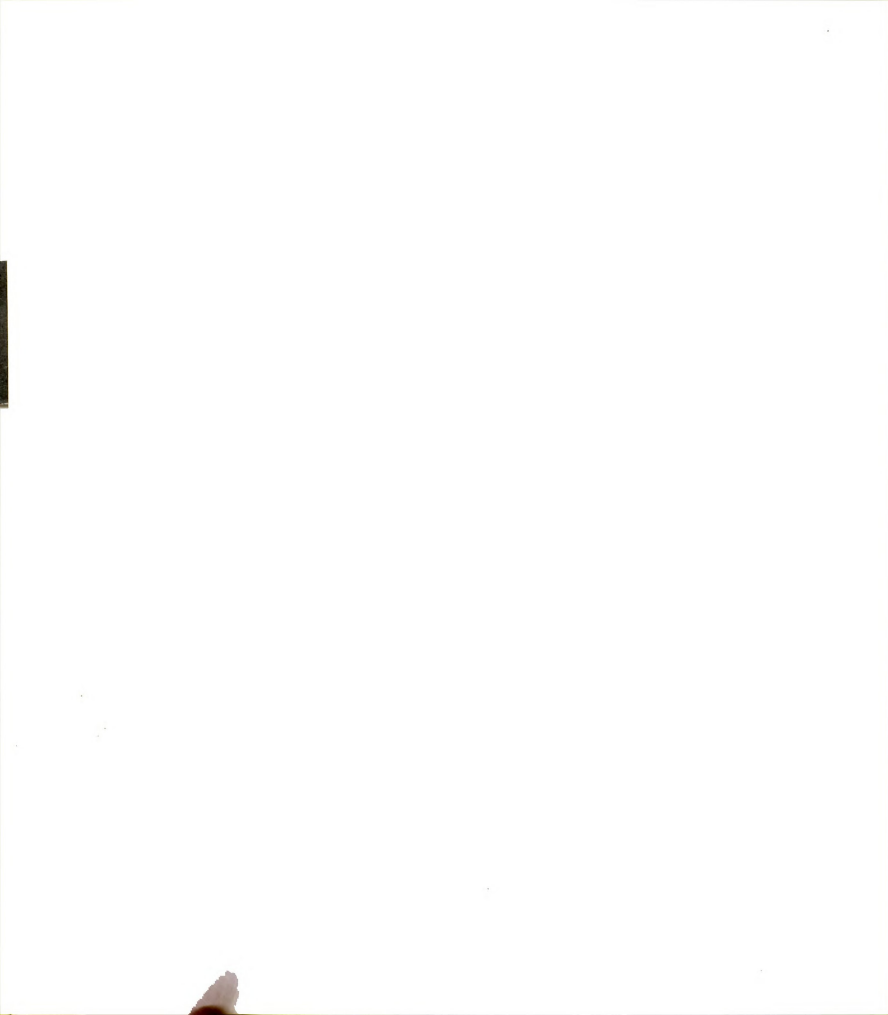
      GO TO 152
1 IF(FLOW.EQ.300.0)GO TO 210 128
  IF(FLOW.EQ.600.0)GO TO 202
  IF(FLOW.EQ.800.0)GO TO 203
  IF(FLOW.EQ.1000.0)GO TO 204
  YK=10.0
  YA=3.33
  GO TO 206
210 YK=160.0
  YA=13.33
  GO TO 206
202 YK=40.0
  YA=6.66
  GO TO 206
203 YK=22.5
  YA=5.00
  GO TO 206
204 YK=14.40
  YA=4.00
206 IF(YK.GE.1.) GO TO 91
  YK=1.
  GO TO 93
91 JK=YK
  YKC=JK
  YQ=YK-YKC
  R=RANF(1)
  IF(R.LT.YQ) GO TO 92
  YK=YKC
  GO TO 93
92 YK=YKC+1
93 K1=YK
  TR=1.0
  DO 95 I1=1,K1
    R=RANF(1)
95 TR=TR*R
  Y=-ALOG(TR)/YA
2 ABT=ABT+Y
  IF(ABT.GT.XLINT) GO TO 999
  IABT=ABT
  ICT=CT
  NOCY=IABT/ICT
  XNOCY=NOCY
  TT=CT*(ABT/CT-XNOCY)
  IF(TT.LE.RT) GO TO 4
  IF((NWG.EQ.0).AND.(NWR.EQ.0))GO TO 41
  GO TO 42
41 FAET=ABT+FARRT
42 IF(NOCY-NNOCY) 7,7,6
4 IF((NWG.EQ.0).AND.(NWR.EQ.0))GO TO 43
  GO TO 45
43 FAET=ABT+(RT-TT)+3.8+FARRT
45 IF(NOCY-NNOCY)5,5,6
5 IWR=IWR+1
  NWR=NWR+1
  MSIG1=0
  GO TO 1
6 NNOCY=NOCY
  GO TO 8
7 IF(LDIWG.EQ.KDIWG) GO TO 105
106 MSIG1=1
  IWG=IWG+1

```

```

GO TO 1 129
105 IF((TT-RT).GE.Y) GO TO 115
YC=Y
GO TO 116
115 YC=TT-RT
116 IIM=NWG+NWR
IF(YC.LE.(XHEAD(IIM)+TMOVE))GO TO 113
LDIWG=KDIWG
KDIWG=IWG
GO TO 106
110 NWG=NWG+1
GO TO 106
8 ABT=ABT-Y
IF(IM.EQ.0) GO TO 9
JPS=JPS+IM
9 IWTT=IWR+IWG
JPS=IWTT-IPS
IF(JPS.GT.N)GO TO 11
IM=0
GO TO 11
10 JPS=N
IM=N-JPS
11 IPS=IPS+JPS
IPASS=JPS
ABTT=FAET
IF(ABTT.LE.XLVLT) GO TO 15
GO TO 49
15 ABTT=XLVLT
49 IF(ABTT-ABAT)17,17,40
40 IF(IAS.EQ.0)GO TO 27
IF((ABTT-XABAT).GE.T) GO TO 47
IF(ABTT.GE.XABAT) GO TO 147
GO TO 17
147 WAIT=1
XABTT=ABTT
XABAT=ABTT
GO TO 17
47 JL=JL+1
IF(WAIT.EQ.1) GO TO 141
XLT(JL)=XABAT
GO TO 142
141 XLT(JL)=XABTT
142 IAS=IAS-1
WAIT=0
GO TO 40
17 IF(DIST.EQ.100.)GO TO 171
IF(DIST.EQ.200.)GO TO 172
IF(DIST.EQ.350.)GO TO 173
IF(DIST.GE.500.)GO TO 174
171 IF(JPS.GE.10)GO TO 176
GO TO 277
172 IF(JPS.GE.10)GO TO 178
GO TO 179
173 IF(JPS.GE.10)GO TO 180
GO TO 281
174 IF(JPS.GE.10)GO TO 282
GO TO 283
176 YYK=5.7829
YYA=1/0.3613
GO TO 117
277 YYK=6.9326

```




```

YYA=1/0.3247
GO TO 117
179 YYK=8.6382
YYA=1/0.2971
GO TO 117
178 YYK=8.2475
YYA=1/0.2758
GO TO 117
281 YYK=9.1641
YYA=1/0.3263
GO TO 117
180 YYK=8.259
YYA=1/0.297
GO TO 117
283 YYK=9.9046
YYA=1/0.3031
GO TO 117
282 YYK=8.2617
YYA=1/0.3003
117 IF(YYK,GE,1.)GO TO 81
YYK=1.
GO TO 83
81 IK=YYK
YYKC=IK
YYQ=YYK-YYKC
R=RANF(1)
IF(R,LT,YYQ) GO TO 82
YYK=YYKC
GO TO 83
82 YYK=YYKC+1
83 KK=YYK
TR=1.0
DO 85 I2=1, KK
R=RANF(1)
85 TR=TR*R
YY=-ALOG(TR)/YYA
FAET=ABTT*YY
JPS=JPS-1
ABTT=ABTT*YY
IF(JPS,EQ,0)GO TO 19
GO TO 49
19 XLVLT=ABTT
NWR=0
NWG=0
GO TO 700
27 R=RANF(1)
X=-EXP*ALOG(R)
ABAT=ABAT+X
IAS=IAS +1
IENT=IENT*1
JA=JA+1
IF(JL,EQ,0) GO TO 46
IF(ABAT,LT,XLT(JL))GO TO 145
GO TO 46
145 WAITS=XLT(JL)-ABAT+WAITS
XABAT=XLT(JL)+THOVE
XAT(JA)=XABAT
GO TO 40
46 XABAT=ABAT
XAT(JA)=ABAT
GO TO 40

```



```

999 DO 30 JT1=1,JL
      TIMM=XLT(JT1)-XAT(JT1)
      TIMMS=TIMMS+ TIMM
131
30 CONTINUE
      XJL=JL
      AVEWM=TIMMS/XJL
      TIMSS=TIMMS+WAITS
      AVEINS=TIMSS/XJL
      PRINT 32, IPS
      PRINT 33, AVEWM
      PRINT 34, AVEINS
      PRINT 35, JL
      PRINT 39, FLOW, EXP, T, DIST
39 FORMAT(* MAIN FLOW=*,F10.4,* MINOR FLOW=*,F10.4,* T=*,F4.2,*
C DISTANCE=*,F10.4)
32 FORMAT(* VOL VEH PER HR = *,I10)
33 FORMAT(* AVE WAITING TIME IN THE MERGING PLACE = *,F10.4)
34 FORMAT(* AVE WAITING TIME IN THE SYSTEM = *,F10.4)
35 FORMAT(* VOL IN MINOR STREAM = *,I10)
      END

```



C
C
C
C
C
C

132
SIMULATION PROGRAM FOR PHASE THREE MODEL.

```

PROGRAM MERGE3(OUTPUT=65)
DIMENSION XHEAD(50),XAT(1000),XLT(1000),QXLT(1000),GXAT(1000)
XHEAD(1)=3.8
XHEAD(2)=6.9
XHEAD(3)=9.6
XHEAD(4)=12.0
XHEAD(5)=14.2
DO 150 II=6,50
XHEAD(II)=XHEAD(II-1)+2.1
150 CONTINUE
SP=14.5
XDIST=800.
NJA=0
QLVLT=0
IENT=0
QXLT(1)=0
MJL=0
QARTT=0
QTIMS=0
QWAIT=0
EXPP=10.
EXP=10.
TMOVE=2.
DIST=500.
T=3.
FLOW=1000.
XLIMIT=3600.
N=0
XLVLT=0
NJA=0
MIAS=0
IPASS=0
TIMSS=0.
TIMMS=0.
JL=0
NNOCY=0
ABT=0.
ABTT=0.
JJ=0
GT=40.
RT=20.
IAS=0
JA=0
XLT(1)=0
WAITS=0
WAIT=0
XFART=XDIST/SP
QABAT=-EXPP*ALOG(RANF(1))
ABAT=-EXP*ALOG(RANF(1))
IPS=0
IM=0
JPS=0
XLVLT=0.
LDING=0

```



```

KDIWG=0
IWR=0
IWG=0
MSIG1=0
CT=GT+RT
NWG=0
NWR=0
FARRT=DIST/SP
152 JJ=JJ+1
IF(CT-XHEAD(JJ))1,151,151
151 N=N+1
GO TO 152
1 IF(FLOW.EQ.300.)GO TO 210
IF(FLOW.EQ.600.)GO TO 212
IF(FLOW.EQ.800.)GO TO 213
IF(FLOW.EQ.1000.)GO TO 214
YK=10.0
YA=3.33
GO TO 206
210 YK=160.0
YA=13.33
GO TO 206
202 YK=40.0
YA=6.66
GO TO 206
203 YK=22.5
YA=5.00
GO TO 206
204 YK=14.40
YA=4.00
206 IF(YK.GE.1.) GO TO 91
YK=1.
GO TO 93
91 JK=YK
YKC=JK
YQ=YK-YKC
R=RANF(1)
IF(R.LT.YQ) GO TO 92
YK=YKC
GO TO 93
92 YK=YKC+1
93 K1=YK
TR=1.0
DO 95 I1=1,K1
R=RANF(1)
95 TR=TR*R
Y=-ALOG(TR)/YA
2 ABT=ABT+Y
IF(ABT.GT.XLIMT) GO TO 999
IABT=ABT
ICT=CT
NOCY=IABT/ICT
XNOCY=NOCY
TT=CT*(ABT/CT-XNOCY)
IF(TT.LE.RT) GO TO 4
IF((NWG.EQ.0).AND.(NWR.EQ.0))GO TO 41
GO TO 42
41 FAET=ABT+FARRT
42 IF(NOCY-NNOCY) 7,7,6
4 IF((NWG.EQ.0).AND.(NWR.EQ.0))GO TO 43
GO TO 45

```




```

43 FAET=ABT+(RT-TT)+3.8+FAET
45 IF(NOCY-NNOCY)5,5,6
5 IWR=IWR+1
NWR=NWR+1
MSIG1=0
GO TO 1
6 NNOCY=NOCY
GO TO 8
7 IF(LDIWG.EQ.KDIWG) GO TO 135
106 MSIG1=1
IWG=IWG+1
GO TO 1
105 IF((TT-RT).GE.Y) GO TO 115
YC=Y
GO TO 116
115 YC=TT-RT
116 IIM=NWG+NWR
IF(YC.LE.(XHEAD(IIM)+TMOVE))GO TO 118
LDIWG=KDIWG
KDIWG=IWG
GO TO 106
110 NWG=NWG+1
GO TO 106
8 ABT=ABT-Y
IF(IM.EQ.0) GO TO 9
JPS=JPS+IM
9 IWTT=IWR+IWG
JPS=IWTT-IPS
IF(JPS.GT.N)GO TO 10
IM=0
GO TO 11
10 JPS=N
IM=N-JPS
11 IPS=IPS+JPS
IPASS=JPS
ABTT=FAET
IF(ABTT.LE.XLVLT) GO TO 15
GO TO 49
15 ABTT=XLVLT
49 IF(ABTT-ABAT)17,17,40
40 IF(IAS.EQ.0)GO TO 27
IF((ABTT-XABAT).GE.T) GO TO 47
IF(ABTT.GE.XABAT) GO TO 147
GO TO 17
147 WAIT=1
XABTT=ABTT
XABAT=ABTT
GO TO 17
47 JL=JL+1
IF(WAIT.EQ.1) GO TO 141
XLT(JL)=XABAT
GO TO 142
141 XLT(JL)=XABTT
142 IAS=IAS-1
WAIT=0
GO TO 40
17 IF(DIST.EQ.100.)GO TO 171
IF(DIST.EQ.200.)GO TO 172
IF(DIST.EQ.350.)GO TO 173
IF(DIST.GE.500.)GO TO 174
171 IF(JPS.GE.10)GO TO 176

```



```

GO TO 277
172 IF(JPS,GE,10)GO TO 178
GO TO 179
173 IF(JPS,GE,10)GO TO 15. 135
GO TO 281
174 IF(JPS,GE,10)GO TO 282
GO TO 283
176 YYK=5.7829
YYA=1/0.3613
GO TO 117
277 YYK=6.9326
YYA=1/0.3247
GO TO 117
179 YYK=8.6382
YYA=1/0.2971
GO TO 117
178 YYK=8.2475
YYA=1/0.2758
GO TO 117
281 YYK=9.1641
YYA=1/0.3263
GO TO 117
180 YYK=8.259
YYA=1/0.297
GO TO 117
283 YYK=9.9046
YYA=1/0.3031
GO TO 117
282 YYK=8.2617
YYA=1/0.3003
117 IF(YYK,GE,1.)GO TO 81
YYK=1.
GO TO 83
81 IK=YYK
YYKC=IK
YYO=YYK-YYKC
R=RANF(1)
IF(R,LT,YYO) GO TO 82
YYK=YYKC
GO TO 83
82 YYK=YYKC+1
83 KK=YYK
TR=1.0
DO 85 I2=1, KK
R=RANF(1)
85 TR=TR*R
YY=-ALOG(TR)/YYA
FAET=ABTT*YY
JPS=JPS-1
ABTT=ABTT*YY
IF(JPS,EQ,0)GO TO 19
GO TO 49
19 XLVLT=ABTT
NWR=0
NWG=0
GO TO 700
27 R=RANF(1)
X=-EXP*ALOG(R)
ABAT=ABAT*X
IAS=IAS +1
IENT=IENT*1

```

```

JA=JA+1
IF(JL.EQ.0) GO TO 46      136
IF(ABAT.LT.XLT(JL))GO TO 145
GO TO 46
145 WAITS=XLT(JL)-ABAT+WAITS
XABAT=XLT(JL)+TMOVE
XAT(JA)=XABAT
GO TO 40
46 XABAT=ABAT
XAT(JA)=ABAT
GO TO 40
700 IENT=0
IPASS=IPASS+IENT
QABTT=XFART
IF(QABTT.LE.QLVLT)GO TO 315
GO TO 349
315 QABTT=QLVLT
349 IF(QABTT-QABAT)317,317,340
340 IF(MIAS.EQ.0)GO TO 327
IF((QABTT-QQXAB).GE.T)GO TO 447
IF(QABTT.GE.QQXAB)GO TO 447
GO TO 317
447 QWAIT=1.
QQAAT=QABTT
QQXAB=QABTT
GO TO 317
347 MJL=MJL+1
IF(QWAIT.EQ.1.)GO TO 341
QXLT(MJL)=QQXAB
GO TO 442
341 QXLT(MJL)=QQAAT
442 MIAS=MIAS+1
QWAIT=0
GO TO 340
317 IF(IPASS.GE.10)GO TO 478
YHK=8.2617
YQA=1/0.3003
GO TO 417
478 YHK=9.9046
YQA=1/0.3031
417 IF(YHK.GE.1) GO TO 481
YHK=1.
GO TO 483
481 IHK=YHK
YHKC=IHK
YHQ=YHK-YHKC
R=RANF(1)
IF(R.LT.YHQ)GO TO 482
YHK=YHKC
GO TO 483
482 YHK=YHKC+1
483 MK=YHK
TR=1.0
DO 485 I3=1,MK
R=RANF(1)
485 TR=TR*R
YYQ=-ALOG(TR)/YQA
XFAET=QABTT+YYQ
IPASS=IPASS-1
QABTT=QABTT+YYQ
IF(IPASS.EQ.0)GO TO 319

```



```

      GO TO 349
319  QLVLT=QABTT
      GO TO 2
      137
327  XQ=-EXPP*ALOG(RANF(1))
      QABAT=QABAT+XQ
      MIAS=MIAS+1
      NJA=NJA+1
      IF(MJL.EQ.0)GO TO 346
      IF(QABAT.LT.QXLT(MJL))GO TO 445
      GO TO 346
445  WAITS=QXLT(MJL)-QABAT+WAITS
      QQXAB=QXLT(MJL)+TMOVE
      QXAT(NJA)=QQXAB
      GO TO 340
346  QXAT(NJA)=QABAT
      QQXAB=QABAT
      GO TO 340
999  DO 30 JT1=1,JL
      TIMM=XLT(JT1)-XAT(JT1)
      TIMMS=TIMMS+TIMM
30  CONTINUE
      DO 330 MJT1=1,MJL
      QTIMM=QXLT(MJT1)-QXAT(MJT1)
      QTIMS=QTIMS+QTIMM
330  CONTINUE
      MSM=JL+MJL
      XMSM=MSM
      SUMM=TIMMS+QTIMS
      TIMSS=TIMMS+WAITS
      AVEWM=SUMM/XMSM
      AVEIWS=TIMSS/XMSM
      PRINT 32, IPS
      PRINT 33, AVEWM
      PRINT 34, AVEIWS
      PRINT 35, JL
      PRINT 35, MJL
      PRINT 39, FLOW, EXP, T, DIST
39  FORMAT(*      MAIN FLOW=*,F17.4,*MINOR FLOW=*,F17.4,*      T=*,F4.2,*,
C    DISTANCE=*,F17.4)
32  FORMAT(* VOL VFP PER HP = *,I17)
33  FORMAT(* AVE WAITING TIME IN THE MERGING PLACE = *,F17.4)
34  FORMAT(* AVE WAITING TIME IN THE SYSTEM = *,F17.4)
35  FORMAT(* VOL IN MINOR STREAM = *,I17)
      END

```


REFERENCES

REFERENCES

1. Adams, W.F. "Road Traffic Considered as a Random Series," Journal of the Institute of Civil Engineers. (November, 1936): 121.
2. Bleyl, R.L. "Speed Profiles Approaching a Traffic Signal," Bureau of Highway Traffic Report, Pennsylvania State University, 1972.
3. Blumenfeld, D.E., and Weiss, G.H. "On Queue Splitting to Reduce Waiting Times," Transportation on Research, 4. (1969): 141-144.
4. Blumenfeld, D.E., and Weiss, G.H. "On the Robustness of Certain Assumptions in the Merging Delay Problem," Transportation on Research, 4. (1970): 125-139.
5. Cochran, W.G. "The X^2 Test of Goodness of Fit," Annals of Mathematical Statistics, Vol.23 (1952): 245 & 315.
6. Cox, D.R. Renewal Theory. London, Methuen, 1962.
7. Draper, N.R., and Smith, H. Applied Regression Analysis. New York: Wiley, 1966.
8. Drew, D.R. Traffic Flow Theory and Control. McGraw-Hill, New York: 1968.
9. Grace, M.J. and Potts, R.B. "A Theory of the Diffusion of Traffic Platoons," Operation Research, Vol 12, (1964): 255-72.
10. Graham, E.L., and Chenu, D.C. "A Study of Unrestricted Platoon Movement of Traffic," Traffic Engineering (April, 1962): 11-13.
11. Grecco, W.L., and Sword, E.C. "Prediction of Parameters for Schahl's Headway Distribution," Traffic Engineering (February, 1968): 36-38.
12. Greenshields, B.D., Shapiro, D., and Erickson, E.L. Traffic Performance at Urban Street Intersections. New Haven: Yale Bureau of Highway Traffic, (1947).
13. Hamming, R.W. Numerical Methods for Scientists and Engineers, New York: McGraw-Hill, 1962.

14. Herman, R., and Weiss, G. "Comments on the Highway-Crossing Problem," Operation Research, Vol.9, No.6 (1961): 828-40.
15. Herman, R.; Potts, R.B.; and Rothery, R.W. "Behavior of Traffic Leaving a Signalized Intersection," Traffic Engineering and Control. (January, 1964): 529-33.
16. ITE Technical Committee 6P6. "Land Use and Demography Growth Versus Forecast," Traffic Engineering, Vol.47, (March, 1977): 42-44.
17. Kell, J.H. "A Theory of Traffic Flow on Urban Streets," Proceedings of the 13th Annual Western Section Meeting, Institute of Traffic Engineers. (1969): 66-70.
18. Kendall, D.G. "Some Problems in the Theory of Queues," Journal of the Royal Statistical Society, Series B, Vol.13 (1951): 151-185.
19. Lewis, B.J. "Platoon Movement of Traffic from an Isolated Signalized Intersection," Highway Research Board Bulletin, 178, (1958): 1-11.
20. Major, N.G., and Buckley, D.J. "Entry to a Traffic Stream," Proceedings of the Australian Road Research Board, Vol.1, Part 1 (1962): 206-228.
21. Massey, F.J. "The Kolmogorov-Smirnov Test for Goodness of Fit," Journal of American Statistical Association, Vol.4 (1951): 68-78.
22. Nemeth, E.A., and Vecellio, R.L. "Investigation of the Dynamics of Platoon Dispersion," Highway Research Record, No.334 (1970): 23-33.
23. Nemeth, E.A., Vecellio, R.L., and Treiterer, J. "Effect of Signal Spacing on Platoon Dispersion," Engineering Experiment Station, Ohio State University, Final Report EES 311, (July, 1973).
24. Neter, J., and Wasserman, W. Applied Statistical Models. Homewood, Ill.: IRWIN, (1974).
25. Newell, G.F. "Statistical Analysis of Flow of Highway Traffic Through a Signalized Intersection," Applied Math, Vol.13 (1956):
26. Pacey, G.M. "Progress of a Bunch of Vehicles Released from a Traffic Signal," Road Research Laboratory, Crowthorne, England, RRL Report RN/2665, (1956).

27. Robertson, D.I. "TRANSYT: A Traffic Network Study Tool," Road Research Laboratory, Crowthorne, England, RRL Report LR/253, (1969).
28. Tanner, J.C. "The Delay to Pedestrians Crossing a Road," Biometrika, Vol.38 (1951): 383-392.
29. Tolle, J.E. "The Lognormal Headway Distribution Mode," Traffic Engineering and Control, Vol.13. (May, 1971): 22-24.
30. Weiss, G.H., and Maradudin, A.A. "Some Problems in Traffic Delay," Operation Research, Vol.10, No.1 (1962): 74-104.



MICHIGAN STATE UNIVERSITY LIBRARIES



3 1293 03085 5427